DISSERTATION

ADDRESSING THE THREAT OF FROST DAMAGE ON PEACH FLORAL BUDS THROUGH LARGE-SCALE COLD HARDINESS PHENOTYPING, DYNAMIC WEATHER MODELING AND NON-TARGETED METABOLOMIC AND PROTEOMIC ANALYSIS

Submitted by

David Sterle

Department of Horticulture and Landscape Architecture

In partial fulfillment of the requirements

For the Degree of Doctor of Philosophy

Colorado State University

Fort Collins, Colorado

Summer 2023

Doctoral Committee:

Advisor: Ioannis Minas

Julia Sharp
Jessica Prenni
Horst Caspari

ABSTRACT

ADDRESSING THE THREAT OF FROST DAMAGE ON PEACH FLORAL BUDS THROUGH LARGE-SCALE COLD HARDINESS PHENOTYPING, DYNAMIC WEATHER MODELING AND NON-TARGETED METABOLOMIC AND PROTEOMIC ANALYSIS

Cold damage to reproductive tissues is the greatest threat to the profitability of peach (*Prunus persica*) growers worldwide. Cold hardiness is the extent to which peach floral buds super-freeze without suffering lethal damage. Although no changes are visible externally to floral buds for much of the dormant season, cold hardiness fluctuates as they acclimate, deacclimate and respond to abiotic stressors such as temperature or drought. A greater understanding of the mechanisms involved in these fluctuations involves accurate and frequent measurement of the extent to which cold hardiness is changing, and the ambient weather factors influencing the changes, at different stages of the dormant season. Warmer or more erratic temperature changes during the dormant season threatens peach floral buds to more frequently receive frost damage if cold hardiness becomes misaligned with the timing of lethally cold weather events.

Statistical analysis of the trends and forces impacting the cold hardiness of floral buds can help identify significant patterns. These patterns can be used to better understand the physiological mechanisms affecting cold hardiness changes, and they can be used to help predict the impact of weather conditions on cold hardiness. In addition to their use in a practical sense by growers to aid in frost management decisions, accurate cold hardiness prediction models can be used to estimate what effects foreseeable climate effects can have on the outlook of future peach production.

Metabolic changes are known to occur in dormant plants, although the effects of the metabolome in peaches on cold hardiness are unknown. Changes associated with cold hardiness likely follow several trends. One such trend is the fluctuations of metabolic abundances across the season, which are more associated with the endodormancy, and ecodormancy phases and the prebloom phase. These trends likely take place every dormant season as buds undergo a steady process of acclimating and deacclimating. Another trend is the response floral buds exhibit in response to acute cold events, in order to rapidly increase cold hardiness. The study of this response necessitates the monitoring of cold hardiness as well as the metabolic shift to the weather event. The response can be further elucidated by comparing cold hardiness and metabolic changes between genotypes that have different cold hardiness phenotypes. By exploring changes a cold hardy genotype undergoes, geneticists may be able to target certain metabolic expressions that may increase the frost tolerance of future cultivars.

Since frost damage can be so destructive to peach production, it is necessary to understand the risks to the peach industry moving forward surrounding climate change, and it is also necessary to understand the extent to which frost tolerance can be improved in future cultivars. This study uses a multifaceted approach to cold hardiness which involves improved and large-scale cold hardiness phenotyping using differential thermal analysis, dynamic weather prediction models and associated metabolic regulation understanding.

ACKNOWLEDGMENTS

I would like to first acknowledge my wife Danielle for her insight, support and generosity she has provided to me through the last few years. At times I needed every ounce of each. And thank you to my daughter Ellia for your big loving personality, and for the sacrifices you didn't have a choice in making when Papa was too tired to be much fun.

Next, I would like to acknowledge our pomology lab: Jeff Pieper, Brendon Anthony and Jake Pott. It is great to look back and see the progress we have all made in the last several years, and I credit much of that to the talent and character of those in this group.

To Emily Dowdy and Bryan Braddy, thanks for keeping this farm running smoothly each of the nine years I have been involved in some capacity at WCRC Orchard Mesa. It requires a lot of strength and dedication to work hard outside each day.

To my mom who has never wavered in her support even if it meant a son and granddaughter were out of arms-reach 99% of the time. To my dad who couldn't be prouder and who provided for our family growing up working in the scorching hot California sun for over forty years while rarely taking any kind of vacation.

Thanks to Dr. Rich Rosecrance who first put the idea of graduate school into my mind and setting me down this path. Thanks to Dr. Jessica Davis for taking me on as a graduate student and being a patient mentor for me as I flailed about trying to learn how to do research for the first time.

Thanks to everyone in my committee for your expertise and support over the years, each bit means so much when you are not located on a main campus. Dr. Horst Caspari for constantly swapping notes about cold hardiness and weather for the last six years. Dr. Julia Sharp for the statistical guidance that has helped data analysis become something I really enjoy. Dr. Jessica

Prenni for being a strong student advocate and for helping guide and redirect my metabolomic and proteomic research.

And lastly to my advisor Dr. Ioannis Minas for providing some Macedonian energy to balance my more laconic style. For the excitement, determination, and vision you bring to your pomology research program which has benefited our lab, local industry, and the CSU Ag Experiment Station as a whole.

TABLE OF CONTENTS

LIST OF TABLES

LIST OF FIGURES

CHAPTER ONE

OPTIMIZED DIFFERENTIAL THERMAL ANALYSIS SHEDS LIGHT ON THE EFFECT OF TEMPERATURE ON PEACH FLORAL BUD COLD HARDINESS AND TRANSITION FROM ENDO- TO ECODORMANCY

1.1. Introduction

Cold damage to reproductive tissues is the greatest limiting factor to peach (*Prunus persica*) production in the world. Peach floral buds exhibit supercooling with a dynamic cold tolerance level which changes throughout the dormant season in accordance with time, environmental and weather conditions, and genotype. Xylem discontinuity is one strategy which allows peach floral buds to supercool (Ashworth, 1984; Liu et al., 2019), preventing ice crystals from forming in the floral primordia. The dormant season, post leaf senescence through bloom, has two phases which are characterized by unique physiological behaviors associated with the accumulation of thermal time. The first phase, endodormancy, is the period where plants gradually acclimate and gain cold hardiness (H_c) as a response to external temperatures, until they reach a maximum and growth is controlled from within the floral bud until a genetically predetermined chilling exposure requirement is met (Lang et al., 1987). The second phase, ecodormancy, is the period of growth after the chilling requirement has been met, where external temperatures determine the gradual loss of H_c and the acceleration of deacclimation until bloom (Lang et al., 1987). “Chilling” generally refers to the accumulation of thermal time within different thresholds which are relatively cool, yet greater than 0 ºC, although recent literature has determined certain species achieve greater yields only when sufficient sub-freezing chilling is accumulated (Preedy et al., 2020). Depending on the phase of dormancy, the response of the plant organs to different temperature stimuli varies dramatically.

Orchard frost protection tools are necessary to consistent tree fruit production in many areas; however, the associated benefit from the temporary temperature rise in the orchard is relatively small, often averaging only 1.5 ºC with wind machines at common spacings (Beyá-Marshall et al., 2019). To effectively use frost protection tools, there must be an accurate and an up-to-date understanding of the critical temperatures which would be lethal for floral tissues (Minas and Sterle, 2020). Additionally, development of predictive cold hardiness models requires the accumulation of a large data set across numerous years in which changes in lethal temperatures (LTs) are compared with unique local growing conditions for informed real-time frost protection decision making (Sterle et al., *unpublished*). Therefore, in order to have a complete understanding of H_c and the parameters affecting it for successful frost protection or cold damage mitigation, it is necessary to have practical and efficient methods of determining the level of H_c which is in turn affected by dormancy stage.

Oxidative browning (OB) observation following natural or artificial freezing is a standard method of assessing cold damage or monitoring H_c in plant tissues and more specifically in floral buds (Proebsting and Mills, 1978; Szalay et al., 2010). This method requires the freezing of floral buds inside of a programmable freezing chamber, and the removal of the buds at various temperature intervals. After remaining at 21 ºC for 24 hours, buds are dissected to determine the probability of lethality. Green tissue is judged to be viable while brown tissue indicates non viability due to presence of oxidated phenolic compounds released from cell membranes damaged by the formation of ice crystals during the freezing event (**Figure 1.1**). A positive aspect of OB is that it is capable of determining lethal temperatures of floral buds at any phenological stage. Furthermore, this method simulates a pattern which is often seen in ambient conditions, and ensures all tissue reaches the same minimum temperature. Unfortunately, in order for OB to be

effective samples need to be removed at distinct temperatures. The range of temperature intervals must be greater than the lethal temperature range in order to extrapolate the critical temperatures from the analysis. This can have negative ramifications such as not being able to calculate certain quantiles from the data or limiting the precision of the data. In addition, judging the colors of floral primordia tissue is subjective and time-consuming and limits the capacity for the assessment of larger sample volumes.

Differential thermal analysis (DTA) can be used to obtain frequent, large-scale data sets that represent the lethal freezing points of peach floral buds. Early DTA cold hardiness techniques involved the placement of thermocouples in a single bud, greatly limiting the number of lethal events which were observed (Quamme, 1986). Modern DTA methodology uses thermal electric modules (TEM) to detect temperature gradient changes from the latent heat of fusion released when supercooled water from floral primordia (e.g., ovaries) freeze (Mills et al., 2006; Minas and Sterle, 2020; Quamme, 1991). The TEMs are arrayed on plates which are subjected to progressively colder temperatures within a programable freezing chamber. As extracellular water freezes heat is released in a non-lethal exotherm referred to as the high temperature exotherm (HTE). The temperature at which the lethal freezing event occurs is termed the low temperature exotherm (LTE) and represents the temperature at which a particular floral bud lost its ability to grow into a healthy fruit (Burke et al., 1976; Mills et al., 2006). In peach, a freezing event at this temperature level in the orchard will result in oxidation, desiccation, and finally the abortion of the floral bud which further adds to the challenge of estimating the actual winter damage to inform management decisions as well. Improvements to the DTA methodology that lead to increased signal to noise ratio can provide more accurate lethal temperature estimation across larger data sets. DTA-estimated LTs can be associated with weather data for H_c prediction models

development or with biochemical and/or molecular data to better characterize cold stress related physiological responses during dormancy in perennial fruit tree crops.

This work focuses on continuing the development of DTA into a reliable and efficient tool for determining precise lethal temperatures of peach floral buds. DTA has the potential to provide large-scale data which can support decision making for frost protection during the dormant season. These data can also be used to better understand the environmental temperature effects on physiological changes related to H_c within peach floral tissues during the transitions across the different phases of dormancy. In addition, the use of such a powerful tool for comparative studies can help define optimum horticultural management strategies and/or genotype selection for future plantings to mitigate the negative consequences of cold damage in tree fruit production systems.

1.2. Materials and Methods

Dormant peach [*Prunus persica* (L.) Batsch] flower buds from 9-year-old 'Redhaven' scions grafted on 'Lovell' rootstock were tested for cold hardiness (H_c) using artificial freezing in combination with differential thermal analysis (DTA) or oxidative browning (OB). Buds were collected weekly (beginning in mid-October of 2016) from one-year-old shoots of moderate vigor that had no obvious signs of damage and were located at the mid-canopy position of 15 randomly selected trees. The sampling location was the Colorado State University's Experimental Orchard at Western Colorado Research Center, Orchard Mesa, Colorado (39.042230, -108.469492). For regular DTA assessment samples were collected from the orchard and buds were then separated and randomly assigned to 13 sets of 10 buds each (in total 130 buds per time point). Three complete sets (30 buds) were kept as a control and were not frozen for visual evaluation of oxidative browning to check orchard variability and estimate existing field cold damage. The remaining 10 complete sets (100 buds) were then used for DTA utilizing an optimized system in the Minas Lab

that was build based on a previously developed system to sense H_c of large volumes of grape bud samples (Mills et al., 2006). Sampling method was followed proportionately, but with appropriately varied sample sizes for the three optimization experiments maintaining 10 buds per TEM in any case.

The OB method is a standard method for observing cold damage of fruit tree floral buds exposed to naturally occurring or artificial freezing temperatures (Stushnoff and Junttila, 1986). Samples of 30-cm long one-year-old fruiting shoots were placed in a programmable freezing chamber in several replicated bundles. The starting temperature in the freezing chamber was set to the ambient outside temperature and was then dropped 4 ºC over 30 minutes (step-drop), and then held at the lower temperature for 30 minutes. The process was repeated, and samples were removed at predetermined temperature thresholds. A bundle of four to eight fruiting shoots containing between 20 and 40 floral buds was removed at each of three to four different temperature intervals after holding at the targeted temperature for 30 minutes. Following removal, the shoots were then brought to 21 ºC and high relative humidity (~90%) for 24 hours, to allow for oxidative browning to become evident. The buds were longitudinally sectioned with a razor blade through the ovary. Green tissue was judged to be viable while brown tissue indicates nonviability due to presence of oxidized phenolic compounds released from damaged cell membranes following ice crystals formation in response to the freezing event (**Figure 1.1**). The fraction of bud mortality was tallied for each temperature regime, and a linear regression line with a quadratic term was fitted for temperature against the percent lethality observed within the bundle at that temperature. The resultant regression was then used to calculate lethal temperature (LT) quantiles (LT_{10}, LT_{50}, and LT_{90}). In addition to OB the three evaluations performed for validation of DTA accuracy, OB was performed three other dates October 26, 2016, March 8 and March 13, 2017 when DTA was not

able to detect LTEs of the supercooled peach floral primordia. Targeted removal temperatures were -10 ºC, -15 ºC and -20 ºC on October 26, -7 ºC, -12 ºC, -15 ºC, and -18 ºC on March 8 and -3 ºC, -5 ºC, -7 ºC and -9 ºC on March 13.

The original DTA system used for this study was adapted from Mills et al., 2006, and modifications were made as a result of various optimization experimental trials. The DTA assembly was composed of three 29 cm × 27 cm aluminum plates which were fastened together using bolts, with the plates spaced by rubber hosing, so that each plate was 2.5 cm apart so that heat would dissipate following exotherms (**Figure 1.2A**). Attached to each aluminum plate were eleven evenly spaced 4.5 cm × 5.5 cm × 1.5 cm lidded aluminum bins, each containing a single thermoelectric module (HP-127-1.4-1.5-72 high performance module, TE Technology, Inc., Traverse City, MI). The TEM detected temperature gradients by producing a small electric charge due to the heat of fusion released from exotherms (**Figure 1.2B**). The DTA assembly could accommodate at least 300 peach floral buds in total, across 30 sample TEMs and 3 reference TEMs.

Sample buds were excised from one year old fruiting shoots using a grafting knife, in pairs of two floral buds. Each bud pair was immediately wrapped in aluminum foil to prevent desiccation. Five foil-wrapped pairs of buds were placed within ten lidded bins on each plate, and enclosed with foam insulation pads (**Figure 1.2**), which ensured buds remained in close contact with the TEM. One centrally located TEM per plate did not get filled with buds, to act as a reference TEM cell. The voltage data from the reference TEM was subtracted from the data generated from each sample TEM on the same plate, this removed some amount of noise caused by minute thermal gradients in the system. Within each reference cell two copper/constantin thermocouples were placed to monitor the temperature within the reference cell when neighboring

cells experienced exotherms. In total, 100 ‘Redhaven’ floral buds were loaded into the DTA assembly per regular “run”.

The DTA assembly was then loaded into a programmable freezer (Tenney Jr. Test Chamber, Model TUJR 1.22 cu.ft., Thermal Product Solutions, New Columbia, PA). To perform the DTA “run”, the freezer was programmed for a cooling rate of 4 $^{o}C \cdot h^{-1}$. At the start of the program the temperature was held at 4 ^{o}C for 1 h and then dropped to -36 ^{o}C in 10 h at 4 $^{o}C \cdot h^{-1}$ (rate-drop), then returned to 4 ^{o}C in 10 h (Mills et al., 2006). A digital multimeter (Keithley Integra Series 2700 multimeter, Keithley Instruments, Cleveland, OH) measured each TEM voltage signal every 8 seconds. The signals were sent to a PC and then output directly to an Excel spreadsheet. Exotherms were identified by plotting the TEM signals (mV) against the temperature (^{o}C) (**Figure 1.2B**). This voltage rapidly increases when the thermal energy of a high temperature exotherm (HTE) or low temperature exotherm (LTE) is released. Only LTEs are representative of lethal events as it corresponds to supercooled water freezing within the primordial tissue of the bud, which results in membrane leakage and oxidative damage. HTE occur consistently at temperatures between -5 ^{o}C to -10 ^{o}C and as a result of intercellular water freezing (Kovaleski, 2021). Despite the much larger thermal energy release caused by HTE, this peak does not correspond to a lethal freezing event. TEM voltage signals were plotted against the reference TEM cell temperature and the LTs which were necessary to kill floral primordia were observed, based on the temperature at the time of the LTE appearance per flower bud. Parametric survival analysis was performed in JMP Pro 15 (SAS Institute Inc., Cary, NC,), to estimate LT quantiles (LT_{10}, LT_{50}, and LT_{90}) for the LTE data generated by DTA. For each sampling date Weibull, Lognormal, Exponential, Frechet, and Loglogistic distributions were tested to determine which distribution was the best fit

for the data (**Figure 1.2c**). The specific quantiles were estimated as "time quantiles," substituting absolute values for temperature for time in this context.

To test the validity of the DTA methodology using rate drop (**Figure 1.2d**), lethal temperature estimates coming from LTE analysis were validated against estimates created by using OB and step drop (**Figure 1.2e**) with artificial freezing three times throughout the dormant season (December 1, 2016, February 8, 2017 and February 15, 2017; **Figure 1.2f**). For OB, temperature was dropped incrementally using the step-drop method (see Section 2.2), while when using DTA a 4 $^{o}C \cdot h^{-1}$ rate drop was employed (see Section 2.3). Buds exposed to freezing temperatures were warmed for 24 h and longitudinally sectioned as described in section 2.2. Linear regression analysis including a quadratic term was used to create a temperature versus percent oxidative damage curve for OB. The LT_{10}, LT_{50}, and LT_{90} lethal temperature quantiles were then compared between DTA and OB to validate the use of DTA using the rate-drop method (**Figure 1.2b**).

An experiment was performed with the DTA system in an attempt to increase the signal of LTE over the noise perceived by fluctuating temperature gradients created by the TEMs. LTE signal heights were compared in cells which were insulated with two different insulating materials: 9 mm thick closed foam insulation pads (control), and 9 mm thick mylar insulation pads (MIP) (**Figure 1.3a**). MIP pads were constructed of three layers of 3 mm thick metalized mylar bubble insulation. Three hundred floral buds were loaded into 30 separate cells with a total of 150 buds in 15 cells with foam pads (control treatment), and 150 buds in 15 cells with MIP (experimental treatment). Peak height was measured for each LTE (n=134 total LTE for foam, and n=137 total LTE for MIP) from the base of the peak to the apex of each peak in mV. Differences were compared using one-way ANOVA in JMP Pro 15. Graphs were created using Prism v9.0 for Mac OS X (Graph Pad Inc., San Diego, CA, USA).

Significant temperature swings within strong air currents in the chamber of the programmable freezer can cause noise to appear in the data output produced by the DTA. This noise can be detrimental to the accurate identification of LTE peaks. A simple comparison of the noise generated in the mV output was conducted using two consecutive runs, one in which the DTA assembly was placed inside of a temperature resistant nylon bag slipped over the entire DTA assembly (**Figure 1.3b**). Three hundred buds were loaded into 30 cells across all three plates of the DTA assembly, on November 15, 2016 (control unbagged) and November 21, 2016 (bagged). In order to fairly quantify noise in the system, absolute fluctuations in voltage from the mean were calculated in each cell, for 80 minutes at temperatures less than -25 ºC. Only temperatures lower than -25 ºC were used because this range provided a span of signal which was consistent with the rest of the range of temperatures and yet only included noise, not having additional signals from HTE or LTE (actual temperature range of LTE temperatures was -12.6 ºC to -24.7 ºC). Absolute fluctuations were quantified by taking the absolute value of the difference of each individual adjusted voltage signal (measured every 8 seconds within each TEM cell for a total of 600 voltage measurements per TEM cell) and the mean voltage signal from the cell. Absolute fluctuations in voltage signal were compared using the corresponding plates as covariates and compared between the two runs using ANOVA to determine difference in the amount of noise detected.

The ability of DTA to perceive lethal freezing events diminished incrementally during ecodormancy in early February, as LTEs were no longer detected by the system. DTA measurements were deemed unreliable if greater than 40% of live buds failed to yield recognizable LTE in the graphical output of the data (**Figure 1.4**). To regain the perception of LTE an additional optimization step was included into the DTA protocol. Starting February 8, 2017, the temperature of the freezing chamber with the DTA trays loaded was held at a non-lethal temperature for the

phase of dormancy (-2 ºC) for a period of 12 hours (Liu et al., 2019) before dropping steadily as before at a rate of 4 ºC · h^{-1} until the terminal temperature (-36 ºC) for LTE detection. The exposure of the buds to the non-lethal freezing conditions caused condensation of the supercooled water in the floral primordia to a level that would allow subsequent LTE detection. This method increased the number of perceptible LTEs for the following 4 weeks at which point the number LTEs was again too low for reliable prediction of lethal temperatures even with this optimized LTE recovery protocol. Starting March 8, 2017 OB was used to estimate lethal temperatures until full bloom as described in section 2.2.

Predicted DTA floral bud damage was validated also against four naturally occurring lethal freezing events in the field (**Table 1.1**), on dates when temperatures were lower than LT_{10} as predicted by DTA. These frost events took place on January 6, 2017 (T_{min}=-19.2 ºC), February 26, 2017 (T_{min}=-9.7 ºC), March 1, 2017 (T_{min}=-8.2 ºC), and March 7, 2017 (T_{min}=-5.9 ºC). Samples of 30 floral buds were brought to the Minas Lab on the same day immediately after the freeze and held at 21ºC for 24 hours and then longitudinally sectioned to observe the percentage of buds with OB in the floral ovaries. The sum of the cumulative damage from the in-situ frost events was compared with the estimated cumulative damage from the most recent DTA data from dates preceding the frost events.

Chill hours (0-7.2 ºC) accumulation was calculated for comparison with trends in LTEs detection using a chill calculating tool developed by Erez and Fishman (Erez et al., 1989). Dynamic chill portions, Utah chilling units, and chilling hours (<7.2 ºC) were also calculated using the same tool. Because of the lack of a universally accepted chilling estimation model, this work focused primarily on the chill hours (0-7.2 ºC)(Fadón et al., 2020). Chill hours were selected as the primary

chill estimation model because of a greater prevalence of cultivar specific chilling information available related with this model.

1.3. Results and Discussion

Freezing temperatures can kill plant tissues when ice crystals form in the symplast, but not when ice forms in the extracellular spaces (apoplast) (Wisniewski et al., 2014). The standard method to determine cold damage after natural or artificial freezing to floral tissues consists in detecting the presence of tissue browning caused by oxidized phenolic compounds that are released from the damaged cellular membranes by ice crystal formation following a 24 h incubation (**Figure 1.1**). The advantage of the OB method is that it can be performed at any phenological stage. However, it is labor intensive and not friendly for large data volumes acquisition towards prediction models development. In addition, artificial freezing with OB is limited by the number of targeted temperature regimes that the plant tissue is exposed that is not necessarily an accurate representation of the distribution of the lethal temperatures of the sample population (Proebsting and Mills, 1978; Szalay et al., 2010). The OB method also requires some prior knowledge of cold hardiness in order to capture the minimum and maximum temperatures which are lethal to buds, while ensuring this range is narrow enough to accurately identify the median lethal temperatures. In contrast to the OB method, the type of data DTA yields is an individual lethal temperature for each individual floral bud, which is higher in resolution, and more descriptive of the distribution of lethal temperatures within a sample population. The DTA system used in the present study (**Figure 1.2a**) proved able to precisely identify HTEs and LTEs in peach floral buds from sample populations of up to 300 floral buds in a single run. Prior to DTA methodology optimization (see section 3.2), there was reliable identification of HTE and LTE in 'Redhaven' peach buds from November 2, 2016 through January 30, 2017. However, the OB method still remains a critical tool

in evaluating cold hardiness because it is not limited to as narrow of an effective-use time frame as is DTA and can be used prior or after that frame (**Figure 1.1**). In addition, OB is the most reliable method to perform validation tests for the accuracy of DTA-based cold hardiness estimations throughout the season (**Figure 1.2f**).

Peach floral bud cold hardiness in the form of lethal temperature quantiles (LT_{10}, LT_{50}, and LT_{90}) were estimated from the LTE data generated by DTA following parametric survival analysis. Weibull, Lognormal, Exponential, Frechet, and Loglogistic distributions were tested to determine which distribution was the best fit for the LTE data per sampling date. Consistently, Weibull distributions provided the best fit for the data based on having the lowest Akaike information criterion (AICc) and were selected for LTs estimation using the created continuous probability or survival distribution plots (**Figure 1.2c**). On the other hand, a quadratic linear regression line was used to fit for LT against the percent lethality observed as oxidative damage within the bundle at that temperature regime in OB. The resultant regression was used to calculate the LT quantiles (LT_{10}, LT_{50}, and LT_{90}) for OB. The LT_{10}, LT_{50}, and LT_{90} quantiles were then compared to validate the use of DTA using the rate-drop method against the standard OB following the stepwise drop method.

At three timepoints throughout the season, artificial freezing coupled with the DTA and OB methods were compared for cold hardiness assessment on 'Redhaven' peach floral bud samples taken at the same day. The OB method was tested using the step-drop cooling pattern which has been historically used in western Colorado and elsewhere (**Figure 1.2b**). In contrast, a rate-drop method was used in the DTA methodology, so it was necessary to compare the accuracy of the two systems against one another. Across the three dates the two methods alternated which predicted the lowest LT_{50}, and the average difference between the two methods was only 0.4 ^{o}C

and was not statistically significant. Similar results were found at five different test times during the 2016/17 and 2017/18 dormant season with six different wine grape cultivars (Sterle and Caspari, *unpublished*). The slight difference for LT_{50} is accounted for by natural variability in the sample populations and was considered to be negligible.

The workflow of OB has less initial setup time but requires active management to retrieve samples from the freezing chamber at appropriate temperature intervals. Whereas DTA workflow requires more setup time, but the process is progressing automatically once begun, and therefore gives additional flexibility to the user in terms of start time. With either method the results can be analyzed the following day, and the overall time each method takes is roughly similar for the analysis of 300 buds. The raw data are distinct as DTA provides exact temperatures when LTEs occur, whereas OB provides the number of dead buds versus alive buds at relatively few regularly spaced temperature intervals. The individual lethal temperatures observed using DTA allow for a more realistic distribution curve to be made for each individual date. Better describing the LT quantiles can aid in the development of more precise hardiness prediction models (Sterle and Minas, *unpublished*).

Differentiation of LTE peaks in processed output is a critical part of the usage of DTA. Increased signal and decreased noise increase the efficacy of LTE differentiation. The increase in LTE peak height using different insulating materials within each TEM cell was tested. The hypothesis was that within a TEM cell, the mylar insulation pads (MIP) would reflect thermal energy released by LTE directly back to the TEM plate. With closed foam pads acting as a control treatment and MIP an experimental treatment, LTE peak height was compared across the two treatments in a combined DTA run. Use of MIP resulted in a significant (P<0.0001) 94% increase in a signal height from a mean of 0.117 to 0.227 mV (**Figure 1.3a**). This insulation method

increased the number of LTE peaks that can be detected and may increase the efficacy of DTA for other crops, which have exotherms which are more difficult to detect because of lower floral primordia intracellular water content.

The original DTA apparatus was setup so that air would freely move through the plates, however it was noticed that this led to increased amounts of noise detected in cells which were located nearest to the freezing chamber fan. This noise originated from differences between the temperature gradients working on the TEM in the reference cell in comparison to the different sample cells on the plate. The cells located nearest to the reference cell were consistently less noisy. An intermitted experiment was conducted to evaluate potential further improvements of the DTA system performance by reducing the amount of noise present within the data related with the freezer fan. To reduce the extremes in temperature gradients across the DTA plates, a temperature resistant nylon baking bag was slipped over the entire DTA apparatus. This data was compared across two adjacent DTA runs, by calculating the absolute mean deviations from signal mean mV output (**Figure 1.3b**). The result was an overall reduction in noise of 29.2% across all cells, with the cells on the noisiest plate reducing by an average of 55.5% ($p=0.022$). This represents a tremendous increase in the clarity of the data generated by DTA.

In summary, optimizations like the use of the nylon bag to cover the entire stack of TEM plates and the use of MIP to cover the individual TEM cells reduced the noise of the system and doubled the LTE signal, greatly improving the detection limits and accuracy of the DTA estimates saving significant amount of time in the data processing portion of the procedure. Increased signal to noise ratio also may make the data easier to process algorithmically without risking errant data.

In early February the percentage of detectable LTEs of the total amount of sampled floral buds was 38% or decreased by 55% between January 30, 2016 and February 7, 2017 as buds began

to deacclimate. The loss of detectable LTEs was first noted in 'Redhaven' upon the accumulation of 900 chilling hours (0-7.2 ºC). Immediately once this decrease was observed a modified DTA protocol was developed and tested for the recovery of LTEs during this late stage of dormancy which is called ecodormancy. The LTE recovery protocol involved pre-exposure of the floral buds to -2 ºC for a period of 12 h before running the standard rate of 4 ºC · h^{-1} temperature drop, as proposed previously (Liu et al., 2019). The addition of the pre-conditioning step resulted in an increase in the proportion of LTE detected from 38% to 79% of the total sampled floral buds (**Figure 1.4**). This approach allowed for an extended period of time in which DTA could estimate hardiness with a high enough quantity of peaks to yield reliable LT estimates. On March 6, 2017, 35% of the expected number of LTE were still detected, which is similar to the number of LTEs detected without the LTE recovery protocol when for the first time a significant decrease in detectable LTEs was observed (27 days prior; **Figure 1.5**). The mid-deacclimation period of ecodormancy is an important period to have estimates of LTs of peach floral buds because of the gradual decrease in cold hardiness as they approach visual bud swell and bloom time, which results in a greater risk of cold injury.

The use of DTA showed a dramatic shift in peach cold hardiness as the weekly detected LTEs of floral buds acclimated and deacclimated in the period between leaf senescence and bloom (**Figure 1.5**). Floral bud intracellular supercooled water freeze and subsequent LTE detection from the DTA system using the standard and the LTE recovery protocol was possible from November 2, 2016 until March 6, 2017 (**Figure 1.5**). Before and after this period OB was used for cold hardiness assessment. To generate a visual representation of the seasonal progression of 'Redhaven' peach floral bud cold hardiness the OB- and DTA-based LT quantiles estimations (LT_{10}, LT_{50}, and LT_{90}) across the dormant season were plotted against the ambient minimum (min),

mean, and maximum (max) daily temperatures (T) (**Figure 1.6**). Floral buds generally became hardier (acclimated) in early autumn from October 18, 2016 (LT_{50}=-14.2 ºC) when OB was first used to assess cold hardiness until the coldest time of year when the hardiest lethal temperatures were measured based on DTA on January 9, 2017 (LT_{50}=-23.9 ºC; **Figure 1.5 and 1.6**). Hardiness was then gradually lost as daily temperatures rose until the final DTA measurement performed on March 6, 2017 (LT_{50}=-8.9 ºC) or the final OB assessment was performed on March 8, 2017 (LT_{50}=-8.6 ºC). During the early acclimation stage post-leaf senescence, LT_{50} dropped from -16.0 ºC to -19.1 ºC three days after the first significant frost event (less than -6.5 ºC on November 18, 2016). This was the first dramatic change in peach floral bud cold hardiness measured, and it suggests that the low minimum temperature was associated with the change. Another significant increase in hardiness was seen between January 3, 2017 and January 9, 2017 after a significant freezing event (January 7, 2017) in which the low temperatures reached -19.2ºC and the maximum temperatures did not rise above 0 ºC for a period of three days. As a result of this event the LT_{50} dropped from -21.8 to -23.9 ºC. This increase in hardiness was associated with a prolonged period at sub-zero temperatures, when previously the LT_{50} had appeared to have stabilized around -21.5 ºC. From February until early March, peak height (mV) in DTA output dramatically increased (**Figure 1.5**). The observed height increase is likely because of the influx of extracellular water into the growing and developing peach floral primordia, leading to a larger release of thermal energy as the heat of fusion during the artificial freezing events that are captured by the DTA.

A key component to the successful use of DTA and any other cold hardiness assessment methodology is the generation of floral bud LT prediction data which comports with field status. The ultimate validation of the developed methodology is when there is a natural freezing event in which the ambient temperatures are lower than the estimated critical temperatures, allowing the

recording of the actual cold damage in situ. Field cold damage following three separate natural freezing events (-9.7 ºC on February 26, 2017; -8.2 ºC on March 1, 2017; and -5.9 ºC on March 7, 2017) was compared with the expected damage as predicted by DTA prior the frost (**Table 1.1**; **Figure 1.6**) to validate the accuracy of the estimates. The sum-total of the observed damage across all events was 58% dead floral buds, whereas the expected damage from the DTA was estimated at 55% dead floral buds. In addition, the DTA setting presented in this study did not predict any significant damage for 'Redhaven' peach floral buds as a result of the extreme freeze on January 7, 2017 (**Figure 1.6**) and this was also confirmed by independent in situ OB observations on samples collected on January 9 (data not shown). Results from the field validation demonstrate a high level of accuracy using the DTA method, and they impart a high level of confidence in the use of DTA as a tool for large-scale cold hardiness assessment of peach floral buds. It is worth highlighting the importance of field validation for the use of the LTE recovery protocol as well (**Figure 1.3**). During the mid-deacclimation period of ecodormancy it is important to have estimates of LTs of peach floral buds because of the gradual decrease in cold hardiness as they approach visual bud swell and bloom time, which results in a greater risk of cold injury. This was evidenced by the three lethal frost events that occurred in late February and early March (bud swell), i.e. during a period when the DTA was performed following the LTE recovery protocol. It highlights the significant impact of this approach to generate critical LT data that could support grower informed frost protection decision making. It also indicates that the LTE recovery protocol did not affect the outcome of the LTEs by changing the lethal freezing temperatures of the buds (**Figure 1.6**). Further, it demonstrates that although there was only ~40% of the expected LTE peaks observed in late February early March, the estimated cold hardiness levels were still an accurate indicator of the actual LTs in field.

On January 24, 2017, 868 chill hours (0-7.2 ºC) had accumulated (**Figure 1.7**), approximately equal to the chilling requirement needed by 'Redhaven' to enter ecodormancy (Weinberger, 1950; Fadón et al., 2020). According to other chilling models, 56.4 dynamic chill portions, 1517 Utah model chill units, and 1658 chill hours (<7.2 ºC) had accumulated at that time (**Figure 1.7**). Satisfaction of chilling coincided with a dramatic 55% loss in the number of LTEs captured by DTA (**Figure 1.4 and 1.7**). The loss in LTEs occurred once two conditions were met: the accumulation of 868 chilling units, and the first accumulation of growing degrees day (T_{base}=7 ºC) post chill satisfaction, on February 7, 2017 (this time point is indicated with an asterisk and an arrow in **Figure 1.7**). It is possible therefore, that the development of xylem vessel elements which leads to the loss of LTEs (Ashworth, 1984; Liu et al., 2019) may be closely related to chilling satisfaction. Allowing for this, DTA may sense the transition from endodormancy to ecodormancy, through the initial loss of LTEs. The hypothesis that the loss of detectable LTEs occurs at the transition from endo- to ecodormancy is supported by data showing that a low-chill cultivar 'Sierra Rich' had lost more LTEs on February 7, 2017 (86% loss), whereas the high-chill cultivar 'Cresthaven' had lost fewer LTEs (35%) (Minas and Sterle, 2020).

The possibility that DTA may be able to sense the transition to ecodormancy would expand the usefulness of DTA as a tool to evaluate and compare cultivars if this link can be validated by future work. Gaining a greater understanding of the precise timing of the transition to ecodormancy can also have an impact on the study of metabolic, proteomic, and transcriptomic shifts which may be happening as a result of chilling satisfaction. This possibility also allows for greater evaluation of chill satisfaction models when comparing cultivars from multiple locations under disparate environmental conditions.

1.4. Conclusions

This work highlights the reliable generation of large-scale cold hardiness data for peach floral buds using an optimized DTA methodology. Additionally, this work demonstrates several experimentally-tested and field-validated techniques and protocols which greatly enhance the quality of the DTA data that extend the useful period for using it in peach floral buds during dormancy and especially during spring deacclimation. Seasonal trends as well as daily changes in cold hardiness can easily be measured by DTA with a high level of confidence. Chill satisfaction was followed by a significant decrease in detectable LTEs using DTA, once the first growing degree day (T_{base}=7.2 ºC) was experienced. This indicates that in addition to the capacity for precise large-scale cold hardiness data acquisition DTA may also have the ability to detect a significant developmental event in peach floral buds, the transition from endodormancy to ecodormancy.

1.5. References

Ashworth, E.N., 1984. Xylem development in prunus flower buds and the relationship to deep supercooling . Plant Physiol. 74, 862–865. https://doi.org/10.1104/pp.74.4.862

Beyá-Marshall, V., Herrera, J., Santibáñez, F., Fichet, T., 2019. Microclimate modification under the effect of stationary and portable wind machines. Agric. For. Meteorol. 269–270, 351–363. https://doi.org/10.1016/j.agrformet.2019.01.042

Burke, M.J., Gusta, L. V, Quamme, H.A., Weiser, C.J., Li, P.H., 1976. Freezing and injury in plants. Annu. Rev. Plant Physiol. 27, 507–528. https://doi.org/10.1146/annurev.pp.27.060176.002451

Erez A., Fishman S., Linsley-Noakes G.C., Allan P. 1989. The dynamic model for rest completeion in peach buds. II International symposium on computer modelling in fruit research and orhard management, 276, 165-174.

Fadón, E., Herrera, S., Guerrero, B.I., Guerra, M.E., Rodrigo, J., 2020. Chilling and heat requirements of temperate stone fruit trees (*Prunus* sp.). Agronomy 10, 409. doi10.3390/agronomy10030409

Kovaleski, A., 2022. Woody species do not differ in dormancy progression: differences in time to budbreak due to forcing and cold hardiness. Proceedings of the National Academy of Sciences of the United States of America, 119 (19). 10.1073/pnas.2112250119

Lang, G.A., Early, J.D., Martin, G.C., Darnelll, R.L., 1987. Endodormancy, paradormancy, and ecodormancy- physiological terminology and classification for dormancy research. HortScience 22, 371–377.

Liu, J., Lindstrom, O.M., Chavez, D.J., 2019. Differential thermal analysis of 'Elberta' and 'Flavorich' peach flower buds to predict cold hardiness in Georgia. HortScience 54, 676–683.

https://doi.org/10.21273/HORTSCI13518-18

Mills, Lynn J, Ferguson, J.C., Keller, M., 2006. Cold-hardiness evaluation of grapevine buds and cane tissues. AJEV 57, 194–200.

Minas, I.S., Sterle, D. G., 2020. Differential thermal analysis sheds light on the effect of environment and cultivar in peach floral bud cold hardiness. Acta Hortic. 1281, 385–391. https://doi.org/10.17660/ActaHortic.2020.1281.51

Preedy, K., Brennan, R., Jones, H., Gordon, S., 2020. Improved models of the effects of winter chilling on blackcurrant (*Ribes nigrum* L.) show cultivar specific sensitivity to warm winters. Agric. For. Meteorol. 280, 107777. https://doi.org/10.1016/j.agrformet.2019.107777

Proebsting, E. L. and Mills, H.H., 1978. Low temperature resistance of developing flower buds of 6 deciduous fruit species. Journal Am. Soc. Hortic. Sci. 103, 192–198.

Quamme, H.A., 1986. Use of thermal analysis to measure freezing resistance of grape buds. Can. J. Plant Sci. 952, 945–952.

Quamme, H.A., 1991. Application of thermal analysis to breeding fruit crops for increased cold hardiness. HortScience 26, 513–517. https://doi.org/10.21273/hortsci.26.5.513

Stushnoff, C., Junttila, O., 1986. Seasonal development of cold stress resistance in several plant species at a coastal and a continental location in North Norway. Polar Biol. 5, 129–133. https://doi.org/10.1007/BF00441691

Szalay, L., Timon, B., Németh, S., Papp, J., Tóth, M., 2010. Hardening and dehardening of peach flower buds. HortScience 45, 761–765. https://doi.org/10.21273/hortsci.45.5.761

Wisniewski, M., Gusta, L., Neuner, G., 2014. Adaptive mechanisms of freeze avoidance in plants: A brief update. Environ. Exp. Bot. 99, 133–140. https://doi.org/10.1016/j.envexpbot.2013.11.011

Weinberger, J. H., 1950. Chilling requirements of peach varieties. HortScience 56, 122-28.

1.6. Tables

Table 1.1. Differential thermal analysis (DTA) validated against in-situ freezing events through comparison of seasonal cumulative damage. Control samples taken at the time of every DTA run were longitudinally sectioned to observe the extent of oxidative damage in each sample. From January 6, 2017 through March 7, 2017 observed cumulative in-situ field damage was used to validate the DTA predicted field damage over the same period. Field validation confirmed that DTA was accurately representing the lethal temperature thresholds of peach floral buds under ambient conditions.

Date of killing frost event	Minimum T (°C)	Observed field damage (%)	DTA predicted damage (%)
January 6, 2017	-19.17	3	0
February 26, 2017	-9.72	21	27
March 1, 2017	-8.17	24	16
March 7, 2017	-5.88	10	12
Total		58	55

Table 1.2 Validation of deferential thermal analysis (DTA) compared to oxidative browning method (OB) for accuracy in peach floral bud lethal temperature prediction. Oxidative browning method (OB) was used to validate differential thermal analysis (DTA) in parallel runs on three dates, December 1, 2016, February 8, 2017, and February 15, 2017. Lethal temperature quantiles LT_{10}, LT_{50}, and LT_{90} were calculated for each method and compared. For each date the mean difference for the three quantiles was less than 1 ºC, indicating a high level of precision between the two methods.

Lethal temperature quantile	Oxidative browning method estimation	DTA method estimation	Difference
12/01/2016			
LT_{10}	-19.23	-18.77	0.46
LT_{50}	-21.47	-20.96	0.51
LT_{90}	-23.70	-22.49	1.21
02/08/2017			
LT_{10}	-16.46	-18.37	-1.91
LT_{50}	-20.55	-20.76	-0.21
LT_{90}	-23.64	-22.44	1.20
02/15/2017			
LT_{10}	-16.31	-16.38	-0.07
LT_{50}	-19.78	-18.87	0.91
LT_{90}	-21.13	-20.64	0.49

Figures 1.7.

Figure 1.1 Evaluation of cold damage of dormant and pre-bloom peach floral buds using the oxidative browning method (OB) at two different phenology stages. Samples were taken following artificial or naturally occurring freeze during the dormant and green calyx phenology stages. Buds were longitudinally sectioned with a razor blade through the ovary after being incubated at 21 ºC and high relative humidity (90-95%) for 24 hours. Floral buds

are considered viable if all portions of the pistil remain green and considered dead if browning is present to any portion of the pistil tissue.

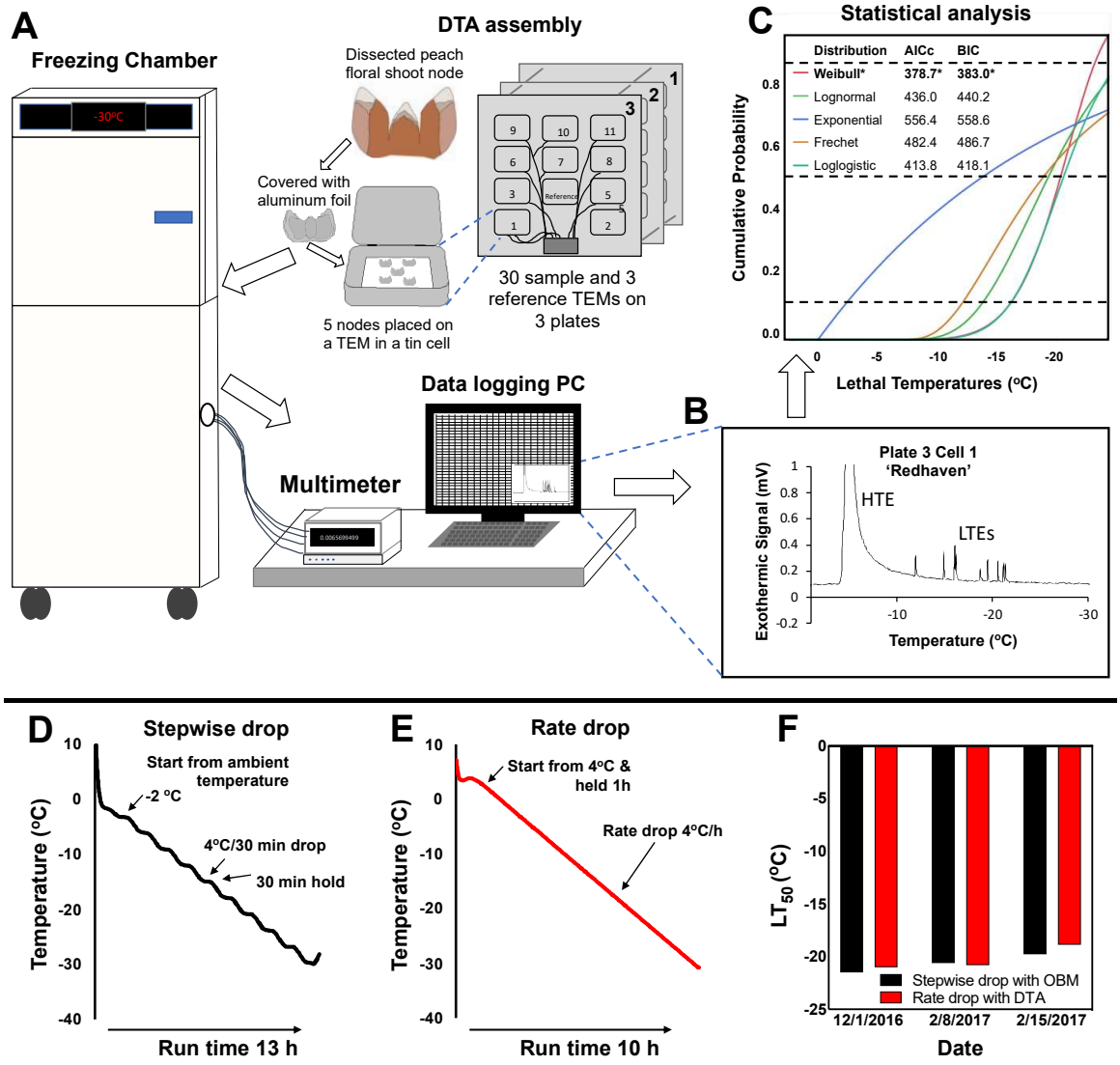

Figure 1.2 Graphical representation of differential thermal analysis (DTA) data acquisition system workflow for detection and data analysis of low temperature exotherms (LTEs) indicating the minimum survivable temperatures of up to 300 peach floral buds per run. Peach floral bud pairs were removed from shoots before being covered in aluminum foil and enclosed in tin cells atop thermal electric modules (TEM). As the chamber cooled, an electric signal was monitored by a digital multimeter and data was logged onto a PC (A). TEM signal (mV) data populate figures which display the amount of electricity being generated as a result of supercooled water freezing events within the peach floral tissue. High temperature exotherms (HTE) are nonlethal freezing events, and LTE represent lethal events to floral tissues (B). Lethal temperatures were then compiled, and lethal temperature quantiles were calculated after fitting a sample population of lethal temperatures to a Weibull distribution (C). Two different methods of

temperature drop were evaluated, stepwise drop (D) and rate drop (E), for consistency among the LT measurements (F).

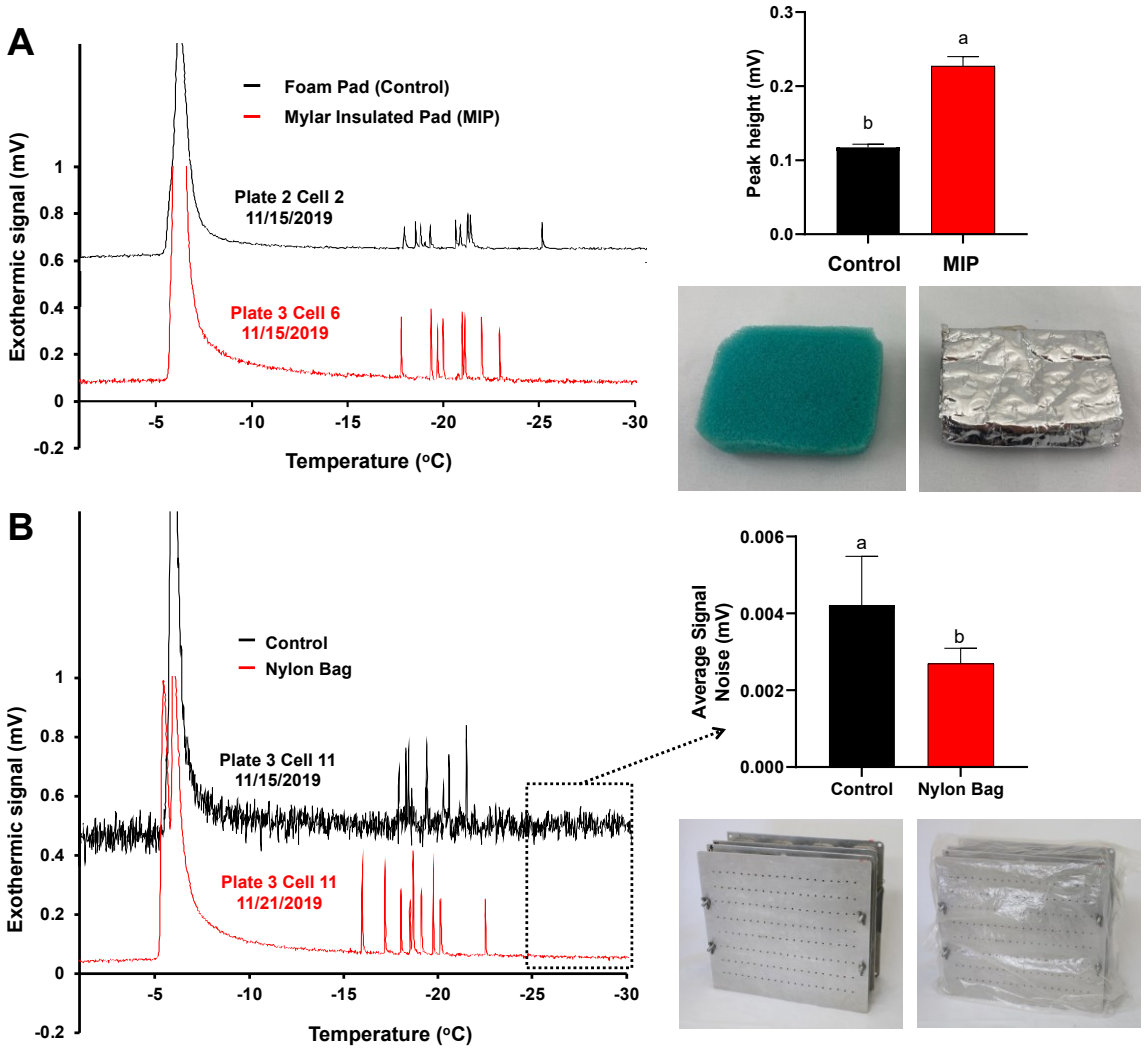

Figure 1.3 Experimental improvements to differential thermal analysis (DTA) signal amplitude and to the reduction of noise amplitude. A signal amplification study was conducted in which two different insulating materials were compared to determine whether the low temperature exotherm (LTE) signal generated from a thermoelectric module (TEM) could be improved. The standard 9 mm closed foam insulating pads (control) were compared to 9 mm of mylar insulation pads (MIP), to evaluate whether the increased thermal reflectivity of the MIP would increase the strength of the signal by reflecting radiating LTE heat of fusion back towards the TEM. Mean peak heights were compared using one-way ANOVA (P=0.05) (A). A signal noise reduction experiment was conducted to test the effect of covering the DTA assembly with a nylon bag on lowering the signal noise. Absolute fluctuations from the mean noise level were compared between adjacent DTA runs, with and without the nylon bag treatment. Mean absolute fluctuations per treatment followed by a different letter are statistically significant when analyzed using ANOVA (P=0.05) (B).

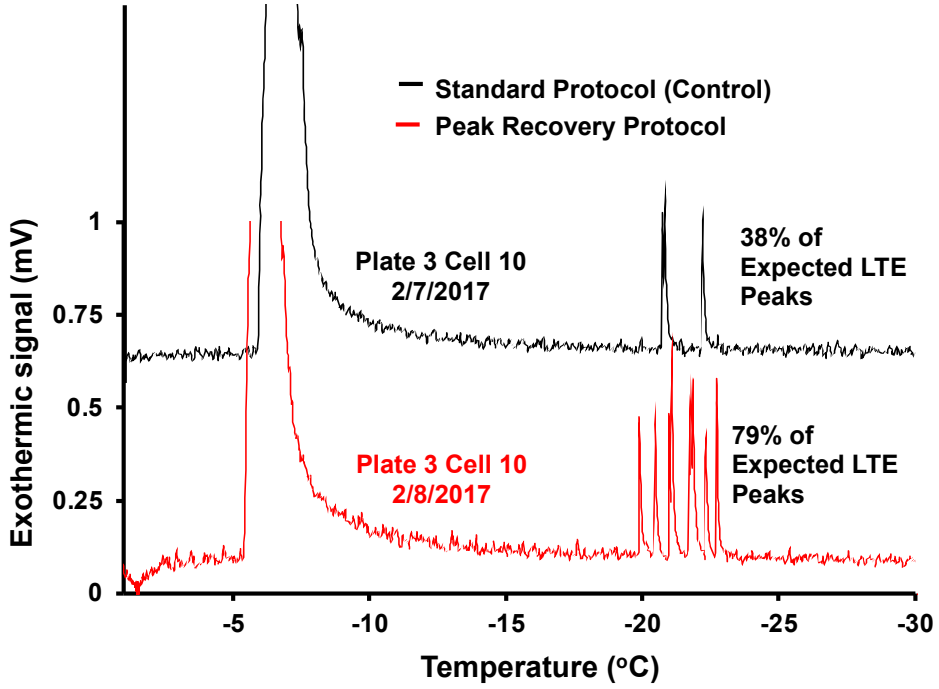

Figure 1.4 Experimental optimization of low temperature exotherm (LTE) signal recovery for ecodormant peach floral buds. An experiment to test an LTE signal recovery protocol was conducted to increase the span of the dormant season in which DTA could be reliably used to detect peach floral bud LTEs. Starting February 7, 2017, a dramatic decrease in the number of detectable LTE peaks was noticed. On February 8, 2017, the freezing chamber was programmed to first run for 12 hours at -2 °C prior to the regular DTA 4 °C · h^{-1} rate drop in order to increase the detectable number of LTE peaks. The total number of detected LTE peaks rose from 38% of expected peaks to 79% of expected peaks.

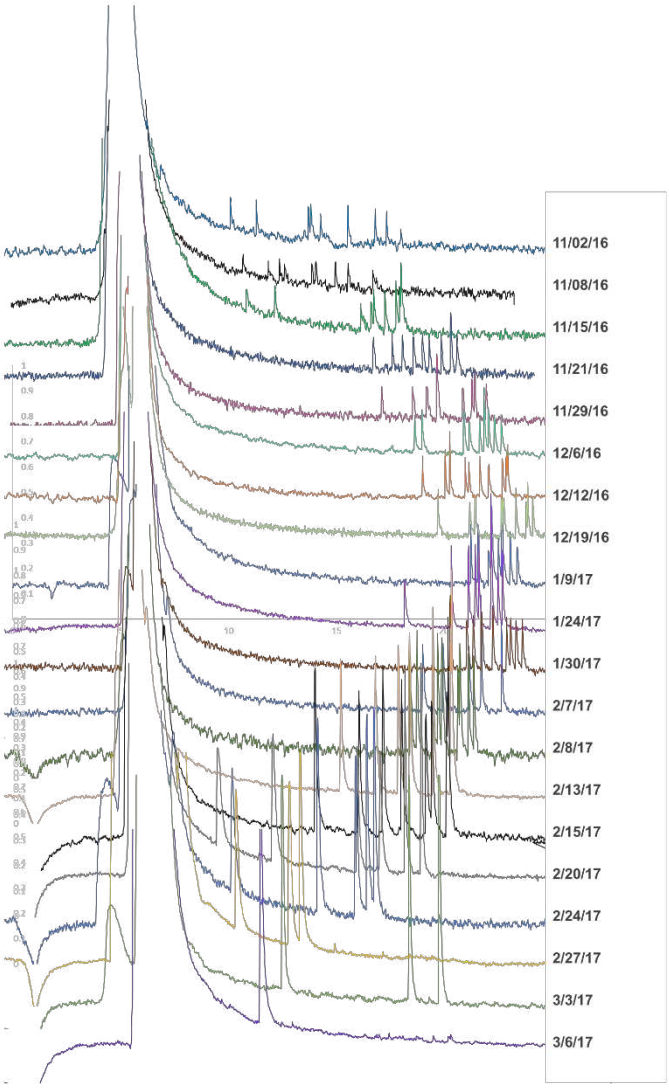

Figure 1.5 Large scale differential thermal analysis (DTA) from November 2, 2016 through March 6, 2017 shows clear trends of acclimation and deacclimation throughout the dormant period. The graphical representation of peach floral bud acclimation, maximum hardiness and deacclimation is exhibited through weekly LTE recordings from a single TEM cell per run that are vertically arrayed to illustrate the seasonal progression, while using the same scale for each different date in the array. Peak cold hardiness was observed January 9, 2016, which coincided with the coldest week of the year. As buds began to deacclimate and swell, low temperature exotherms (LTE) dramatically grew, as increased water content in floral primordia resulted in a larger exothermic energy release for each LTE. The y-axis refers to the millivoltage difference from a single TEM cell on March 6, 2017, while all other curves share the same scale.

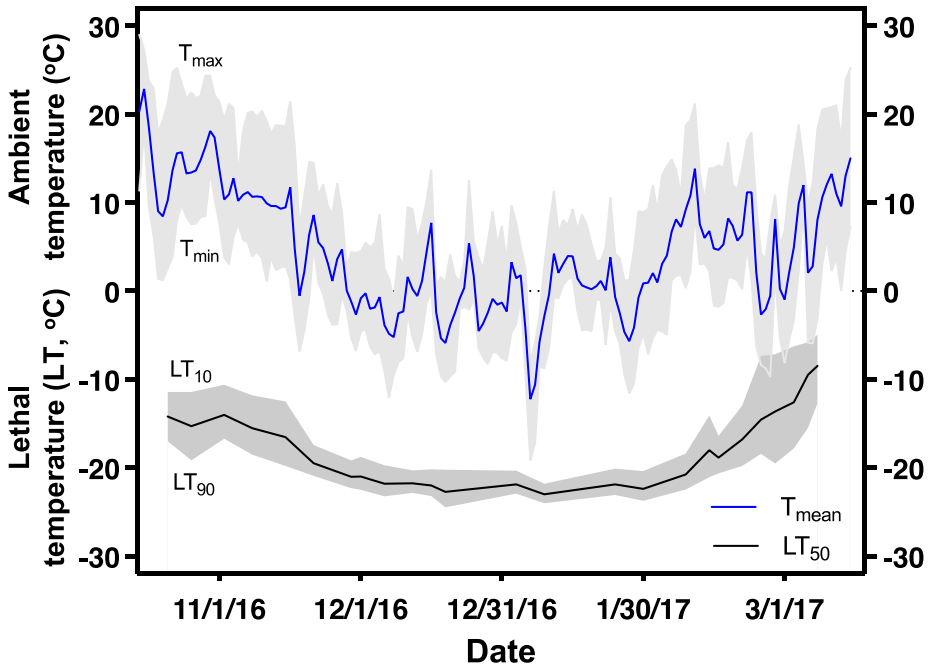

Figure 1.6 Seasonal patterns of temperature and cold hardiness, expressed as lethal temperature quantiles for 10, 50 and 90% flower bud loss (LT_{10}, LT_{50} and LT_{90}) of 'Redhaven' flower buds. Daily temperature data and observed lethal temperatures from the CSU's experimental orchard at WCRC-OM, Grand Junction, CO, were combined to show how despite general seasonal symmetry, extreme events result in low temperatures crossing lethal temperature thresholds in peach floral buds. As low temperatures generally dropped overall from November 2016 to early January 2017, cold hardiness followed the same trend. Rising temperatures from late January until March 2017 corresponded to a loss of cold hardiness as buds deacclimated towards the spring bloom period. In November 18, 2016 the first significant frost event reached -6.5 ºC and the observed cold hardiness in the following observations increased dramatically. Another significant frost event took place on January 7 2017, and this was also correlated with an increase in cold hardiness in the next observation. Three lethal cold events were seen on February 26, 2017 (-9.7 ºC), March 1, 2017 (-8.2 ºC), and March 7, 2017 (-5.9 ºC) which were below the observed lethal temperature threshold for 10% mortality. These events were used to validate observed DTA data with observed cumulative field damage (see **Table 1**) to show no significant difference between observed cumulative field damage (58% mortality) and expected cumulative damage from DTA data (55% mortality).

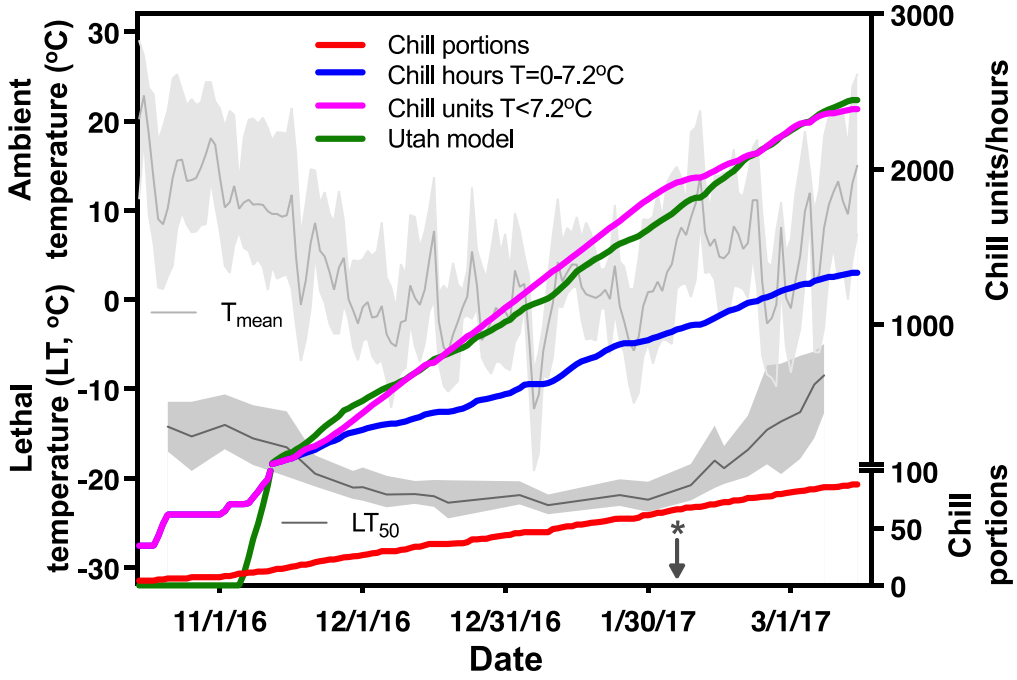

Figure 1.7 Chilling accumulation in combination with observed cold hardiness data, daily temperatures throughout the 2016-2017 dormant season. The relationship between cold hardiness and chill accumulation was observed. 868 chill hours (0-7.2 ºC), 56.4 dynamic chill portions, 1517 Utah model chill units, and 1658 chill hours (<7.2 ºC) were accumulated on January 24, 2017. DTA incrementally began losing the ability to detect LTE, once the first growing degree days (T_{base}= 7 ºC) were accumulated beyond this thermal-time point (indicated with asterisk). The loss of LTE may therefore be an indication that chilling satisfaction has been reached and buds are transitioning from an endodormant to an ecodormant state.

CHAPTER TWO

FACT SHEET: SPRING PEACH FLORAL BUD COLD HARDINESS: REEXAMINING CLASSIC PRE-BLOOM PHENOLOGY CRITICAL THRESHOLDS

2.1. Introduction

Cold damage on floral tissues represents the greatest threat to profitable yields for peach growers. Differential thermal analysis (DTA) can be used to accurately measure precise lethal temperatures of hundreds of peach floral buds during a relatively short process (Mills et al., 2006; Minas et al., 2020; Minas, 2023). While DTA reliably provides accurate data from post-leaf senescence through bud swell, DTA loses the capacity to detect lethal temperatures during deacclimation. As peach floral buds deacclimate following chilling satisfaction in the lead up to bloom time, cold hardiness is rapidly lost as the buds begin to rapidly change. Moisture content begins to rise as xylem connectivity is restored to the reproductive organs. It is also known that a multitude of metabolic changes are happening within the floral tissues, as dormancy is released and gradually exposing vulnerable female reproductive organs to freezing temperatures. Accurate knowledge of cold hardiness during these critical phenological stages will help growers more effectively protect their crops.

Pre-bloom floral buds being extremely vulnerable to damage is a well-established reality for peach growers worldwide. However, when previous studies have documented freezing thresholds across different phenological stages it was done with antiquated technology, and with a cultivar (‘Elberta’) which is no longer widely planted by Colorado and other peach growers around the world. This study tests cold hardiness of ‘Cresthaven’ and ‘Suncrest’ peach, two widely grown mid-season peach cultivars, across many stages of bud phenology.

Flower petal phenotype is often considered to be an indication of a lack of hardiness because of past experience with cultivars with large, showy petals, such as 'Suncrest,' leading many to believe they are less hardy than cultivars with small and non-showy petals such as 'Cresthaven' (**Figure 2.1)**. This characteristic has not been sufficiently compared to identify whether the difference in hardiness is real or perceived. Another characteristic commonly associated with hardiness is the place of origin in which a cultivar was bred. Cultivars coming from California are often considered more tender, whereas those originating in Michigan are considered more-hardy. Whether the difference in mid-winter hardiness is universally true, or more-likely to be true is an open question. Warmer region breeders often prioritize selection of cultivars with low chilling requirements in order to ensure a full and uniform bloom. 'Suncrest' requires around 550 chill hours (between 0 ^{o}C–7.2 ^{o}C), and 'Cresthaven' requires around 850 chill hours. Cultivars bred in cold locations are more likely to be selected by breeders if they develop a consistent track record of surviving cold events, so there is a selection mechanism which could be expected to lead to more cold hardy lineages of peach.

Affecting orchard temperatures through frost protection measures is energy intensive and has limited efficacy (Beyá-Marshall et al., 2019). While floral buds deacclimate, they quickly lose cold hardiness. Since grower profitability depends on the survival of floral buds, it is necessary to know the precise temperature at which floral buds are vulnerable to frost damage. Therefore, it is necessary to revisit classic studies of heritage cultivars to ensure each phenology stage of currently used cultivars are as cold hardy during deacclimation.

2.2. Materials and Methods

From March 18 to April 18, 2022, 25 samples of fruiting shoots (proleptic) were taken every 2-4 days from mature 'Suncrest' (9 yr. old) and 'Cresthaven' (10 yr. old) trees. Samples were taken

from a uniform height of ~1.5 m above ground level. The distal ends of shoots were removed, only leaving the primary fruit bearing part of each shoot, the basal 30 cm section. For each day, a phenology stage was ascribed to each cultivar. The phenology stage was the most advanced stage which described at least 40% of the buds in the sample for each cultivar. Fifteen floral buds per date were weighed, freeze dried, and re-weighed to determine the moisture content at each stage. Sample shoots were frozen within a programmable freezing chamber (Tenney Jr Test Chamber, Model TUJR 1.22 cu.ft., Thermal Product Solutions, New Columbia, PA, USA), being lowered to 4 sets of predetermined temperatures per date. Temperature within the chamber dropped at a rate of 4^0C per hour. Each predetermined target temperature was set to hold for 30 minutes, and one set of 5 shoots per cultivar were removed before dropping to the next targeted temperature. All shoots were left at room temperature and high relative humidity conditions for 24 hours, and then longitudinally sectioned with a razor blade. Survival was determined by the presence or absence of significant oxidative browning to pistil of each flower bud per target temperature. Percentage of dead buds were tallied for each individual temperature. Linear regression was used to determine the relationship between percent mortality and temperature. Slope and intercept were calculated through linear regression, and then used to calculate LT_{10}, LT_{50}, and LT_{90}.

2.3. Results and Discussion

Several surprising results came about through this study with regards to cold hardiness of buds of different cultivars and phenology stage (**Figure 2.2**). Critically, there was a great difference in the projected cold hardiness of 'Elberta' from classic literature, at bud stages 2-4 ("green calyx"- "pink tip"). The average LT_{50} of 'Suncrest' and 'Cresthaven' compared to the LT_{50} of 'Elberta,' across phenology stages, was 2.9 ^{o}C less hardy at Stage 2- "green calyx," 3.9 ^{o}C less hardy at Stage 3- "red calyx," and 1.7 ^{o}C less hardy at Stage 4- "pink tip." There was very little

difference between the two cultivars at equal bud stages, despite their apparent phenotypic differences. ‘Suncrest’ was less hardy overall however, since it reached Stage 3- “red calyx,” a tender stage two days earlier. Ultimately ‘Suncrest’ reached full bloom one day earlier (April 7, 2022) than ‘Cresthaven’ (April 8, 2022). There were almost perfect linear relationships between LT_{50}, and bud moisture content (R^2= 0.97 for ‘Suncrest’, and R^2= 0.98 for Cresthaven; **Figure 2.3**) and did not differ by cultivar. The relationship between phenology stage and moisture content was a nearly perfect logarithmic curve (R^2=0.98; **Figure 2.3**) and did not differ between cultivars.

These results reveal the value of testing classical assumptions, such as bud hardiness, developed in other locations with outdated cultivars, using locally specific research. The results also provide a new perspective on the perceived differences between attributes such as location of breeding program origin (CA vs. MI), flower petal size (large and showy vs. small and non-showy) and chilling requirement (550-850 chill hours, 0-7.2 ºC). While there was a difference between the two cultivars, the only real difference was a slight acceleration in bud phenology development in the ‘Suncrest.’ It is important to understand that this relationship will not necessarily hold true for every cultivar.

2.4. Conclusion

These results highlight that the differences between cultivars is more complicated than binary comparisons across several traits, and that low chill, large showy petals of CA bred peach cultivars are not implicitly far less cold hardy than their MI alternatives. The results suggest that cold hardiness differences between two phenologically different cultivars are more related to the bud stage of each cultivar (**Figure 2.4 and 2.5**). Also noteworthy is the relationship that moisture content has with both cold hardiness and phenology stage.

2.5. References:

Beyá-Marshall, V., Herrera, J., Santibáñez, F., Fichet, T., 2019. Microclimate modification under the effect of stationary and portable wind machines. Agric. For. Meteorol. 269–270, 351–363. https://doi.org/10.1016/j.agrformet.2019.01.042

Mills, Lynn J., Ferguson, J.C., Keller, M., 2006. Cold-hardiness evaluation of grapevine buds and cane tissues. Am. J. Enol. Vitic. 57, 194-200.

Minas, I.S., Sterle, D., 2020. Differential thermal analysis sheds light on the effect of environment and cultivar in peach floral bud cold hardiness. Acta Hortic. 1281, 385–391. https://doi.org/10.17660/ActaHortic.2020.1281.51

Minas, I. S. (2023, March 12). *Cold hardiness*. Pomology Ioannis S. Minas. Retrieved March 28, 2023, from https://agsci.colostate.edu/minas/tree-fruit-information/cold-hardiness/

2.6. Figures

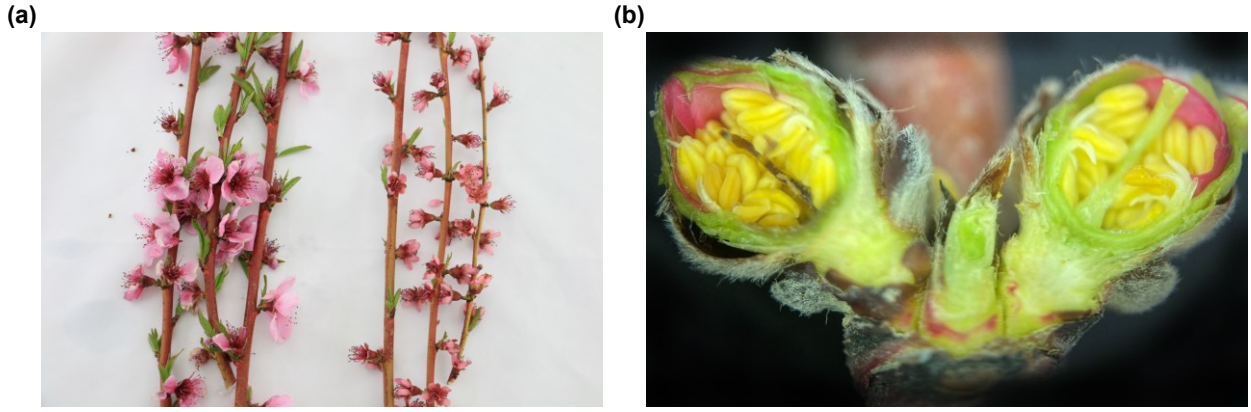

Figure 2.1. External and internal morphology of peach floral buds. (a) Samples of 1 ft long fruiting shoot sections during bloom, demonstrating stark differences in flower morphology. Three 'Suncrest' shoots are on the left and three 'Cresthaven' shoots are on the right. (b) Longitudinally sectioned buds of 'Suncrest' during stage 3-"Red Calyx". Showing live pistil within the right bud, and an oxidized pistil the left bud which would prevent pollination of these flowers. The viability of anthers and petals indicated by a lack of oxidative browning, indicates these tissues were more frost tolerant during this stage.

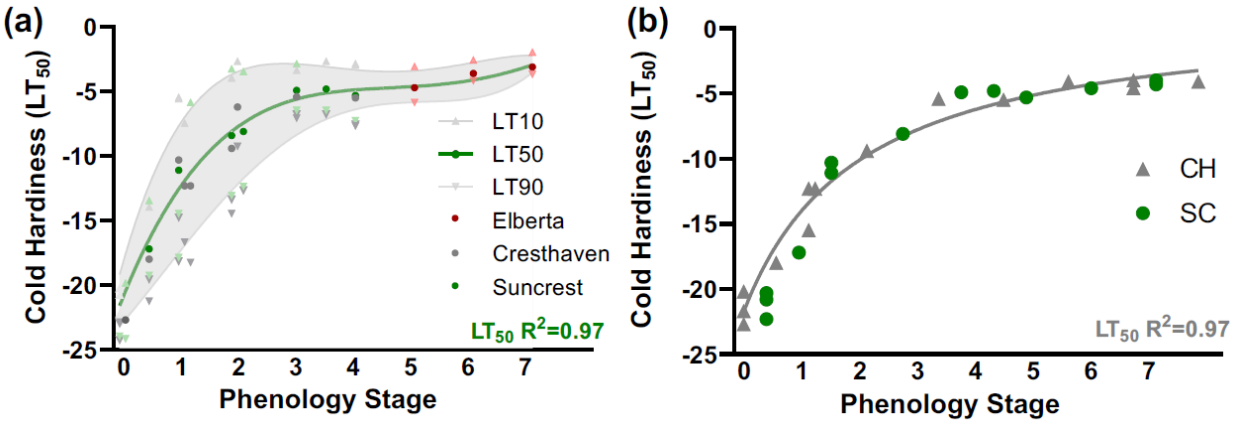

Figure 2.2. Relationship of cold hardiness with phenology stage of two different cultivars (a) Redeveloped lethal temperature thresholds for peach floral buds as determined by rigourous oxidative browning testing across seven phenological stages. (b) Lethal temperatures (LT_{50}) for 'Suncrest' and 'Cresthaven' peach floral buds along with a logarithmic regression curve highligting the relationship between developmental stage and LT_{50}.

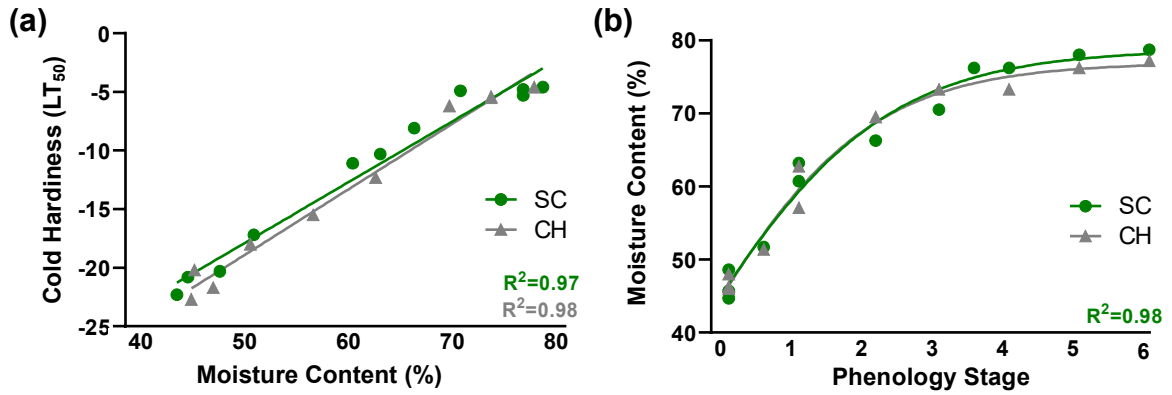

Figure 2.3. Relationships among cold hardiness, moisture content and developmental stage. (a) Linear regression showing that 97-98% of the variability in LT_{50} is explained by the moisture content of the floral bud, with no meaningful difference between the two cultivars. (b) Logarithmic non-linear regression showing that 98% of the variability in moisture content is explained by the developmental growth stage.

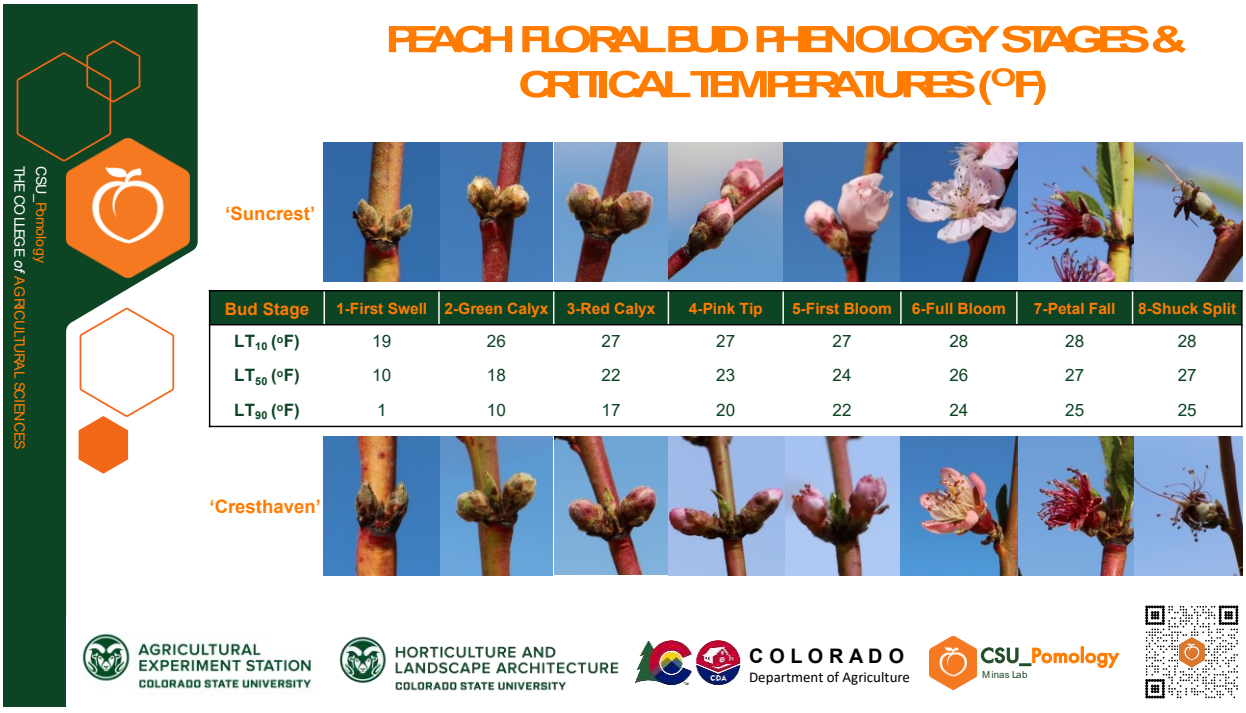

Figure 2.4. Visual phenology stage identification chart with critical temperature thresholds (ºF). Bud phenology stages of two morphologically different cultivars, displaying the difference in appearance of two common types of peach flowers. Lethal temperatures were measured every 2-4 days from March, 18-April 18, 2022.

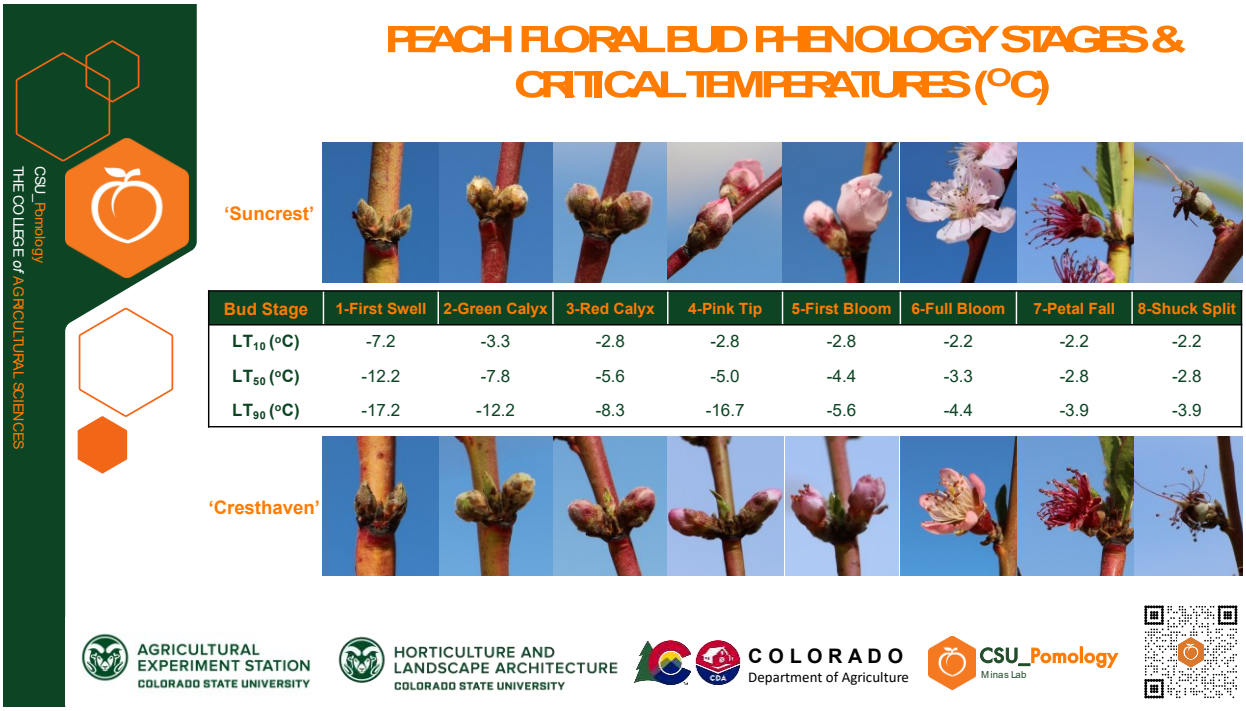

Bud Stage	1-First Swell	2-Green Calyx	3-Red Calyx	4-Pink Tip	5-First Bloom	6-Full Bloom	7-Petal Fall	8-Shuck Split
LT_{10} (°C)	-7.2	-3.3	-2.8	-2.8	-2.8	-2.2	-2.2	-2.2
LT_{50} (°C)	-12.2	-7.8	-5.6	-5.0	-4.4	-3.3	-2.8	-2.8
LT_{90} (°C)	-17.2	-12.2	-8.3	-16.7	-5.6	-4.4	-3.9	-3.9

Figure 2.5. Visual phenology stage identification chart with critical temperature thresholds (ºC). Bud phenology stages of two morphologically different cultivars, displaying the difference in appearance of two common types of peach flowers. Lethal temperatures were measured every 2-4 days from March, 18-April 18, 2022.

CHAPTER THREE

MODELING DORMANT PEACH FLORAL BUD COLD HARDINESS USING LARGE-SCALE THERMAL AND DYNAMIC WEATHER DATA

3.1. Introduction

Crop loss due to cold damage of floral tissues is a primary factor in determining the economic viability of the peach [*Prunus persica* (L.) Batsch] industry in many growing regions throughout North America and the world. Cold hardiness (H_c) is the extent to which a floral bud is able to supercool, in order to withstand sub-freezing temperatures. Novel climate conditions threaten to misalign the prevailing trends of H_c expression and cold weather events. This misalignment may result in more growing locations less reliably productive.

Predicting H_c is valuable for site selection, orchard management and frost protection decisions, especially when considering the future effects of climate change. However, predicting H_c is difficult since the floral buds acclimate or deacclimate differently depending on the growing climate or weather conditions, and the stage of dormancy. Endodormancy begins in autumn after leaf abscission and is the phase of dormancy during which growth inhibition of structures within the floral or vegetative bud is physiological rather than environmental. During endodormancy, growth is inhibited even if it is exposed to favorable for growth environmental stimuli (Lang et al., 1987). Environmental stimuli related to dormancy include: photoperiod length, light quality, and ambient temperature (Heide, 2008). After sufficient chilling units have been accumulated during endodormancy the dormant buds transition to ecodormancy which is governed by the entire plant's response to environmental conditions unfavorable for growth (Lang et al., 1987). Heat accumulation, hydration, availability of nutrients, and time are some factors associated with ecodormancy. It is broadly accepted that chilling and heat accumulation have a well-established

negative correlation; with more chilling, less heat is required for budbreak (Kovaleski et al., 2022). As ecodormancy progresses the buds will visibly swell and eventually bloom. These processes are genetically programmed and involve physiological changes that include carbohydrate composition, reactive oxygen species and antioxidant levels, phospholipid composition and hydric status which are not clearly understood yet (Erez et al., 1997; Li et al., 2009; Maurel, 2004; Viti et al., 2012; Yamane et al., 2011; Yu et al., 2020). Cold hardiness will generally increase during fall with cooling temperatures, until the endodormancy barrier (CST), a genotypically controlled chilling satisfaction threshold, is reached leading to ecodormancy (Ferguson et al., 2011). During ecodormancy, buds will begin to gradually lose H_c as thermal time above a threshold (T_{base}), measured in growing degree days (GDD), accumulates, until bloom when the H_c is at its least cold-hardy (Proebsting and Mills, 1978). Temperature impacts on bud dormancy and development are well documented, therefore the effects of a warming climate on these processes must be understood to forecast the sustainability of peach production worldwide.

Current H_c can be estimated by dissecting floral buds which have been previously exposed to freezing temperatures to look for oxidative browning (OB) caused by phenolic compounds oxidation. These compounds are released from damaged cell membranes by the formation of ice crystals during the freezing event and their presence on the floral primordia is associated with the loss of reproductive viability (Proebsting and Mills, 1978; Szalay et al., 2010). Differential thermal analysis (DTA) is a technique which can be used to detect exotherms caused by freezing floral primordia in dormant peach floral buds (Quamme, 1986; 1991). An updated DTA methodology uses thermal electric modules (TEM) to detect temperature gradient changes from the latent heat of fusion released when supercooled water from floral primordia (e.g., ovaries) freezes (Mills et al., 2006; Minas and Sterle, 2020). High temperature exotherms indicate the non-lethal freezing of

extracellular water, while low temperature exotherms indicate the lethal freezing of the floral primordia. These methods are necessary for H_c determination, as bud external appearance does not change during the dormant period, until the weeks immediately preceding bloom, when the buds can be visually assessed for H_c given their phenological stage (Szalay et al., 2018). Large numbers of lethal temperatures (LT) can be observed relatively quickly using DTA, that help obtain precise estimations of seasonal changes in H_c, (Ferguson et al., 2011; Mills et al., 2006). Lethal exotherms in peach can be detected during the endodormancy period which begins in autumn and continues until early stages of ecodormancy and before bud swell. Prior to endodormancy and post bud swell OB can be used to determine peach H_c thresholds (Minas and Sterle, 2020). Large data sets using both methods can provide important reference values to be used in conjunction with meteorological data to build accurate H_c predictive regression models which can inform frost control management leading to increased profitability.

Cold hardiness prediction models have been developed for various crops such as: winter wheat, grape, cherry, and other deciduous tree species (Anisko et al., 1994; Ferguson et al., 2014; Salazar-Gutiérrez and Chaves-Cordoba, 2020). Anisko et al. (1994) used a stepwise model-building procedure to arrive at regression models that predict hardiness given different measures of thermal time, photoperiod, and aggregated temperatures from clusters of time in the recent meteorological history. Dynamic models have also been developed which build upon previously predicted hardiness values by calculating how much the buds may have acclimated or de-acclimated relative to a previously estimated H_c based on the recent conditions (Ferguson et al., 2014; Salazar-Gutiérrez and Chaves-Cordoba, 2020). These methods all have validity and may elucidate some differences among cultivars, including acclimation and de-acclimation rates at different stages, and CST. As such, each model should be judged by how well it fulfills the desired

outcomes, whether this be identifying phenotypic differences among genotypes or accurate prediction for practical orchard management purposes.

To be economically viable, an orchardist needs to consider the frequency and severity of the frost risk that occurs in a prospective orchard location. Estimating the frequency and severity of frost risk is complicated when considering the effect climate change will have in that same location. Crop load management is considered during dormant pruning, and H_c prediction is useful for informed pruning and optimum crop load decisions. In addition to site selection, and crop load management, knowing the precise H_c of floral buds from fall to spring is critical to frost protection decision-making during freezing events, typically using wind machines and overhead sprinkler irrigation. Efficacy of wind machines depends on the amount of difference of inversion temperature, and proximity to wind machines. It has been demonstrated that stationary wind machines can increase the average temperature of a 4-ha area by 1.5 ºC, and portable wind machines increased temperatures to this extent for less than 1 ha (Beyά-Marshall et al., 2019). Lu et al. (2018) demonstrated a 2.8 ºC increase in temperatures using overhead sprinkler irrigation, however, irrigation water is often not available for use by growers in winter months in colder regions. Economic crop loss can increase dramatically with small decreases in temperature. Given the small temperature increase the wind machine can provide, being able to accurately predict H_c is critical to optimize their usage. Since H_c is prone to change throughout the season, and responds differently to changes in the environment depending on the stage of dormancy as well as proximity to bloom time, it is necessary to develop low-error H_c estimation methods for sufficient frost protection decision-making.

The accuracy of previously created dynamic models for other deciduous tree fruit species may be insufficient to instruct management decisions for peach. Some models have resulted in

error terms that are often greater than the T increase which could be expected using a wind machine at spacings of 1 machine per 4 ha (Ferguson et al., 2011; Ferguson et al., 2014; Beyά-Marshall et al., 2019; Salazar-Gutiérrez and Chaves-Cordoba, 2020). The large error terms reduce the practical use of the predictive model since the error is large compared to the benefit provided by standard frost management activity. For multiple regression models which predict accurately on different data sets, parsimonious variable selection is necessary. Overparameterization on the other hand can lead to extremely highly fit data but will not predict accurately outside of the model training dataset. Thus, for model accuracy an optimized number of variables per model should be included, and validated against independent datasets, while using variables that are not overly colinear.

Multiple regression models could easily be linked to automated data collection systems, once trained and validated with a dataset within a growing region. In this study, regression models were created to estimate peach H_c during the different stages of dormancy (endodormancy and ecodormancy), at different thresholds of crop survival (LT_{10}, LT_{50}, and LT_{90}) using between 4,690 and 6,880 observations per cultivar across four years as a robust dataset for model training and validation. The primary goal was to develop H_c prediction models with minimized root mean squared error of prediction (RMSEP), to the extent that H_c models could reliably be used for practical orchard management purposes (RMSEP<1.5 ^{o}C), while making parsimonious models and avoiding overparameterization.

3.2. Materials and Methods

3.2.1. Plant material and data collection location

Four peach cultivars ‘Redhaven’ (RH), ‘Cresthaven’ (CH), ‘Sierra Rich’ (SR), and ‘Suncrest’ (SC) that were grown under standard commercial practices in the experimental orchard of Colorado State University (CSU) at Western Colorado Research Center at Orchard Mesa (WCRC-OM) in

Grand Junction, CO were used for peach H_c assessment over a period of four dormant seasons from 2016/2017 to 2019/2020, except for SC which was assessed only for three dormant seasons (2017/2018-2019/2020). Cold hardiness samples were taken from 8-11-year-old trees per cultivar that were grafted on Lovell rootstock, except 'Suncrest' that was 3-6 years old and grafted on 'Viking' rootstock. Experimental trees were managed and irrigated according to local commercial production practices and trained in an open-center training system (open-vase for CH and RH and perpendicular-V for SR and SC) and were planted at a spacing of 4 × 4.5 m (for CH and RH) or 1.5 × 4.5 m (for SR and SC) and a planting density of 510 (for CH and RH) or 1195 (for SR and SC) trees per ha.

3.2.2 Peach lethal temperature estimation

Peach floral bud H_c was measured over twenty sampling dates in each of four dormant seasons from 2016 to 2020 across peach cultivars except of SC that was assessed only for three dormant seasons (2017-2020). The data collection period for each year was from October (post leaf senescence) through March. For each sampling date, 70-80 floral buds were collected from one year old proleptic shoots of moderate vigor that were growing at uniform height of 1.2-1.8 m across 15 experimental trees per cultivar. Overall, the number of floral buds assessed for RH, CH, SR, and SC were: 6,090, 6,880, 6,800, and 4,690 respectively. Differential thermal analysis (DTA) was used until low temperature exotherms (LTEs) ceased to be seen, which corresponded to bud swell, typically in mid-February (Minas and Sterle, 2020). In the time between bud-swell and full bloom, dissection and oxidative browning was used to identify lethal temperatures (Proebsting and Mills, 1978).

Peach floral bud H_c was evaluated using DTA following the methods developed in Minas Lab and described previously (Mills et al., 2006; Minas and Sterle, 2020; Tanner et al., 2021).

Pairs of floral buds were detached from the one-year-old fruiting shoots and wrapped in aluminum foil, then placed within cells containing thermoelectric modules (TEMs). Temperature was dropped at a rate of 4 ºC to -36 ºC, in a programmable freezing chamber (Tenney Jr Test Chamber, Model TUJR 1.22 cu.ft., Thermal Product Solutions, New Columbia, PA, USA). Lethal floral bud temperatures were detected by thermocouples and exothermic reactions related to freezing events were detected by TEMs as a voltage response using a multimeter data acquisition system (Keithley 2700, Tektronix, Beaverton, OR). Using the accompanying software (Tektronix, Keithley ExceLinx™ for Instruments, Beaverton, OR) the data were input to a spreadsheet for analysis in Microsoft Excel. Parametric survival analysis was performed using JMP Pro 15.0 (SAS Institute, Inc., Cary, NC). For each sampling date, cumulative low temperature exotherm to lethal temperature (LT) data were fit to a model using a logistic function to best fit the nonlinear data (Minas and Sterle, 2020). Using the Weibull regression model, LTs where 10%, 50%, and 90% (LT_{10}, LT_{50}, and LT_{90}) of buds that were considered dead were estimated for each sampling date throughout the four dormant season-span.

Between bud-swell (February 10^{th}-20^{th} depending on the year) and bloom, floral bud hardiness was measured using the oxidative browning method. Five replicated sets of six 15 cm sections of peach fruiting wood for each cultivar were bundled separately. One replicated bundle were saved as an untreated control to establish preexisting oxidative damage present at the time of sampling. The remaining four replicates were placed within the Tenney Jr. freezing chamber, programmed to drop from 4 ºC at a rate of 4 ºC per hour. Bundles were removed from the freezing chamber at four different target temperatures at 2.5 ºC intervals. Cold temperature treated bundles were kept at high relative humidity at 21 ºC for 24 hours to allow for oxidative browning to take effect in the case of freeze damaged tissue. After 24 hours buds were manually sectioned with a

razor blade and pistil tissues were examined for lethal damage, as indicated by brown tissue. The percentage of total buds that were fatally damaged was tallied for each cultivar across each temperature treatment. Linear regression was used to find a line of best fit, and the equation of this line was used to calculate lethal temperature quantiles (LT_{10}, LT_{50}, LT_{90}).

3.2.3 Weather data collection and calculation

Hourly temperature and weather data were collected by CoAgMET, a CSU's statewide network of weather stations, and specifically by the weather station located at WCRC-OM (https://coagmet.colostate.edu). Weather station temperature and humidity sensor model HMP45C (Vaisala, Helsinki, Finland) height was set at 1.5 meters. Average temperatures were considered the average of the maximum and minimum daily temperature values (**Figure 3.1**). Accumulated chilling hours were counted on an hourly basis, by summing the number of hours between 0-7 ºC each day after October 1st of each dormant season (Bonhomme et al., 2010; Luedeling et al., 2013; Okie and Blackburn, 2011; Weinberger, 1950). Chill portions were calculated using the dynamic chill portions calculating tool (Erez et al., 1989). Growing degree days (GDD) were calculated on a daily basis, by summing the number of degrees above the threshold temperature (T_{base}) the average temperature was for each day (Grossman and DeJong, 1995). Three different T_{base} were used: 0 ºC, 5 ºC and 7 ºC, with literature citing T_{base} from 4-10 ºC (Linsley-Noakes and Allan, 1994; Whiting et al., 2015), expanding the covered range to include T_{base} 0 ºC. Addition of T_{base} 0 ºC was deemed necessary after a survey of the literature revealed the representation of mostly warmer growing climates. The hypothesis was that phenologic development may take place at cooler temperatures, but may not be well captured in studies where less time was spent at these lower temperatures, contrary to this study. Aggregated temperature variables $T_{mean,1\text{-}4}$, $T_{max,1\text{-}4}$, and $T_{min,1\text{-}4}$ were calculated daily, representing the average of the previous four days' mean, maximum

and minimum temperatures, respectively. In addition, mean, maximum and minimum temperatures the day of sampling as well as 1, 2, 3, 4-, 5-, 6-, and 7-days prior were also used as potential model building variables.

3.2.4 Selecting predictor variables

To select strong predictor variables for LT prediction model training, Pearson correlation matrices were created using the weather variables previously mentioned. These weather variables (**Figure 3.2 and 3.3**) and the LT quantiles of the four peach cultivars from three to four consecutive dormant seasons (**Figure 3.1**) were analyzed using correlation matrices. Many of the regressor variables had Pearson correlation coefficients which indicated strong positive ($r>0.8$) or negative correlations ($r<-0.8$) with H_c and with other regressor variables. Inclusion of highly correlated variables in the models without justification, was minimized to reduce the risk of overparameterization. This was done by checking correlation of variables within the same models for high correlation in the correlation matrices.

As expected, various temperature measurements had significant correlation to LT, including each individual maximum, minimum and mean temperatures from the seven days prior to a H_c measurement. The correlation was reduced beyond four days. In order to capture recent temperature fluctuations without compromising model parsimony, the average of the previous four days' mean, maximum and minimum temperatures were identified as terms to be considered for inclusion in model creation. These temperature parameters ($T_{mean,1\text{-}4}$, $T_{max,1\text{-}4,}$ and $T_{min,1\text{-}4}$) represent the recent temperatures to which the buds were exhibiting a short-term response (recent climate history). Additionally, the day of the year (days post October 1st), photoperiod length, chill portions, chilling hours, and accumulated growing degree day counts with base thresholds of 7 ^{o}C, 5 ^{o}C, and 0 ^{o}C were considered, given their individual correlations with H_c. These variables capture

aspects of seasonal progression in terms of time and experienced thermal time, which locate the H_c of the floral buds within a plausible range of values for different points in the season. Cultivar was used as a categorical variable in model selection to compare differences in intercept (baseline H_c) or slope (change in H_c in relation to a unit change in the predictor) among the cultivars.

3.2.5 Cold hardiness (H_c) model development and validation

Endodormancy and ecodormancy H_c prediction models were developed using an exploratory model building approach. Stepwise model selection was used to find combinations of variables which formed accurate models across different portions of the dormant season. Model validation was done independently following two methods: 1) by segregating each date (between 2016 and 2020) in which a cultivar was sampled into a training set and a validation set at a ratio of 2:1 and 2) by using six sampling dates coming from a distinct dormant season (2021) from the ones used to create the models. Effort was made to include as few terms into each model as possible for a resulting parsimonious model. Interaction terms were added only if highly significant (P<0.005) and if deemed physiologically justifiable. LT_{50} was used as the primary dependent variable in both endodormancy and ecodormancy models to select significant predictor variables. Subsequently, the selected variables were then used to train models for LT_{10} and LT_{90} as well, which were validated in the same fashion as LT_{50}.

Endodormancy and ecodormancy model variables were selected separately using an estimated date where sufficient chilling was accumulated to meet the chilling satisfaction threshold (CST) and enter ecodormancy. January 15th was used as a preliminary stand-in date at which point the data previous to this date were used for preliminary endodormancy H_c model selection, and the data after this date were used for preliminary ecodormancy H_c model selection. Endodormancy and corresponding ecodormancy models were made using training observations on either side of

a number of test CST in commonly suggested ranges of chill accumulation requirements from 600-900 chilling hours or 45-60 dynamic chilling portions (**Table 3.1**; Fadon et al., 2020). The models made for each test CST were validated using the randomly selected validation data set. Validation data were then compared to determine the strongest pairings of endodormancy and ecodormancy models by comparing coefficients of determination (R^2), root mean square errors of prediction (RMSEP), and Akaike information criteria (AIC) (**Table 3.1**).

3.3. Results and Discussion

3.3.1 Genotypic variation in peach floral bud H_c is highest during acclimation and deacclimation

Seasonal mean temperatures reached a low point in early January during the dormant seasons between 2016-2020, with observed peach floral bud cold hardiness (H_c) in terms of LT_{50} following the same seasonal trend (**Figure 3.1**). Generally, the variation among cultivars on a given date was highest in autumn and spring when the acclimation and deacclimation processes were in effect, while variation was lowest from mid-November until through January. Unsurprisingly, this time frame also correlates with both the shortest photoperiod (December 21st) and the coldest time of year. Low mid-winter temperatures contributed to stability in the LT_{50} values that further underscore the slower physiological activity of the floral tissues during the endodormancy phase that protects them from unfavorable environmental conditions. Average maximum H_c (LT_{50}) for the different cultivars was: -23.5 ºC for RH, -24.5 ºC for CH, -22.2 ºC for SR, and -24.0 ºC for SC. Consistently, SR was least hardy for most dates each season, while CH and RH had the lowest LT_{50} on average. 'Suncrest' while being of average H_c most dates, exhibited a responsiveness to cold temperatures which allowed it to gain hardiness following relatively extreme cold events that lasted more than two days. 'Suncrest' therefore had the hardiest maximum annual LTs as response to extreme freezing events. The lowest LT_{50} at -25.9 ºC for SC recorded

on January 2, 2019 as a response to being the fifth day of a 10-day long cold event with continuous sub-freezing temperatures (when 711 chilling hours, and 52.7 chilling portions had been accumulated). These differences in traits among cultivars contributed to the decision to include cultivar as an indicator variable within the floral bud H_c models. The propensity of the buds to gain hardiness after multiple days of constantly sub-freezing temperatures, provided insight which led to the testing of aggregated temperatures from multiple recent days for correlations with H_c to be used as predictor variables in model creation.

3.3.2. Selection of predictor variables of recent climate history and seasonal progression for floral bud H_c models calibration

Consideration of the Pearson correlation matrices revealed many potential continuous variables for selection in the endodormancy (**Figure 3.2**) and ecodormancy (**Figure 3.3**) models. There was high correlation between LTs and the individual average daily temperature values for the four days before DTA analysis, with correlation coefficients (r) usually greater than 0.75 between the various temperature variables and measured LT_{50} (r=0.68-0.84 during endodormacy). The temperature values were then combined into separate averages of mean, minimum (min), and maximum (max) temperatures for that previous four-day period span and these were used as continuous variables in the models. Correlations between LT_{10} and predictor variables tended to be weaker than with LT_{50} and LT_{90}. For example, during endodormancy correlation coefficients between $T_{mean,1\text{-}4}$ and LT_{10}, LT_{50} and LT_{90} were 0.77, 0.84 and 0.84, respectively. Aggregating the temperature data into four-day aggregates moderated volatility in model prediction to more accurately portray the gradual changes in H_c observed and reflect the impact of recent climate history in model performance. The predictor with the largest correlation with LT_{50} in endodormancy was $T_{min,1\text{-}4}$ (r=0.84), while the predictor with the largest correlation with LT_{50} in

ecodormancy was GDD_0 (r=0.89). Photoperiod (PP) length in hours was the seasonal progression variable selected for the endodormancy H_c models. While PP had a relatively low correlation with LT_{50} (r=0.63) if used as an individual predictor, its inclusion contextualized the effect $T_{min,1\text{-}4}$ could have at different parts of the dormant season. Days post October 1st (DPO) was one of the seasonal progression variables selected for the ecodormancy H_c models (r=0.72), and had a similar contextualizing role with $T_{max,1\text{-}4}$ (r=0.73) for the H_c prediction post CST.

This approach in the analysis revealed that in western Colorado, perhaps because of the relatively cold winters, GDD_0 was more highly related to ecodormancy H_c than 4 ºC and 7 ºC. This is a novel finding to tree fruit phenology as it is often modelled using warmer base temperature (T_{base}) for GDD calculation between 4 ºC to 10 ºC (Linsley-Noakes and Allan, 1994; Grossman and DeJong, 1995; Valentini et al., 2002; Zavalloni et al., 2006; Mounzer et al., 2008; Whiting et al., 2015; Chaves et al., 2017; Blanco et al., 2020). This is likely because more time is spent in the temperature range between 0-5 ºC than in most fruit growing regions, allowing the model to capture deacclimation that is occurring at lower temperatures, challenging the assumption that an insignificant amount of deacclimation occurs in this lower temperature range. Across all four years there was an average difference of 51 days between the first accumulation of GDD_0 and GDD_7, meaning there were on average 51 days of potential deacclimation effect being lost by using different temperature thresholds in GDD accumulation under ambient conditions. This result indicates that this colder location allows for greater insight into cold temperature chilling and heat accumulation and also highlights the need for research that is specific to a particular region and climate.

3.3.3. CST is critical for accurate endo- and ecodormancy H_c models creation

Physiologically, the CST is generally understood to be a point in dormancy which is reached after crossing a certain chill-time threshold (chilling satisfaction), where endodormancy ends and ecodormancy begins and the floral bud will begin relying upon heat-time accumulation before flowering (Lang et al., 1987). Given that different stimuli are driving deacclimation during ecodormancy, it is necessary for optimum H_c prediction at these distinct phases of dormancy, to establish a point at which the CST is reached. Differences were seen between the predictive accuracy of certain variables on either side of the CST. An example is the high correlation of the $T_{mean,1-4}$ to observed LT_{50} during endodormancy (r=0.84) while in ecodormancy this drops (r=0.67). This illustrates the importance of different stimuli depending on the stage of dormancy, and the need to create separate H_c models for endodormancy and ecodormancy phases.

Different chilling accumulation models are used in various growing regions to most accurately capture the true CST of various plant tissues. For our purposes we used both the dynamic chill portions model (Erez et al., 1989) and the more traditional chilling hours models either "<7.2 ºC" or the "0-7.2 ºC" variations (Weinberger, 1950). Our approach was to use an assumed place-holder CST of January 15th in order to obtain our best modelling variables, before using the two sets of modelling variables (one each for endodormancy and ecodormancy) to compare the prediction efficacy on either side of given CST (**Table 3.1**). Because of the different chilling models and thresholds different combinations of model training data were used for each side of each threshold. It is clear from **Table 3.1** that the model validation data for both the dynamic chill portions model, and the chilling hours model resulted in highly accurate predictive models based on our data. The chilling hours model had consistently lower error terms in our validation process and was therefore selected as the chilling model of choice. In general, endodormancy

models had lower coefficient of determination (R^2) values but also lower RMSEP values than did ecodormancy models.

There was insufficient statistical evidence to definitively select a CST from R^2 or RMSEP alone, because differences in model prediction varied so little across these options (**Table 3.1**). 700 chilling hours was used because it was estimated to be the midpoint among the four cultivars. Published information on experimentally derived CST for various peach cultivars is limited. 'Redhaven' with 850-870 chilling units (0-7.2 ºC) (Fadon et al., 2020), 'Cresthaven' with 950 chilling hours (<7 ºC), 'Suncrest' is cited as having a CST of 650 chilling hours (<7 ºC), and consistent CST for 'Sierra Rich' was unavailable (Okie, 1998). Much of the published data uses the "<7 ºC" model which includes time spent at sub-freezing temperatures. However, in a cold growing climate such as Colorado it is necessary to remove sub-freezing temperatures to more accurately represent the effect of chilling. Therefore, the CST of 950 and 650 for 'Cresthaven' and 'Suncrest' are considerably lower when using the "0-7.2 ºC" model. Taking the available information on the CST of various cultivars into account, we estimated that the range of the four cultivars was approximately 550-850 chilling hours (0-7.2 ºC) with a mean of 700.

Across the four years the CST of 700 chilling units (0-7 ºC) was reached on Jan. 14, Dec. 22, Dec. 26, and Dec. 6 for 2017, 2018, 2019 and 2020 respectively. It has been established that the lower the chilling accumulation the higher the heat requirements and vice versa for flowering date determination in perennial woody plants (Kovaleski, 2022). Our data show the higher chill cultivars (CH and RH) and lower chill cultivars (SR and SC) bloom simultaneously in the high chilling conditions of the Intermountain region. This bloom synchrony in Western Colorado growing conditions among high and low chill cultivars is also contrary to the perception that high chill cultivars bloom significantly later. However, this observation confirms previous reports

stating that chilling requirements are a highly heritable component of flowering date determination and have much stronger effects than heat requirements in *Prunus* species where a high genotype × environment interaction is the case (Castède et al., 2014).

3.3.4. Predictive model parameter selection

Model selection revealed a trend in types of variables which proved effective in H_c prediction on either side of the CST (**Table 3.2**). Both the endodormancy and ecodormancy models included several common elements: cultivar as a categorical term, recent meteorological history variables ($T_{min,1\text{-}4}$, and $T_{max,1\text{-}4}$, respectively), a variable representing seasonal progression (photoperiod, and DPO, GDD_0, respectively), and an interaction for the relationship between temperature or experienced thermal time and time ($T_{min,1\text{-}4} \times$ PP and $GDD_0 \times$ DPO, respectively). This pattern in variable selection could be effective because seasonal progression variables (PP, DPO, GDD_0) define a range of potential H_c values which are likely to occur at different parts of the dormant season, while recent history of temperature values ($T_{min,1\text{-}4}$ and $T_{max,1\text{-}4}$) and cultivar differences adjust based off recent conditions to predict H_c at each stage of the dormant season. Thus, the seasonal progression variables buffer the impact of temperature on H_c. The use of this combination of variables may provide a similar balance to dynamic models which add or subtract predicted to a running H_c tally (Ferguson et al., 2011) through a multiple regressive approach. The endodormancy H_c model includes PP, $T_{min,1\text{-}4}$ and the interaction between PP and $T_{min,1\text{-}4}$ as continuous variables. It cannot be concluded from this study that PP is driving H_c acclimation in fall as it may simply be correlated to other factors such as chill accumulation or time. Minimum temperature is more likely to be directly related to H_c in endodormancy because it accounts for much of the daily fluctuations in H_c which cannot be accounted for by PP alone.

The ecodormancy H_c model includes DPO, GDD_0, $T_{max,1\text{-}4}$, and an interaction term between DPO × GDD_0. This aligns with previous work indicating that heat and time are both highly correlated to the phenological advancement of floral buds in deciduous trees (Chaves et al., 2017; Mounzer et al., 2008; Whiting et al., 2015). However, these results also indicate that there may be a synergistic effect between the intensity of the temperature ($T_{max,1\text{-}4}$), and how quickly GDD_0 are accumulated (DPO × GDD_0). GDD_0 alone incorporates both time and temperature, but the model was greatly improved by including these two terms. Essentially this means that decreases in H_c are not simply governed by a linear relationship with time spent at a temperature range. This indicates that dramatic increases in the temperature, and the quickness at which GDD_0 are accumulated multiply the effect of thermal time. This observation may underscore that time and temperature both have a more polynomial effect on H_c since across the four predictor variables some form of either time information and temperature information are captured within all continuous variables included in each of the models described herein.

3.3.5. H_c model validation with independent data sets reveals high predictive accuracy

Across all four cultivars, the independent validation using 1/3 of the data that were not used for training the H_c models across the four dormant seasons showed an average RMSEP of 0.82 ºC for endodormancy, and 1.08 ºC for ecodormancy. Such model validation performance across all four cultivars for both ecodormancy and endodormancy indicates that our initial focus for H_c prediction with low error (RMSEP<1.5 ºC) can be achieved with large-scale data sets and simple construction with efficient dynamic parameter combination (**Figure 3.4**). This is the most accurate floral bud H_c predictive suite of models known from the literature. Low error predictions were observed from late-October to mid-March, using this suite of models (**Figure 3.5**). The suite of models was constructed parsimoniously, meaning the models were not overparameterized, which

can lead to results which are overly biased to the training dataset. Parsimonious model construction should allow for the maximum amount of flexibility in prediction given the data which went into the model. Accurate prediction across multivarious locations and conditions is expected to decrease with increasing deviations from the training data. Further data could be added to the training and validation datasets and possibly increase the predictability across different growing regions. Such models are expected to provide useful information for peach orchard management purposes and for the development of frost control decision-support systems to be linked with local weather stations and provide real time H_c predictions.

As seen in previous works, the periods immediately preceding bud break, and as floral buds first enter endodormancy in late summer, become more difficult to predict H_c using modelling approaches (**Figure 3.5**). This is in part because supercooling of floral primordia allows DTA LTEs detection later in fall as well as due to the fact that DTA loses the ability to detect LTEs during bud-swell later in spring (Minas and Sterle, 2020). The period before bloom is easily predicted using oxidative browning or visual phenology-based assessments as demonstrated in Szalay et al. (2018), therefore during this period it is not practical to predict using models. On average, in the location of the present study from 2018-2020, visible bud-swell began around March 21st at which point H_c is estimable using OB coupled with artificial freezing or visually using critical phenology temperature charts. Using the created thermal and dynamic weather predictive models and previous phenology-based H_c estimates, we can now accurately estimate H_c through the duration of the dormant period. This is an invaluable resource when managing orchard frost protection, pruning practices, planning labor needs, and evaluating and/or projecting suitability of land for future peach production in regions with cold dormant seasons in a changing environment.

For endodormancy and ecodormancy, H_c model prediction was most accurate for LT_{50} and LT_{90} (**Figure 3.4**). Since models were trained using LT_{50} data, this indicates that LT_{90} is more closely related to LT_{50} than is LT_{10} for peach H_c. Given the majority of floral buds are thinned for optimized fruit quality for commercial markets, we consider survival of roughly 10% of floral buds (the percent of survival at LT_{90}) to represent the economic threshold below which represents a significant crop loss. As a result, the high accuracy of LT_{50} and LT_{90} is more relevant to growers for crop protection than an LT_{10}.

A comparison of the seasonal observed and predicted H_c values shows a high level of accuracy, and responsivity of the models to cold events (**Figure 3.5**). Observed H_c dropped significantly in October and November of 2019 following a severe early frost. The model accurately predicted the dramatic change in H_c as a response to the fall freezing events in 2019. In early January of 2019, the model again predicted a large shift in cold hardiness for a 10-day period (Dec., 29 2018- Jan., 7, 2019) where temperatures did not raise above 0 ^{o}C. It was hypothesized that the different models may predict H_c even more accurately during this period because there are far more observations in mid-winter in comparison to early Autumn. This was true for all cultivars with the exception of 'Suncrest' which shows a unique ability to become hardier after prolonged sub-freezing temperatures. The H_c increase in January 2019 shows that although CH and RH are considered higher chill cultivars, while SR and SC are considered lower chill cultivars, LT_{50} for each cultivar decreased despite accumulating greater than 700 chilling hours. The reliable prediction of this H_c change indicates that these predictive models using large-scale dynamic weather and thermal data are able to accurately predict drops in H_c whether in endodormancy or ecodormancy. Relatively few data have been collected in October and March as DTA does not detect LTEs during these times of acclimation and deacclimation. Future work will focus on

acquiring more data from October and March in order to increase predictability during these months of transition in the different phases of dormancy and growth.

In addition to the H_c models validation approach described above a distinct independent validation was performed during the dormant season of 2021/2022. This extra step in H_c models' validation provides valuable insights on the prediction performance of the created endodormancy and ecodormancy models using LT and weather data from a season that was not previously included in the training of the models. In summary H_c prediction for LT_{50} across the six time points that were selected during the 2021/2022 dormant season highlights the validity of the model creation approach followed in the present study (**Figure 3.6**). Peach floral bud LT_{50} in 2021/2022 dormant season was predicted with high accuracy as indicated by the high coefficient of determination (R^2=0.81-0.93) and the low error (RMSEP=0.54-0.98 ^oC) across the four cultivars modeled. H_c models exhibited equally robust performance for RH, CH and SR with SC performance being more volatile. It is worth highlighting that SC models were created with three dormant seasons of data (2017-2020) whereas the other three cultivars were build using data coming from four dormant seasons (2016-2020). Also, SR validation of H_c prediction accuracy during the 2021/2022 dormant season was performed on five time points instead of six that was the case for the rest of the cultivars due to the loss of significant amount LTEs during the DTA assessment in late February of 2022. As mentioned above H_c model prediction was most accurate for LT_{50} and LT_{90} and more volatile for LT_{10} (**Figure 3.6**).

The prediction performance of H_c models across the four cultivars during an independent dormant season highlights the responsiveness of the created models to extreme weather changes and rapid decreases in temperature across the different phases of dormancy. This performance indicates that these predictive models using large-scale dynamic weather and thermal data are

robust enough to accurately predict the effect of rapid whether changes on H_c during endodormancy or ecodormancy. Future large-scale LT data collection from this and other locations is expected to enhance the sensitivity of the present models by including more erratic dormant seasons with unusually warm or cold periods. However, the performance of the models to the specific weather conditions of a different dormant season, indicates that these models may contain requisite adaptability to also forecast H_c responses to climate change.

3.4. Conclusion

Making accurate predictions of H_c is key to appropriate decision making for cold damage mitigation as well as understanding fruit tree adaptation to future climates. Yet, accurate predictions of H_c remain a major challenge mainly due to poor understanding of dormancy and lack of large-scale data acquisition approaches. Our primary goal was as to use our large dataset comprising the measurement of lethal temperatures from over 24,000 floral buds, each linked with specific weather data across four years, to create models able to accurately predict H_c (RMSEP<1.5 ^{o}C) during both endodormancy and ecodormancy in four separate cultivars.

This work demonstrates that through combined large-scale data, physiological observations, and exploratory statistical analysis, it is possible to create simple multiple linear regression models to predict H_c. This work builds upon previous valuable cold hardiness modelling to develop region specific models with sufficient accuracy to aid in orchard management decision making. All data used in the models can be easily linked to automatic data collection systems, to predict the various outcomes using multiple linear regression models. Historical data can also be used to evaluate prospective growing sites by comparing past climate data with predicted H_c or future hypothetical seasons following different climate change scenarios.

The level of accuracy shown by the independent validation demonstrates the high predictive power of the models (endodormancy, ecodormancy). To our knowledge the models presented herein are the most accurate cold hardiness (H_c) prediction models ever reported for tree fruit. We propose that this suite of models can be used in conjunction to estimate H_c, to a high level of accuracy from the time floral buds are nominally entering dormancy (October 1st in our case), until bud swell, at which point H_c is easily estimated given visual phenological evaluation. This work identifies aggregate values of minimum and maximum temperatures four days prior to a H_c measurement as being strongly correlated to H_c throughout the dormant season. Variables capturing the effect of seasonal progression such as DPO and photoperiod were also highly correlated to H_c throughout the season. Our approach also revealed that an assumption of equal CST across these four cultivars resulted in highly accurate H_c predictions in the study location, which was unexpected because of the wide range of previously estimated chill requirements among these cultivars.

This suite of models can be loaded to online weather databases which are populated by automated weather sensors. These tools will provide growers with an accurate estimate of the hardiness on an ongoing basis, aiding in frost protection decision activities in a changing environment. In addition, accurate weather-based prediction of H_c can help characterize future implications in peach production related to increased risk for cold damage as a result of peach tree exposure to future projected changes of climate and increased frequencies of weather extremes.

3.5. References

Aniśko T., Lindstrom O.M., Hoogenboom G. 1994. Development of a cold hardiness model for deciduous woody plants. Physiologia Plantarum 91, 375-382.

Beyá-Marshall V., Herrera J., Santibáñez F., Fichet T. 2019. Microclimate modification under the effect of stationary and portable wind machines. Agricultural and Forest Meteorology 269, 351-363.

Blanco V., Blaya-Ros P.J., Torres-Sánchez R., Domingo R. 2020. Influence of regulated deficit irrigation and environmental conditions on reproductive response of sweet cherry trees. Plants 9(01), 94.

Castède S., Campoy J.A., García J.Q., Le Dantec L., Lafargue M., Barreneche T., Wenden B., Dirlewanger E. 2014. Genetic determinism of phenological traits highly affected by climate change in Prunus avium: Flowering date dissected into chilling and heat requirements. New Phytol. 202, 703–715.

Chaves B., Salazar M.R., Schmidt T., Dasgupta N., Hoogenboom G. 2017. Modeling apple bloom phenology. In X International Symposium on Modelling in Fruit Research and Orchard Management 1160, 201-206.

Erez A., Fishman S., Linsley-Noakes G.C., Allan P. 1989. The dynamic model for rest completion in peach buds. In II International Symposium on Computer Modelling in Fruit Research and Orchard Management 276, 165-174.

Erez A., Wang S.Y., Faust, M. 1997. Lipids in peach buds during dormancy, a possible involvement in dormancy control. Advances in Horticultural Science 11, 128-132.

Fadón, E., Herrera, S., Guerrero, B.I., Guerra, M.E., Rodrigo, J., 2020. Chilling and heat requirements of temperate stone fruit trees (*Prunus* sp.). Agronomy 10, 409. doi10.3390/agronomy10030409

Ferguson J.C., Tarara J.M., Mills L.J., Grove G.G., Keller M. 2011. Dynamic thermal time model of cold hardiness for dormant grapevine buds. Annals of Botany 107, 389-396.

Ferguson J.C., Moyer M.M., Mills L.J., Hoogenboom G., Keller M. 2014. Modeling dormant bud cold hardiness and budbreak in twenty-three *Vitis* genotypes reveals variation by region of origin. American Journal of Enology and Viticulture 65, 59-71.

Grossman Y., DeJong T.M. 1995. Maximum fruit growth potential following resource limitation during peach growth. Ann. Bot. 75, 561–567.

Heide O.M. 2008. Interaction of photoperiod and temperature in the control of growth and dormancy of *Prunus* species. Scientia Horticulturae 115, 309-314.

Kovaleski A.P. 2022. Woody species do not differ in dormancy progression: Differences in time to budbreak due to forcing and cold hardiness. PNAS 119, e2112250119.

Lang G.A., Early J., Martin G.C., Darnell R.L. 1987. Endo-, para-, and ecodormancy: physiological terminology and classification for dormancy research. Journal of the American Society of Horticultural Science 22, 371-377.

Li Z., Reighard G.L., Abbott A.G., Bielenberg D.G.. 2009. Dormancy-associated MADS genes from the EVG locus of peach [*Prunus persica* (L.) Batsch] have distinct seasonal and photoperiodic expression patterns. Journal of Experimental Botany 60, 3521-3530.

Linsley-Noakes, G. C., & Allan, P. (1994). Comparison of two models for the prediction of rest completion in peaches. *Scientia Horticulturae*, *59*(2), 107-113.

Lu Y., Hu Y., Zhao C., Snyder R.L. 2018. Modification of water application rates and intermittent control for sprinkler frost protection. Transactions of the American Society of Agricultural and Biological Engineers (ASABE) 61, 1277-1285.

Maurel K., Sakr S., Gerbe F., Guilliot A., Bonhomme M., Rageau R., Pétel G. 2004. Sorbitol uptake is regulated by glucose through the hexokinase pathway in vegetative peach-tree buds. Journal of Experimental Botany 55, 879-888.

Mills L.J., Ferguson J.C., Keller, M.. 2006. Cold-hardiness evaluation of grapevine buds and cane tissues. American Journal of Enology and Viticulture 57, 194-200.

Minas I.S., Sterle D. G. 2020. Differential thermal analysis sheds light on the effect of environment and cultivar in peach floral bud cold hardiness. In XXX International Horticultural Congress IHC2018: International Symposium on Cultivars, Rootstocks and Management Systems of Deciduous Fruit and Fruit Tree Behaviour in Dynamic Environments, Acta Horticulturae 1281, 385-392.

Mounzer O.H., Conejero W., Nicolás E., Abrisqueta I., Garcia-Orellana Y.V., Tapia L.M., Vera J., Abrisqueta J.M., del Carmen Ruiz-Sánchez M. 2008. Growth pattern and phenological stages of early-maturing peach trees under a Mediterranean climate. Journal of the American Society of Horticultural Science 43, 1813-1818.

Okie W.R. 1998. Handbook of peach and nectarine varieties: performance in the southeastern united states and index of sames (No. 714). US Department of Agriculture, Agricultural Research Service.

Proebsting E.L., Mills H.H. 1978. Low temperature resistance of developing flower buds of six deciduous fruit species. Journal of the American Society of Horticultural Science 103, 192-198

Salazar-Gutiérrez M.R., Chaves B., Anothai J., Whiting M., Hoogenboom G. 2014. Variation in cold hardiness of sweet cherry flower buds through different phenological stages. Scientia Horticulturae 172, 161-167.

Salazar-Gutierrez M.R., Chaves-Cordoba B. 2020. Modeling approach for cold hardiness estimation on cherries. Agricultural and Forest Meteorology 287, 107946.

Sterle, D. G., & Minas, I. S. (2022). Exploration of environmental variables for peach floral bud cold hardiness prediction in western Colorado. In *X International Peach Symposium 1352* (pp. 285-290).

Szalay L., Timon B., Németh S., Papp J., Tóth M. 2010. Hardening and dehardening of peach flower buds. Journal of the American Society of Horticultural Science 45, 761-765.

Szalay L., Gyökös I.G., Békefi Z. 2018. Cold hardiness of peach flowers at different phenological stages. Horticultural Science 45, 119-124.

Tanner J.D., Chen K.Y., Jenderek M.M., Wallner SJ, Minas IS. 2021. Determining the effect of pretreatments on freeze resistance and survival of cryopreserved temperate fruit tree dormant buds. Cryobiology 101, 87-94.

Valentini N., Me G., Spanna F., Lovisetto M. 2002. Chilling and heat requirement in apricot and peach varieties. In XXVI International Horticultural Congress: Key Processes in the Growth and Cropping of Deciduous Fruit and Nut Trees, Acta Horticulturae 636, 199-203.

Weinberger J.H. 1950. Chilling requirements of peach varieties. In Proceedings of American Society for Horticultural Science 56, 122-128.

Whiting M.D., Salazar M.R., Hoogenboom G. 2015. Development of bloom phenology models for tree fruits. In IX International Symposium on Modelling in Fruit Research and Orchard Management, Acta Horticulturae 1068, 107-112.

Viti R., Bartolini S., Zanol G.C. 2010. Biological changes and active oxygen-scavenging enzymes activities in apricot (*Prunus armeniaca* L.) flower buds during dormancy transitions. In XXVIII International Horticultural Congress on Science and Horticulture for People (IHC2010): International Symposium on the Challenge for a Sustainable Production, Protection and Consumption of Mediterranean Fruits and Nuts, Acta Horticulturae 940, 331-339.

Yamane H., Tao R., Ooka T., Jotatsu H., Sasaki R., Yonemori K. 2011. Comparative analyses of dormancy-associated MADS-box genes, PpDAM5 and PpDAM6, in low-and high-chill peaches (*Prunus persica* L.). Journal of the Japanese Society for Horticultural Science 80, 276-283.

Yu J., Conrad A.O., Decroocq V., Zhebentyayeva T., Williams D.E., Bennett D., Staton M.E. 2020. Distinctive gene expression patterns define endodormancy to ecodormancy transition in apricot and peach. Frontiers in Plant Science 11, 180.

Zavalloni C., Andresen J.A., Flore J.A.. 2006. Phenological models of flower bud stages and fruit growth of montmorency' sour cherry based on growing degree-day accumulation. Journal of the American Society for Horticultural Science 131, 601-607.

3.6. Tables

Table 3.1 Selection of chilling satisfaction threshold (CST). Statistical comparisons of model performances of various LT_{50} prediction models trained and validated using data before and after various levels of chill accumulation. For each chilling satisfaction threshold value tested, both an endodormancy model and an ecodormancy model corresponding to the same amount of chill accumulation was built. The various model pairings were evaluated by comparing the coefficients of determination (R^2), root mean square errors of prediction (RMSEP), and the Akaike information criterion (AIC). Based on an evaluation of all three CST 700 chilling hours (CH) was selected as the best performing CST for the collection of cultivars of the present study.

		Endodormancy LT_{50} Model				**Ecodormancy LT_{50} Model**			
Chill Model	Tested CST	R^2	RMSEP	Valid. (n)	AIC	R^2	RMSEP	Valid. (n)	AIC
Dynamic Chill Portions (CP)	45	0.87	0.84	38	274.1	0.91	1.06	73	392.4
	50	0.88	0.83	53	300.9	0.89	1.06	58	371.9
	55	0.88	0.85	58	335.0	0.91	1.09	53	339.6
	60	0.88	0.85	60	374.5	0.91	1.11	51	310.4
Chilling Hours 0-7 ºC (CH)	600	0.85	0.94	31	221.3	0.90	1.10	80	433.0
	700	0.86	0.85	41	239.2	0.91	1.07	70	419.4
	800	0.87	0.85	49	293.6	0.92	1.07	62	377.0
	900	0.87	0.83	55	354.9	0.92	1.10	56	326.1

Table 3.2. Cold hardiness (H_c) models description. Model parameters and intercepts for the selected LT_{50} models of endodormancy and ecodormancy, built from cold hardiness data from four peach cultivars: 'Redhaven', 'Cresthaven', 'Sierra Rich' and 'Suncrest', for a period of four dormant seasons 2016-2020. Endodormancy and ecodormancy delineated by the chilling satisfaction threshold (CST) the point at which 700 chilling hours was accumulated. PP, photoperiod; $T_{min,1-4}$, minimum temperature for the last 4 days; DPO, days post October 1st; GGD_0, growing degree days using 0 ºC as the base temperature; $T_{max,1-4}$, max T for the last 4 days.

Endodormancy LT_{50} model					
Cultivar	**Intercept**	**PP**	**$T_{min, 1-4}$**	**(PP-9.95 × ($T_{min,1-4}$+2.45)**	
'Redhaven'	-27.85	0.81	0.25	0.23	
'Cresthaven'	-27.98				
'Sierra Rich'	-26.48				
'Suncrest'	-27.88				
Ecodormancy LT_{50} model					
Cultivar	**Intercept**	**DPO**	**GDD_0**	**$T_{max, 1-4}$**	**(DPO-131.88) × (GDD_0-75.76)**
'Redhaven'	-30.13	0.055	0.023	0.17	0.00058
'Cresthaven'	-30.97				
'Sierra Rich'	-29.05				
'Suncrest'	-30.30				

3.7. Figures

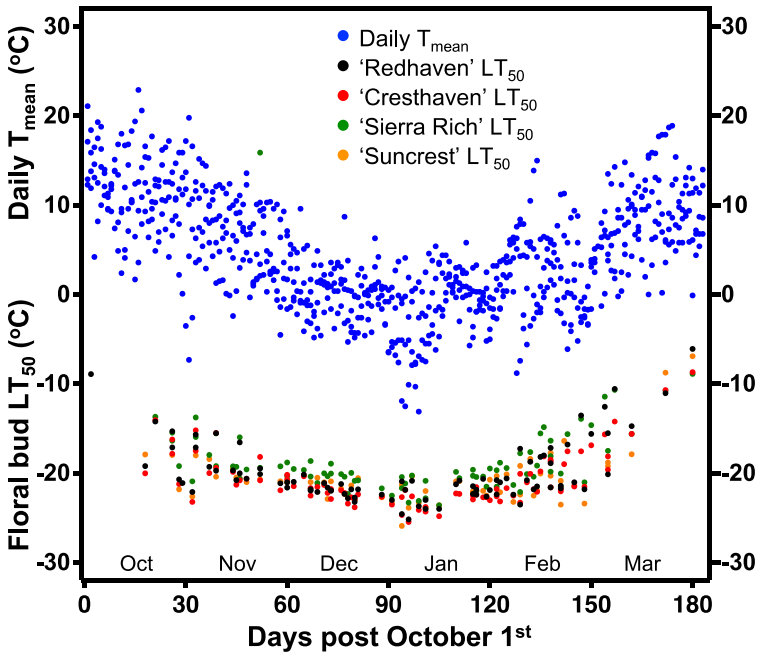

Figure 3.1. Temperature and LT_{50} data used for cold hardiness (H_c) modeling. Daily mean air temperature and observed cold hardiness (expressed as LT_{50}), as determined by differential thermal analysis (DTA), of four peach cultivars ('Redhaven', 'Cresthaven', 'Sierra Rich' and 'Suncrest') grown at CSU's experimental orchard at WCRC-OM, Grand Junction, CO, for a period of four dormant seasons (2016-2020).

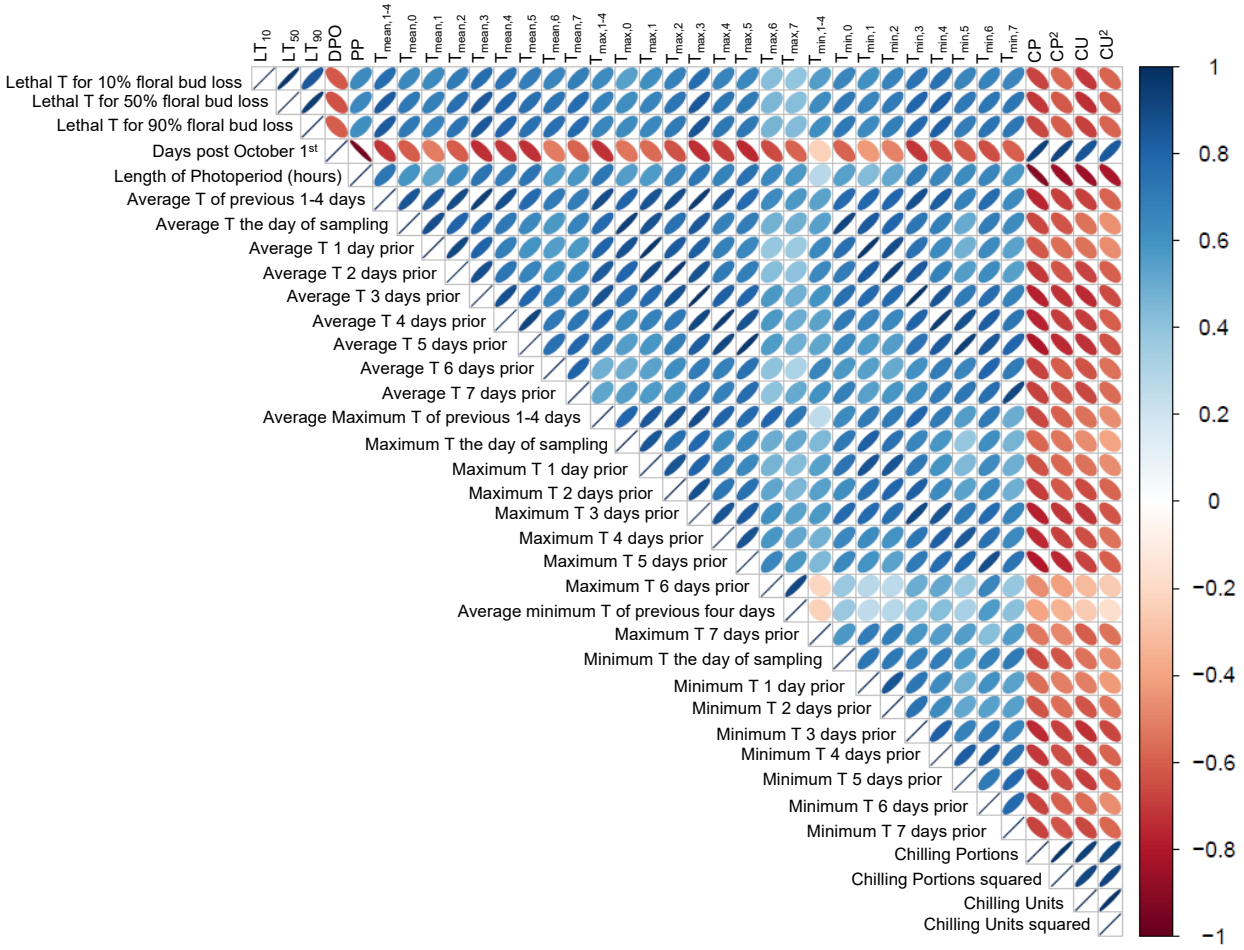

Figure 3.2. Correlations among various variables which were investigated as potential cold hardiness (H_c) predictive variables of four peach cultivars for the endodormancy period (<700 chilling hours). Cultivars studied for four dormant seasons (2016-2020) include: 'Redhaven', 'Cresthaven', 'Sierra Rich' and 'Suncrest'. Data collected from the CSU's experimental orchard at WCRC-OM, Grand Junction, CO, include temperature values for various periods of time prior to H_c measurement, photoperiod length, chill accumulation (expressed as chill portions, chilling hours, chilling portions squared, and chilling hours squared) and the number of days past October 1st.

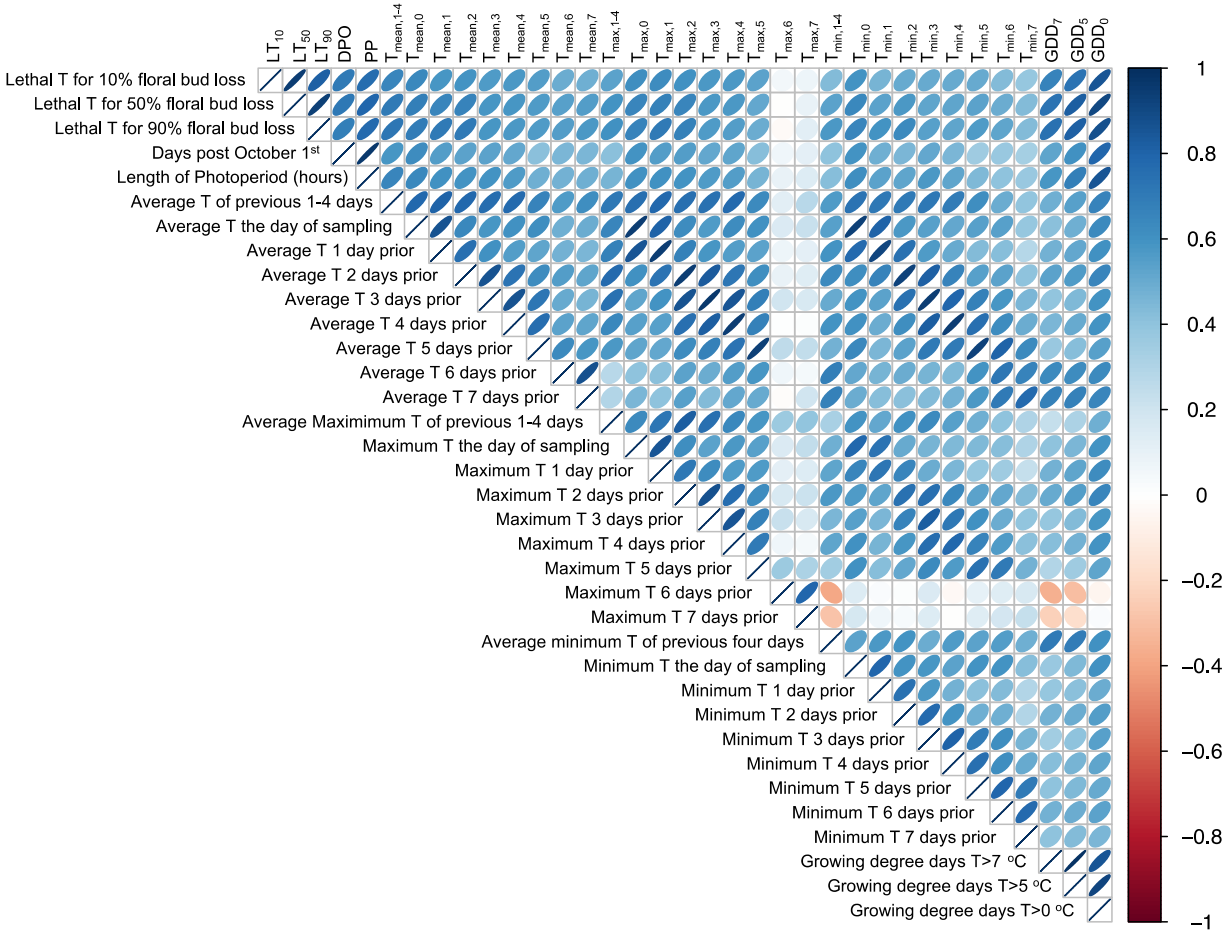

Figure 3.3. Correlations among various variables which were investigated as potential cold hardiness (H_c) predictive variables of four peach cultivars for the ecodormancy period (>700 chilling hours). Cultivars studied for four dormant seasons (2016-2020) include: 'Redhaven', 'Cresthaven', 'Sierra Rich' and 'Suncrest'. Data collected from the CSU's experimental orchard at WCRC-OM, Grand Junction, CO, include temperature values for various periods of time prior to H_C measurement, photoperiod length, growing degree day accumulation with base threshold temperatures of 7 °C, 5 °C, and 0 °C, and the number of days past October 1st.

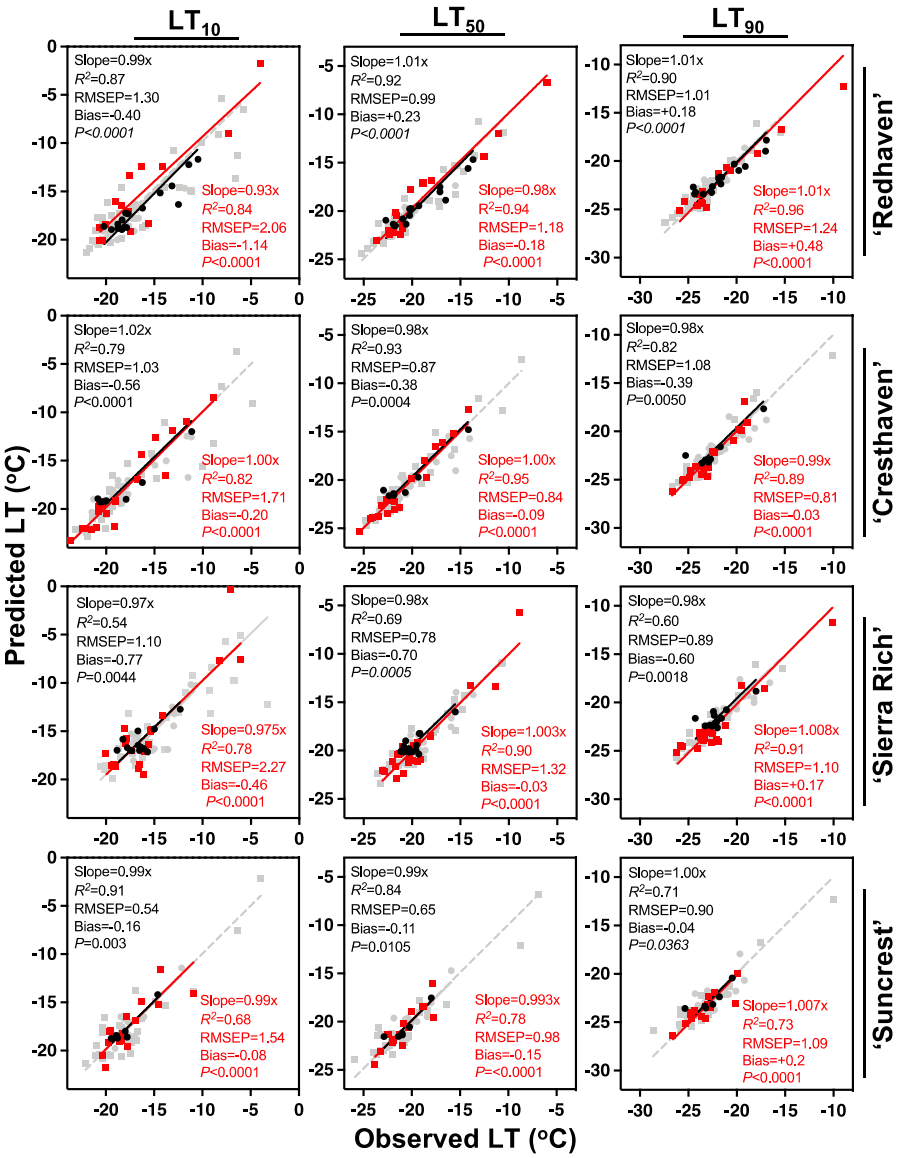

Figure 3.4. Validation of peach floral bud cold hardiness (H_c) prediction models' performance. Comparison between endodormancy (black dots and lines) and ecodormancy (red squares and lines) model predictions and measurements of bud H_c (as determined by DTA and expressed as LT_{50}) for 'Redhaven', 'Cresthaven', 'Sierra Rich' and 'Suncrest', for the dormant seasons (October 1st - March 31st) of from 2016-2020. Slope, coefficient of determination (R^2), bias, significance, and root mean square error of prediction (RMSEP (°C)), were calculated using validation data sets which were independent of model training data sets (grey dots/squares and lines). Data shown in black represent endodormancy H_c validation data, red is ecodormancy H_c validation data and grey is both endodormancy (dots and solid lines) and ecodormancy (squares and breaking lines) H_c training data.

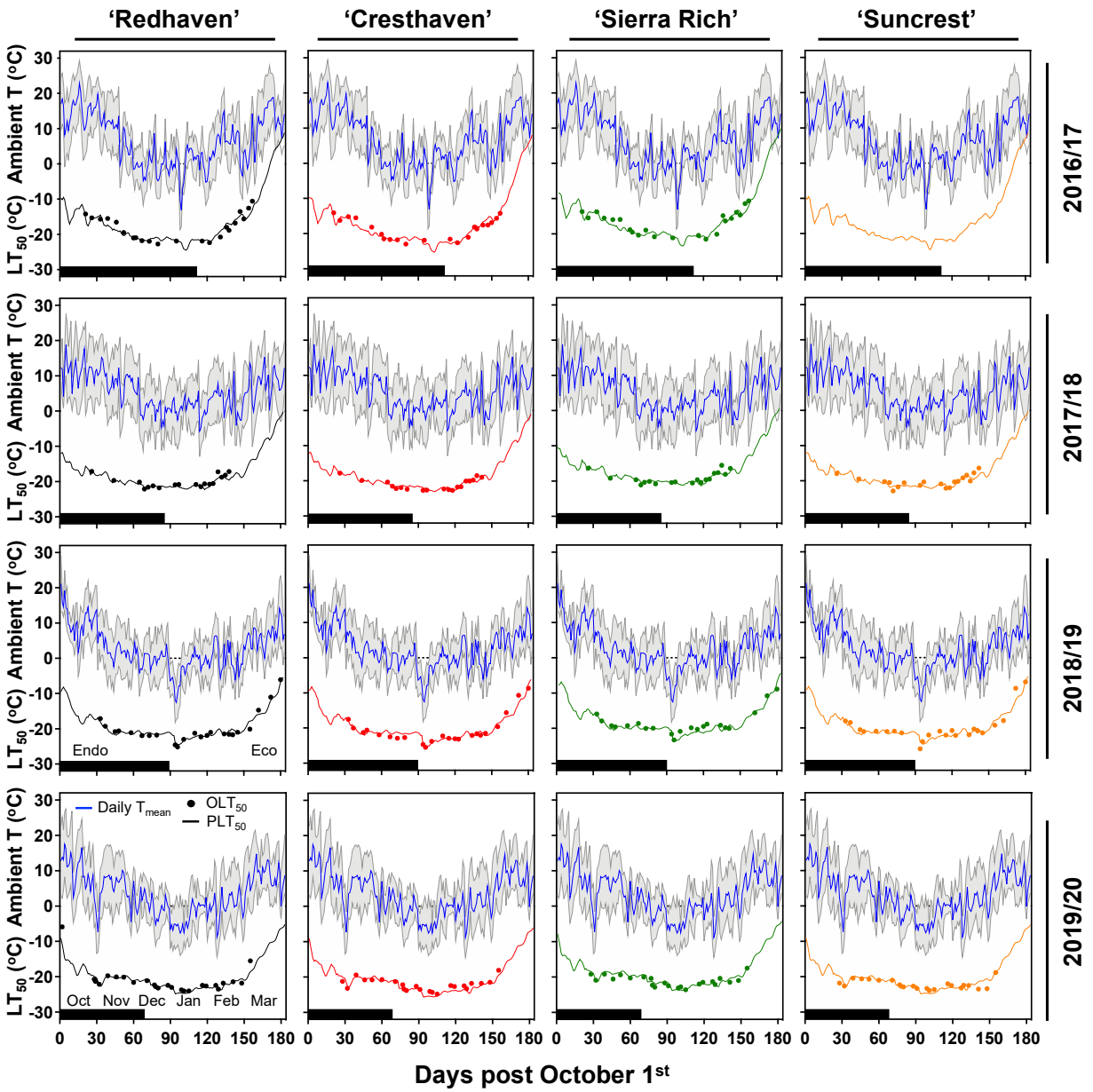

Figure 3.5. Daily LT_{50} prediction and actual data using the created endodormancy and ecodormancy cold hardiness (H_c) models along with weather patterns across four dormant seasons and four peach cultivars. Maximum, minimum and mean air temperatures for October 1st - March 31st of 2016-2020, along with the predicted curve and observed H_c data (as determined by DTA and expressed as LT_{50}) for four peach cultivars: 'Redhaven', 'Cresthaven', 'Sierra Rich' and 'Suncrest'. The use of each H_c model (endormancy or ecodormancy) for each phase of dormancy is indicated on the bottom of each figure cell as a black bar for endodormancy (Endo) or no bar for ecodormancy (Eco). The change from the endodormancy to ecodormancy H_c model every dormant season was determined by the time that the CST is reached at 700 chilling hours (0-7 °C).

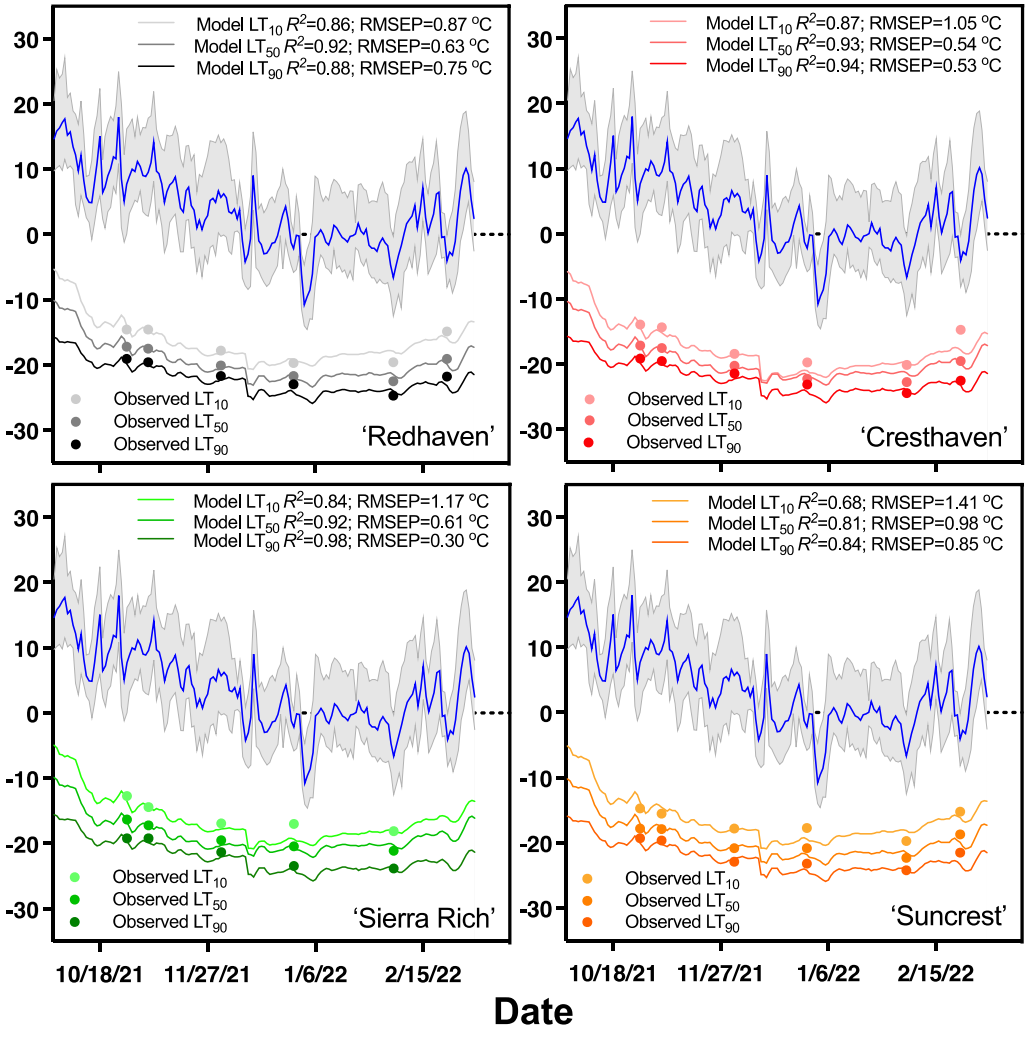

Figure 3.6. Validation of peach floral bud cold hardiness (H_c) prediction models with observations from an entirely independent dormant season. Floral bud H_c observed LT data that were acquired from differential thermal analysis (DTA) across four peach cultivars ('Redhaven', 'Cresthaven', 'Sierra Rich' and 'Suncrest') at six time points during the dormant season of 2021-2022 were used to determine the predictive accuracy of the created H_c models. Coefficient of determination (R^2) higher than 0.8 and root mean square error of prediction (RMSEP (ºC)) of less than 1.0 ºC satisfied the research goals of producing predictive accuracy sufficient to inform management decisions for peach producers managing frost events by conventional means. The ability to accurately predict wide-ranging lethal temperature quantiles using independent data sets increase the confidence that this suite of models may be used to predict H_c accurately even as climate conditions change in the future.

CHAPTER FOUR

INVESTIGATING PEACH FLORAL BUD ECO-PHYSIOLOGY AND METABOLISM DURING DORMANCY USING LARGE SCALE COLD HARDINESS PHENOTYPING AND NON-TARGETED METABOLOMIC AND PROTEOMIC ANALYSIS

4.1. Introduction

Cold damage to reproductive tissues is a primary factor in determining the economic viability of the peach [*Prunus persica* (L.) Batsch] industry in many growing regions throughout North America and the world. Climate change threatens to desynchronize periods of cold hardiness (H_c) in plants, with unusually warm periods and damaging cold events at different times during dormancy and following bud break. Cold hardiness, the threshold at which plant tissues will be irrevocably damaged by subfreezing temperatures, can be accurately measured using differential thermal analysis (DTA) or the oxidative browning technique (Mills et al., 2006; Proebsting, E. L. and Mills, 1978; Minas and Sterle, 2020). Plants as sessile organisms use various physiological means of confronting abiotic stressors such as subfreezing temperatures. Optimizing cultivar selection for H_c can further increase the likelihood of yielding a profitable crop. Global metabolic and proteomic kinetics associated with H_c differences between genotypes remains unknown (Szalay et al., 2010).

It is necessary to gain insight as to how the metabolome and proteome shift over the course of a growing season, and how acute frost events interact with the varying stages of dormancy between both cold hardy and non-hardy cultivars. Traditional breeding includes selection for traits desired for growing under conditions, rather than for specific genes. Cultivar selection for breeding programs in mild environments like California do not necessitate that the genotype exhibits superior H_c during acclimation and mid-winter, instead a low chilling requirement is a desirable

trait for warm climate production (Li and Wang, 2020). Cultivars will be favored in a cold climate such as Michigan, if they exhibit consistent H_c. Thus while low chill requirement and H_c are not mutually exclusive, they are two separate traits which are targeted by breeding programs for adaptation to different growing environments.

Damage to plant cells due to cold is caused by the formation of intracellular ice crystals that destroy cell membranes. In peach, the most critical form of damage is formation of ice crystals within the cells of floral primordia, causing the death of the reproductive organ. Extracellular ice formation in peach is usually not lethal, however it can lead to desiccation due to a developing osmotic gradient within and outside (Gusta et al., 2004; Ruelland et al., 2009) the floral primordial cells eventually resulting in cellular death. Acclimation to freeze events occurs during endodormancy post leaf senescence (Lang et al., 1987), and it is at this time when the floral buds gains the ability to supercool significantly below 0 ºC. Xylem discontinuity is one strategy that allows peach floral buds to supercool, preventing ice crystal formation within the cells of floral primordia (Ashworth and Abeles, 1984; Liu et al., 2019). Endodormancy will last until a genotypically unique chilling threshold is reached, which allows the bud to shift to ecodormancy. Deacclimation occurs during ecodormancy, as the floral tissue begins to phenologically develop until bloom, unless slowed by cool environmental temperatures (Lang et al., 1987). Xylem continuity is reestablished during deacclimation, resulting in a rapid loss of cold hardiness (Hc) (Ashworth, 1982), with the ability to supercool solely dependent upon the physiology of the buds. Throughout this dynamic process differential accumulation of metabolites and/or proteins could affect lethal freezing threshold temperatures of flower buds contributing to the physiological responses to internal and external stimuli occurring during dormancy.

Abiotic stressors such as cold temperatures lead to the creation of reactive oxidative species (ROS). These ROS are phytotoxic byproducts that play a key role in signal transduction (Choudhury et al., 2017; Hernandez et al., 2021; Vimont et al., 2019). The associated compounds within the ascorbate-glutathione cycle (Cooke et al., 2012; Di Ferdinando et al., 2012; Islam et al., 2021; Lu et al., 2018; Waśkiewicz et al., 2014), flavanone 3-hydroxylase (Choudhury et al., 2017; Pelletier and Winkel-Shirley, 1996; Schulz et al., 2016; Shen et al., 2006), peroxidases (Scandalios, 2005) and prenol lipid derivatives such as terpenoids (Vickers et al., 2009) alleviate oxidative stress by scavenging ROS. The ROS signal then leads to the expression of genes that lead to the synthesis of metabolites in response to the cold stress (Zhao et al., 2005). The tetrapyrrole Uroporphyrinogen lll is a precursor to protoporphyrin IX that is known to be part of the signaling system in non-dormant *Arabidopsis* that can impart cold-tolerance through the promotion of cyanide-resistant respiration (Zhang et al., 2016)

Primary metabolites (PM), secondary metabolites (SM) and proteins (PT) carry out many functions related to dormancy and cold stress within the floral buds. Carbohydrates such as sucrose, glucose, sorbitol and raffinose are known to be related to the H_c and development in non-reproductive tissues in peach and related plants (Maurel et al., 2004a, 2004b; Yu et al., 2017; Yun et al., 2014). Associated proteins such as hexokinases are important for sensing plant development (Granot et al., 2013). Proline, a water soluble amino acid, has been associated with H_c or cold stress during dormancy in numerous plants including peach (Shin et al., 2016; Siddique et al., 2018; Yun et al., 2014), and the regulation of proline-associated pentose phosphate pathway that leads to antioxidant phenolic compounds biosynthesis in creeping grasses (Sarkar et al., 2009). In addition, many amino acids such as glutamic acid and isoleucine have been linked with rapid proliferation

during ontogenetic development within floral buds of sweet cherry (*Prunus avium L.*) (Götz et al., 2017).

Despite the ever-growing knowledge of the responses made to abiotic stress by the metabolome and proteome of many plants related to dormancy, much is still unknown. Importantly, it is not well understood which are the principal H_c related metabolic pathways that are associated within distinct peach genotypes, that express hardy or non-hardy phenotypes. Previous works have examined changes in specific classes of compounds or focused on just specific phases of dormancy. Few studies have combined detailed H_c phenotypic analysis with either metabolomic or proteomic data in dormant floral buds of any species. The overall goal of this study was to perform a comprehensive evaluation of the expression of primary and secondary metabolites, as well as proteins across three distinct dormancy phases, responses to freezing events, between a hardy and non-hardy cultivar, in conjunction with robust H_c phenotyping measurements. Our results provide key insights that further our understanding of the physiological responses of dormant peach floral buds that affect H_c.

4.2. Materials and Methods

4.2.1 Plant material and experimental approach

Dormant peach [*Prunus persica* (L.) Batsch] flower buds from 9-year-old 'Cresthaven' or 'Sierra Rich' scions grafted on 'Lovell' rootstock were tested for cold hardiness (H_c) using artificial freezing in combination with differential thermal analysis (DTA) (Minas and Sterle, 2020). 'Sierra Rich' is a non-hardy peach cultivar that was bred in Modesto, California, while 'Cresthaven' is a hardy cultivar that was bred in South Haven, Michigan (Okie, 1998; Zaiger et al., 2002). Floral buds were collected during the dormant season weekly from one-year-old shoots of moderate vigor that had no obvious signs of damage and were located at the mid-canopy position

of 15 randomly selected trees per cultivar. The sampling location was the Colorado State University's Experimental Orchard at Western Colorado Research Center, Orchard Mesa, Colorado (39.042230, -108.469492).

Samples were collected at 25 time points between Oct. 21, 2016 and Mar. 13, 2017. Shoots were sampled from the orchard and buds were then separated and randomly assigned to 16 sets of 10 buds each (in total 160 buds per time point). Ten sets of buds (100 buds) were used for detailed H_c phenotyping using DTA. Three complete sets of buds (30 buds) were kept as a control (not frozen) and were used for visual evaluation of oxidative browning to check orchard variability and estimate preexisting field cold damage. The remaining three sets of 10 buds each were defined as the three biological replicates. The biological replicates were flash frozen in liquid N_2 and stored in a -80 ºC freezer and then lyophilized in preparation for metabolic and proteomic analysis. Of the original twenty-five sampling dates, five dates (Nov. 8, 2016, Nov. 21, 2016, Jan. 3, 2017, Jan. 9, 2017, and Mar. 3, 2017) were selected for metabolomic and proteomic analysis. These five dates were characterized by their stage of dormancy (acclimation, max hardiness, and deacclimation). Additionally, Nov. 8, 2016 and Jan. 3, 2017 were sampled before a significant freezing events (-6.8 ºC and -11.7 ºC, respectively), while Nov. 21, 2016 and Jan. 9, 2017 were sampled after the freezing event. These time points enabled the evaluation of the metabolic reaction to the freezing event across the two cultivars.

4.2.2 Measurement of peach floral bud cold hardiness using differential thermal analysis

Peach floral bud H_c was evaluated using DTA, and weather data was collected following the methods described previously in Chapter 1 and 3. (Minas and Sterle, 2020; Tanner et al., 2021). Five pairs of floral buds were detached from the one-year-old fruiting shoots and wrapped in aluminum foil, then placed within a cell containing a thermoelectric module (TEMs). Ten cells

with TEMs were loaded with buds and one was left empty to serve as the reference. Temperature was dropped at a rate of 4 ºC per hour to -36 ºC, in a programmable freezing chamber (Tenney Jr Test Chamber, Model TUJR 1.22 cu.ft., Thermal Product Solutions, New Columbia, PA, USA). Lethal floral bud temperatures were detected by thermocouples and exothermic reactions related to freezing events were detected by TEMs as a voltage response using a multimeter data acquisition system (Keithley 2700, Tektronix, Beaverton, OR). Using the accompanying software (Tektronix, Keithley ExceLinx^{TM} for Instruments, Beaverton, OR) the data were input to a spreadsheet for analysis in Microsoft Excel. Parametric survival analysis was performed using JMP Pro 15.0 (SAS Institute, Inc., Cary, NC). For each sampling date, cumulative low temperature exotherm to lethal temperature (LT) data were fit to a model using a logistic function to best fit the nonlinear data. Using the Weibull regression model, LTs where 10%, 50%, and 90% (LT_{10}, LT_{50}, and LT_{90}) of buds that were considered dead were estimated for each sampling date throughout the four dormant season-span.

4.2.3. Sample preparation for metabolomic and proteomic analysis.

All samples were removed from -80 ºC lyophilized in original Eppendorf tubes for approximately 30 hours. Dried samples were crushed using "The Stomper" (Next Advance) and subsequently homogenized using the "Bullet Blender" (Next Advance.) After physical disruption, 100 mg of each sample was weighed into a glass autosampler vial. Subsequent biphasic extraction was performed in the glass autosampler vial with a total extraction solvent volume of 1.6 mL. Specifically, 1.2 mL of 40% methanol (75%) 60% methyl-tert-butyl-ether (MTBE) was added to each sample followed by vortexing for 60 minutes at 800 rpm. To induce biphasic separation, 400 µL of LCMS-grade water was added to each vial followed by an additional 15 minutes of vortexing at 800 rpm. The samples were then centrifuged at 2,000 × g for 15 minutes at 4 ºC. Subsequently,

600 µL of polar layer was transferred to a new vial for analysis by GC-MS and stacked injection-LC-MS(Broeckling and Prenni, 2018). 600 µL of non-polar layer was transferred to a new vial for analysis by stacked injection-LC-MS. The remaining protein pellet was kept in -80 ºC until proteomic analysis.

4.2.4 Non-targeted primary metabolic analysis using GC-MS

Fifteen µL of the aqueous phase was dried under N_2, re-suspended in 50 µL of pyridine containing 25 mg mL^{-1} of methoxyamine hydrochloride, incubated at 60 ºC for 1 hour, sonicated for 10 min, and incubated for an additional 1 hour at 60 ºC. Next, 50 µL of N-methyl-N-trimethylsilyltrifluoroacetamide with 1% trimethylchlorosilane (MSTFA + 1% TMCS, Thermo Scientific) was added and samples were incubated at 60 ºC for 45 min, briefly centrifuged, cooled to room temperature, and 100 µL of the supernatant was transferred to a 150 µL glass insert in a GC-MS autosampler vial. Metabolites were detected using a Trace 1310 GC coupled to a Thermo ISQ mass spectrometer (Thermo Scientific). Samples were injected in a 1:10 split ratio. Separation occurred using a 30 m TG-5MS column (Thermo Scientific, 0.25 mm i.d., 0.25 µm film thickness) with a 1.2 mL · min^{-1} helium gas flow rate, and the program consisted of 80 ºC for 30 sec, a ramp of 15 ºC per min to 330 ºC, and an 8 min hold. Masses between 50-650 m/z were scanned at 5 scans · sec^{-1} after electron impact ionization.

4.2.5 Non-targeted secondary metabolic analysis using LC-MS

For LC-MS analysis, a stacked injection approach was used to maximize metabolite coverage (Schauer et al., 2013). The organic layer of the extraction was dried under nitrogen, resuspended in 600 µL of 3 parts toluene 2 parts methanol. 100 µL of this solution was transferred to inserts and 20 µL taken for generating a pooled QC sample. For the aqueous layer 600 µL of methanol was added to current 600 µL of extract and the solution mixed and centrifuged to ensure

polysaccharide and protein depletion. 100 µL of this solution was transferred to inserts and 20 µL taken for generating the pooled QC sample. Two microliter injections were performed in stacked format for each of the organic and aqueous phases.

Samples were analyzed in randomized order, and separation was acheived using a Waters Acquity UPLC CSH Phenyl Hexyl column (1.7 µM, 1.0 × 100 mm), using a gradient from solvent A (water, 0.1% formic acid) to solvent B (Acetonitrile, 0.1% formic acid). Injections were made in 100% A, held at 100% A for 1 min, ramped to 98% B over 12 minutes, held at 98% B for 3 minutes, and then returned to starting conditions over 0.05 minutes and allowed to re-equilibrate for 3.95 minutes, with a 200 $\mu L \cdot min^{-1}$ constant flow rate. The column and samples were held at 65 ºC and 6 ºC, respectively. The column eluent was infused into a Waters Xevo G2 Q-TOF-MS with an electrospray source in positive mode, scanning 50-2000 m/z at 0.2 seconds per scan, alternating between MS (6 V collision energy) and MSE mode (15-30 V ramp). Calibration was performed using sodium iodide with 1 ppm mass accuracy. The capillary voltage was held at 2200 V, source temp at 150 ºC, and nitrogen desolvation T at 350 ºC with a flow rate of 800 $L \cdot h^{-1}$.

4.2.5. Non-targeted proteomic analysis LC-MS

A MixQC sample was made by combining 0.4 µg peptide from each sample. This MixQC was injected approximately every 6th sample. A total of 0.8µg of peptides were purified and concentrated using an on-line enrichment column (Waters Symmetry Trap C18 100Å, 5 µm, 180 µm ID × 20 mm column). Subsequent chromatographic separation was performed on a reverse phase nanospray column (Waters, Peptide BEH C18; 1.7 µm, 75 µm ID × 150 mm column, 45 ºC) using a 90 minute gradient: 5-30% buffer B over 85 minutes followed by 30-45% B over 5 minutes (0.1% formic acid in ACN) at a flow rate of 350 $nL \cdot min^{-1}$. Peptides were eluted directly into the mass spectrometer (Orbitrap Velos, Thermo Scientific) equipped with a Nanospray Flex ion source

(Thermo Scientific) and spectra were collected over a *m*/*z* range of 400–2000, positive mode ionization. Ions with charge state +2 or +3 were accepted for MS/MS using a dynamic exclusion limit of 2 MS/MS spectra of a given *m*/*z* value for 30 s (exclusion duration of 90 s). The instrument was operated in FT mode for MS detection (resolution of 60,000) and ion trap mode for MS/MS detection with a normalized collision energy set to 35%. Compound lists of the resulting spectra were generated using Xcalibur 3.0 software (Thermo Scientific) with a S/N threshold of 1.5 and 1 scan/group.

4.2.6. Data processing for GC-MS and LC-MS

For each sample, raw data files were converted to .cdf format, and matrix of molecular features as defined by retention time and mass (m/z) was generated using XCMS (Smith et al., 2006) package in R software for feature detection and alignment. Outlier injections were detected based on total signal and PC1 of principal component analysis. Features were grouped using RAMClustR (Broeckling et al., 2014).

Metabolites from GC-MS were matched in RAMSearch (Broeckling et al., 2016) by using retention time, retention index and matching spectral data with Golm Metabolome Database (Hummel et al., 2013; Hummel et al., 2007) and NISTv14 (http://www.nist.gov) (Broeckling et al., 2016).

For metabolites from LC-MS, molecular weight was inferred from in-source spectra (Broeckling, 2016) using interpretMSSpectrum (Jaeger, 2016). MSFinder (Tsugawa, 2016) was used for spectral matching, formula inference and tentative structure assignment. Compounds categorized into chemical ontologies using the ClassyFire API (Djoumbou Feunang et al., 2016).

4.2.7. Data processing for proteomic analysis

Tandem mass spectra were extracted, charge state deconvoluted and deisotoped by ProteoWizard MsConvert (version 3.0). Spectra from all samples were searched using Mascot (Matrix Science, London, UK; version 2.6.0) against the Uniprot_Prunus_persica_rev_070918 database (unknown version, 77466 entries) assuming the digestion enzyme trypsin. Mascot was searched with a fragment ion mass tolerance of 0.80 Da and a parent ion tolerance of 20 PPM. Carboxymethyl of cysteine was specified in Mascot as a fixed modification. Oxidation of methionine was specified in Mascot as a variable modification.

Search results from all samples were imported and combined using the probabilistic protein identification algorithms (Nesvizhskii et al., 2003) implemented in the Scaffold software (version Scaffold_4.8.7, Proteome Software Inc., Portland, OR). Peptide thresholds were set (90%) such that a peptide FDR of 0.05% was achieved based on hits to the reverse database (Käll et al., 2008). Protein identifications were accepted if they could be established at greater than 95.0% probability and contained at least 2 identified proteins. Protein probabilities were assigned by the Protein Prophet algorithm (Nesvizhskii et al., 2003). Proteins that contained similar proteins and could not be differentiated based on MS/MS analysis alone were grouped to satisfy the principles of parsimony. Proteins sharing significant peptide evidence were grouped into clusters.

4.2.8. Statistical data analysis of seasonal kinetic fluctuations of metabolites and proteomics

Determination of differences was tested across the selected five time points, Nov. 8, 2016, Nov. 21, 2016, Jan. 3, 2017, Jan. 9 2017, and Mar. 3, 2017. A repeated measures ANOVA was performed using Metaboanalyst 5.0 (www.metaboanalyst.ca), on PM, SM, and PT, with genotype as a covariate. For this analysis, a false discovery rate adjustment was used to correct for multiple testing. Principal component analysis was performed in JMP Pro 15 with all loadings scaled to 1. Final visualizations were developed in GraphPad Prism 9.0 (Graph Pad Inc., San Diego, CA,

USA). Variable clustering analysis was performed in JMP Pro 15 (SAS Institute Inc., Cary, NC) on all significant PT (Statistical details for clusters variables platform, 2023). Variable clustering assigned each PT with others which were most highly correlated over the dormant season. A significance level of 0.05 was used for all tests of significance.

4.2.9. Statistical analysis of changes occurring after major frost events during acclimation and maximum hardiness.

Differences between pre-frost PM and post-frost PM expression were examined using two sample T-test ($p<0.05$, with log2 fold change >0.5). PT and SM differences were examined pre- and post-frost using two samples T-test ($p<0.05$, with log2 fold change >1.5). Visualizations for volcano and bar plots were developed in GraphPad Prism 9.0.

4.2.10. Z-score transformation and combined principal component analysis of primary metabolites, secondary metabolites and proteins.

For combined analysis, the relative abundance (X) of each metabolic or proteomic feature was normalized to a z-score. The following equation was used independently on data from the different detection platforms (GC-MS, LC-MS for secondary metabolites, and LC-MS proteomics), before being combined into a single data set: z= (X-mean)/(standard deviation). The combined z-score data were analyzed using PCA, and variable cluster analysis in JMP Pro 15.

4.3. Results

4.3.1 Detailed physiological characterization of peach floral bud cold hardiness response to seasonal temperature changes across two distinct genotypes during dormancy.

Measurements of floral bud H_c started on October 21, 2016 during bud acclimation, prior to leaf senescence and continued through March 9, 2017 **(Figure 4.1)**. Bud H_c started relatively non-hardy with LT_{50} for 'Cresthaven' and 'Sierra Rich' being -14.1 ºC and -13.7 ºC respectively.

The first significant frost of the season occurred on November 18th, with a low of -6.8 ºC. The marginal increase in H_c of LT_{50} ($MICH_{50}$) in 'Cresthaven' was 3.2 ºC post-frost compared to pre-frost, a shift that represented a relative genotypic increase in H_c 4.6 times greater than that of 'Sierra Rich' **(Table 4.1)**. Following a -11.7 ºC frost event (Jan. 6, 2017, 615 chilling hours 0-7.2 ºC), maximum H_c was reached for the entire dormant season. The $MICH_{50}$ was 1.9 ºC in 'Cresthaven' which was 1.9 times greater $MICH_{50}$ than 'Sierra Rich'. However, the $MICH_{10}$ was 7.3 times greater in 'Cresthaven'. Throughout the dormant season a consistent wider range of lethal temperatures in 'Sierra Rich' compared to 'Cresthaven'. The measured range from LT_{10}-LT_{90} was 1.6 times higher in Sierra Rich across the dormancy for this study, with much greater consistency across the bud population shown with 'Cresthaven' buds. Overall, the two genotypes exhibited distinct H_c behavior throughout the dormant season.

4.3.2. Seasonal kinetics of peach floral bud primary metabolites detected by GC-MS

Principal component analysis of the three replicated samples for each cultivar at each sampling date demonstrates that dormancy stage was a major contributor to PC1 (35.5%) **(Figure 4.2a)**. Influence of dormancy stage is indicated by the separation between the points of different color and the consistent direction to the progressive separation across the different time points. Given the consistency of the separation for samples of the same dormancy stage, it is evident that PC2 (14.4%) is largely capturing the degree that genotype has contributed to primary metabolic differences throughout the dormant season.

Nine known metabolites that were identified using repeated measures ANOVA significantly ($p = <0.0001$-0.0150) vary across time points **(Figure 4.2b)**. The heat map in **Figure 4.2b** confirms conclusions drawn about PC1 of **Figure 4.2a**, the large degree to that these nine metabolites were differentially accumulated over time. Of the 9 significantly changed annotated

metabolites, 6 were amino acids (AA) or AA derivatives. All AA and 4-hydroxyphenyl acetate were at relatively low abundance until deacclimation after which abundance was greatly increased. Allantoin, an imidazole, was at high relative abundance through the dormant season, with peak on January 9 in both cultivars following a major freezing event and after 619 chilling hours had been already accumulated. Raffinose abundance appeared closely associated with H_c, increasing in abundance until a maximum H_c was achieved on January 9. Among all annotated metabolites detected by GC-MS, proline alone differed significantly between genotypes (p=0.001). **Figure 4.2c** illustrates the differences in the metabolites across time, and the striking similarities seen in the expression of each metabolite for each genotype.

4.3.3. Seasonal kinetics of peach floral bud secondary metabolites detected by LC-MS

PCA indicated that genotype was a major contributor to the differences in abundance among secondary metabolites **(Figure 4.3a)**. Clear separation along PC1 (20.7%) is apparent between samples from the same dormancy stage but differing in genotype. It is also apparent that 'Cresthaven' had less variation in secondary metabolite abundance across PC1 and PC2 because there is less separation between points within the same treatments, as compared to 'Sierra Rich'. Influence of dormancy stage is a major contributor to the variation among samples detected by PC2 (16.0%). Vertical separation among time treatments indicates the influence of time on metabolite abundance, although time does not appear to account for differences in the secondary metabolome to the same extent as in the primary metabolome.

Differences (p=<0.0001-0.0439) were found among 64 annotated secondary metabolites across all times during the dormant season using repeated measures ANOVA **(Figure 4.3b)**. Among the 64 significant secondary metabolites 18 differed (p=<0.0001-0.049) between genotypes, as compared to only 1 primary metabolite. This supports the evidence provided by

PCA, that genotype contributes to changes in secondary metabolome more than the primary metabolome.

Lipids and lipid-like molecules accounted for the greatest proportion of significantly changed secondary metabolites (22) of the various represented super-families of molecules, followed by phenylpropanoids and polyketides (11), organic oxygen compounds (5), organoheterocyclic compounds (8) and organic nitrogen compounds (4). The lipid superfamily is further broken into prenol lipids (7), fatty acyls (6), glycerophospholipids (5), steroids (2) and sphingolipids (2). Greater variability throughout the dormant season was seen in the secondary metabolome compared to the primary metabolome across both cultivars, however, most metabolites were still more abundant in deacclimation **(Figure 4.3b)**. Prenol lipids and flavonoids were the two metabolic classes with the greatest number of significant differences between genotypes. Additionally, among the significant prenol lipids (anhydroretinol, retinyl beta-glucuronide, and 2-Octaprenyl-3-methyl-6-methoxy-1,4-benzoquinol), all were significantly higher in abundace in 'Cresthaven', while among the significant flavonoids, all were significantly higher in abundance in 'Sierra Rich'. Oligosaccharides was the last sub family with multiple compounds that differed between cultivar, with suffriticoside E and rubrofusarin both being higher in abundance in 'Cresthaven'. Non-targeted LC-MS analysis of secondary metabolites provided evidence of differences between the genotypes which corresponded to distinct H_c responses.

4.3.4. Seasonal kinetics in peach floral bud proteins detected by LC-MS

Peach floral bud protein PCA showed a clear separation between the deacclimation phase from the other sampling times coming from dormancy **(Figure 4.4a)**. However, the separation among other points and treatments was inconsistent. Twenty-four significant annotated proteins were identified by repeated measures ANOVA to have significantly varied over time (p=0.0001-

0.0453). The only protein found to be significantly different in abundance between the two cultivars was a peroxidase (6G289400) (p=0.021).

Four protein clusters were found, each cluster containing the proteins that had the greatest correlations to others within each respective cluster, using variable clustering analysis. The most interesting pattern was observed for protein cluster 4.2, which represented proteins that increase or decrease in abundance during January, the time of maximum H_c **(Figure 4.4b and 4.4c)**. This included precipitous drops in abundance of 6-phosphogluconate dehydrogenase, flavanone 3-hydroxylase, tubulin alpha chain, peroxidase, but a sizable increase in glutathione peroxidase. Although not statistically significant, proteins in cluster 4.2 demonstrated a trend of higher abundance in 'Sierra Rich' as compared to 'Cresthaven' during January. Furthermore, the relatively higher abundance of flavanone 4-hydroxylase in 'Sierra Rich" supports the findings noted previously in section 3.3, that all significantly different flavonoids between genotypes were higher in 'Sierra Rich'. Compared with heatmaps in **Figures 4.2b and 4.3b**, for the primary and secondary metabolites, the proteomic heatmap 4.4b showed a relatively even distribution of the peak of seasonal expression among all proteins. However, the addition of variable clustering provided insight as to the associations among proteins.

4.3.5 Primary metabolic changes occurring after major frost events during acclimation and maximum hardiness

Volcano plot analysis identified differences (p=0.0001-0.0497) in the primary metabolome in both genotypes and at two dormancy phases following significant frost events at each phase **(Figure 4.5a)**. 'Sierra Rich', the least cold hardy cultivar, had more significant differences than did 'Cresthaven', the hardiest, and in each phase of dormancy there were common metabolic shifts between the genotypes **(Figure 4.5b)**. After the acclimation frost event in November a total of 6

significant changes were observed for ‘Cresthaven’ metabolite abundance, 11 significant changes were observed for ‘Sierra Rich,’ and only one significant primary metabolite was overlapping among cultivars. After the maximum hardiness frost event, 9 primary metabolites significantly changed in ‘Cresthaven’, 17 in ‘Sierra Rich’, and 4 that were overlapping between genotypes.

Carbohydrate structural categories which changed post-freeze varied by genotype **(Figure 5c)**. The summation of the significantly changed primary metabolites in ‘Cresthaven’ in response to freeze and across both dormancy phases had a sugar alcohol: soluble sugar: sugar acid ratio of 2:5:1, while Sierra Rich’ had a ratio of 4:1:2 (**Figure 4.5d**). When considering the primary carbohydrates of the two genotypes, this result highlights a difference in the carbohydrate balance that may provide insight into the differences in H_c responses following freezing events across these phases of dormancy. Metabolite abundance before and after each frost event were examined to identify similarities and significant differences between the genotypes using two sample t-test. The total amino acid content of all significantly changed amino acids and derivatives (**Figure 4.2**) including glutamic acid, proline, glycine, valine, isoleucine, and pyroglutamic acid, was calculated for each date. Amino acid content of ‘Cresthaven’ was 280%-400% the levels of ‘Sierra Rich’ for each of the sampling dates during dormancy and significantly different each date (**Figure 4.5e**; t-test, p=0.0017-0.0434). These important findings support the need for analysis before and after frost events in addition to seasonal trends for discerning metabolic activity in peach dormant floral buds.

4.3.6. Secondary metabolic changes occurring after major frost events during acclimation and maximum hardiness detected by LC-MS

Volcano plot analysis of secondary metabolites detected using LC-MS clearly indicated stark differences among the distinct phenotypic responses to frost, and stark differences related to

the dormancy timing of the frost events (**Figure 4.6a and b**). After the acclimation frost event there was a total of 62 annotated secondary metabolites that significantly (p=0.0005-0.0454; fold change >1.5) changed in 'Sierra Rich', whereas only 12 in 'Cresthaven'(p=0.0085-0.0448). There were 10 significantly changed annotated secondary metabolites that were common to both genotypes. Before the frost during the acclimation phase (November) 'Sierra Rich' and 'Cresthaven' had similar H_c with LT_{50} of -15.5 ºC and -15.9 ºC respectively. But following the frost, these H_c values changed to -16.2 ºC and -19.1 ºC, revealing a much more significant gain of H_c. The 3.2 ºC $MICH_{50}$ in 'Cresthaven' H_c was 4.6 times greater than the relative shift seen in 'Sierra Rich' that had only 0.7 ºC change in H_c. Given the discrepancy in the diversity of the metabolic response in light of the H_c change, the response of 'Sierra Rich' appears more chaotic, and perhaps inefficient. While this was the first major frost event of the dormant season neither genotype received fatal damage to floral tissues with the frost only reaching -6.8 ºC.

The -18.6 ºC frost event during maximum hardiness (January) resulted in a nearly two-fold increase difference in 'Cresthaven' $MICH_{50}$ over 'Sierra Rich'. The number of significant secondary metabolic differences following the frost event was much less dramatic than for the November 2016 event, with 8 and 7 significant changes in 'Sierra Rich' and 'Cresthaven', respectively. The change in the type of behavior seen from 'Sierra Rich' when comparing the metabolic responses after each frost may be related to the prior accumulation of chilling hours (619) meaning that the chill requirement had already likely been satisfied. Whereas 'Cresthaven' was still yet to satisfy the roughly 800 chilling hours requirement and was still surely in endodormancy **(Figure 4.1c)**. This difference in cultivar behavior following a major freezing event at this phase of dormancy (maximum hardiness) is further highlighted by the lack of any

overlapping primary metabolites that changed significantly across both cultivars in response to freeze.

Significant trends were seen when considering the secondary metabolites that had significant increases. Prenol lipids were linked with 'Cresthaven' in the previously mentioned repeated measures ANOVA approach. Thus, across all pre- and post- frost dates that occurred during dormancy (Nov. 9, Nov. 21, Jan. 3, and Jan. 9) the sum of the abundances from each of the 7 previously identified significant prenol lipids were compared. For each date prenol lipid content was significantly ($p=0.0002$-0.0487) more highly expressed, 1.6 to 2.7-fold greater than the expression of 'Sierra Rich'. This significant and consistent trend aligns with increases in H_c and amino acid trends across the same dates **(Figures 4.2c, 4.3bc, 4.5e and 4.6e)**.

Across multiple classes of secondary metabolites, post maximum hardiness frosts resulted in significant gains in 'Cresthaven', whereas the corresponding expression of the same metabolites in 'Sierra Rich' declined, although non-significantly. This difference in behavior was the case among the fatty acids: oleamide and squamocin, and the tetrapyrroles: precorrin 3-B and Uroporphrinogen lll (**Figure 4.3b and 4.6c**). This confounding behavior of 'Sierra Rich' provides more evidence that this type of change in metabolic abundance may be occurring as a result of having satisfied the chilling requirements before January 3, 2017.

4.3.7. Proteomic changes occurring after major frost events during acclimation and maximum hardiness detected by LC-MS

Volcano plot analysis of proteins determined that there was a smaller number of annotated proteins changing significantly in response to frost events compared to secondary metabolites **(Figure 4.7a)**. As indicated in the Venn diagram in **Figure 4.7b**, 'Cresthaven' expressed fewer changes than 'Sierra Rich'. There was not a single significant difference in protein abundance

shared between the two genotypes within the same phase of dormancy. Carboxypeptidase was the only protein to show a significant response after both frost events within a single genotype, which was 'Sierra Rich'. All other instances of protein significance after frosts were unique to one genotype at a single time. Peptidyl-prolyl isomerase was strongly expressed in 'Cresthaven', immediately following the acclimation frost event. The expression of elongation factor 1-alpha post-frost is similar to the trend seen in elongation factor tu **(Figure 4.4c)** suggesting a trend in translational activity following cold stress in ecodormant buds. Although only significant in 'Sierra Rich' post maximum hardiness frost, the 5-(hydroxymethyl) glutathione dehydroxylase was consistently higher post frost events compared to pre frost events, in both genotypes, supporting the role of the glutathione-ascorbate cycle in ROS scavenging.

4.3.8. Multiple domain approach reveals most influential relationships in metabolic and proteomic trends with integration of primary and secondary metabolism with proteome of dormant peach floral buds

The interconnectivity of the largest detectable scope of metabolic and proteomic activity was interrogated by PCA and variable clustering of z-scored data **(Figure 4.8a and b)**. Clear separation is observed as vertical spacing between the two genotypes was apparent and was clearly a major contributing factor to PC2 (15.0%). Dormancy phase was a major contributing factor to PC1 (17.6%) with apparent horizontal separation even if individual dates tended to have some overlap. Separation within genotype was more pronounced in 'Sierra Rich', even though the variability was also more apparent. Expanded variation is an indicator of an inconsistent response to dormancy phase and frost events. Coupled with a minimal gain in H_c, the response of 'Sierra Rich' can be considered a disordered response of multiple cycles within bud organelles to being

overly cold stressed. ‘Cresthaven’, in contrast, proceeded through the dormant season in a consistent linear trend, with minimal variation within groups of replicates.

Variable clustering was useful when used in combination with PCA, specifically in identifying meaningful groupings within over 4,000 individual data points from the combined metabolic and proteomic analyses **(Figure 4.8b)**. PCA elucidated the cluster analysis by revealing trends in how genotype and dormancy stage influence the abundance of various metabolites and proteins within the clusters. Dormancy stage followed diagonal linear progression ending in quadrant 2 of the PCA. Averaging across genotype results in a strong linear diagonal trend originating in quadrant 4 with the acclimation replicates. Dormancy stage was a major contributor to the metabolites and proteins within cluster 8.1. Positively correlated metabolites and proteins within cluster 8.1 were grouped in an area of strongest influence on dormancy stage top left of quadrant 2, while negatively correlated features grouped in the exact opposite position in quadrant 4. This combined approach helped to identify a cluster of annotated, closely correlated metabolites contributing to ‘Cresthaven’, given the position of the clusters around ‘Cresthaven’ replicates withing the PCA plot. Clusters 8.2 and 8.8 contain a mix of prenol lipids, glycerophospholipids, and oligosaccharides, supporting evidence found in earlier analyses. The approach highlighted key associations unique to the genotypically cold hardy cultivar.. Cluster 8.5 was clearly associated with ‘Sierra Rich,’ and was primarily made up of proteins as opposed to the previously mentioned clusters 8.2 and 8.8 that were dominated by metabolites. Several stress related compounds were found to be related to ‘Sierra Rich’ including the isoflavanoid, isorobustin, as well as proteins within cluster 8.5: peroxidase (6G289400), 6-phosphogluconate dehydrogenase, and glutathione peroxidase. These results provide unprecedented insight into the metabolic and proteomic changes that are associated with changes in peach floral bud H_c.

4.4. Discussion

The greatest threat to peach production worldwide is cold damage to tender reproductive tissues. Although peach uses an "avoidance" strategy and remain dormant throughout the coldest times of the year, it remains physiologically active during this period (Burke et al., 1976; Wisniewski et al., 2014). Underlying metabolic and proteomic composition of floral buds plays a key role in determining the H_c of the floral buds. This study provides the first detailed physiological characterization of H_c in conjunction with untargeted primary and secondary metabolomics, and proteomics. The first goal of this study is to identify how primary and secondary metabolites, and proteins change with cold hardiness at different stages of a dormant season. The second goal is how metabolites and proteins change after acute frost events. The third goal is how these global changes are associated among metabolites and proteins. The fourth goal is to identify differences in metabolites and proteins between a hardy genotype and a non-hardy genotype to identify compounds which play a large role in determining the H_c trait.

4.4.1 Seasonal shifts in peach floral bud H_c, metabolome and proteome

Peach floral buds entered endodormancy during leaf senescence in mid- to late October, 2016. While floral buds of each cultivar already possessed the ability to supercool significantly below freezing (LT_{10} < -12 ^{o}C, across both cultivars), further acclimation did not take place until after the first freezing event (-6.8 ^{o}C; November 18,, 2016). Following this event the H_c of 'Cresthaven' increased dramatically, while a very subtle shift in H_c was detected in 'Sierra Rich' (**Figure 4.1**; **Table 4.1**). Throughout the rest of the dormant season a distinct phenotypic H_c difference was evident between the two cultivars. 'Cresthaven' acclimated with a consistently hardier trend culminating in maximum hardiness on January 9, 2017. 'Sierra Rich' reached maximum hardiness on the same date, however, H_c was already lost temporarily on December 12,

2016 following warming daily temperatures, despite already experiencing 20 nights of subfreezing temperatures since mid-November 2016. The H_c range (difference between LT_{90} and LT_{10}) was 60% wider for 'Sierra Rich'. 'Cresthaven' remained unambiguously more cold hardy, with a narrowing range and lower lethal temperatures, throughout the dormant season until March 9th, 2017 when phenologic growth and development was quickly advancing towards bloom on March 23, 2017.

PCA of primary metabolites showed there were distinctions between genotypes, and clear trends between dormant stages **(Figure 4.2a)**. Repeated measures ANOVA, accounting for multiple testing issues using false discover rate (FDR), was used as a conservative measure of the changes in peach floral bud primary, and secondary metabolites, and proteins across five time points encompassing acclimation, maximum hardiness, and deacclimation. Of the 54 annotated primary metabolites nine were significantly different across the time points ($p=<0.0001$-0.0150). These nine metabolites were dominated by AA and were in highest abundance during deacclimation, and conversely lower abundance during acclimation and maximum hardiness **(Figure 4.2b and c)**. Deacclimation is associated with higher AA content as buds are entering ontogenetic development, in preparation for bloom. Proline has long been associated with responses to cold stress and cold tolerance protecting plants as an osmolyte, a signaling molecule, as an antioxidant, and as a step of the metabolism of several pathways such as the pentose phosphate, the phenylpropanoid, and the tricarboxylic acid pathways (Hayat et al., 2012; Kaur and Asthir, 2015; Sarkar et al., 2009; Shin et al., 2016; Yun et al., 2014). Proline was the only compound expressed differently between the genotypes, with the greatest abundance difference occurring during acclimation and deacclimation.

Allantoin is considered to be an efficient nitrogen transport compound, annotated to be associated with H_c in other plant species, by initiating abscisic acid (ABA) synthesis (Kaur et al., 2016; Watanabe et al., 2014; Yu et al., 2017). Abundance of allantoin peaked for both genotypes on Jan., 9 2017 along with maximum hardiness, confirming allantoin's association with peach floral bud H_c. Studies have associated raffinose family oligosaccharides with H_c and dormancy in peach as well as other plants (Nishizawa-Yokoi et al., 2008). The relationship of raffinose with H_c was also confirmed in this study as raffinose abundance was consistently higher during both maximum hardiness dates (January 3 and 9, 2017), in both genotypes. Contrary to expectations, raffinose was the only significantly changing carbohydrate across all time points by ANOVA. Other studies have found carbohydrates such as glucose, fructose and sorbitol to vary significantly in many peach tissues as bud break is approaching (Maurel et al., 2004b; Michailidis et al., 2018).

The secondary metabolome had overall more significant compounds, and more differences between genotypes, which was expected since secondary metabolites are associated with responses to abiotic stress. PCA analysis of secondary metabolites indicated clear distinctions in expression between genotypes, and a clear linear trend over time, with 'Sierra Rich' having more variability between reps. The clear linear trend was seen in the heatmap as well, with most of the secondary metabolites observed at highest abundance in deacclimation **(Figure 4.3b)**. Among the 64 annotated significantly changed secondary metabolites, several other oligosaccharides were detected such as suffriticoside E and rubrofusarin. The abundance of both oligosaccharides was much greater in 'Cresthaven', with highest abundance of suffriticoside E occurring during acclimation, and highest abundance of rubrofusarin occurring during maximum hardiness. Seven flavonoid compounds were found to be significantly different in abundance across the five dormancy stages and the two cultivars, with 3 genotypic differences, all in favor of 'Sierra Rich'.

These three flavonoids included: kaempferol 3-rhamnosyl-(1->2)(6''-acetylgalactoside)-7-rhamnoside, kaempferol 3-galactoside-7-rhamnoside, quercetin 3-(4''-acetylrhamnoside)-7-rhamnoside. Flavonoids including kaempferol derivatives, quercetin derivatives and proteins related to flavonoid biosynthesis are known to be related to abiotic stress as well as having an involvement in bud dormancy of *Prunus* spp. (Ashraf et al., 2018; Bai et al., 2013; Baldermann et al., 2018; Di Ferdinando et al., 2012). However, we did not observe a corresponding increase in cold hardiness for 'Sierra Rich' with higher flavonoid abundance. It is possible that the higher abundance of flavonoids was served as a signal ROS scavenging in the more cold-stressed genotype.

Overall, the superclass of lipids, and lipid-like molecules accounted for over 1/3 of the significantly changed secondary metabolites. Prenol lipids is a class of compounds comprised of terpenes and terpenoids which are also known to be related to stress responses in plants. Of the 7 prenol lipids found to change significantly throughout the season, 3 compounds were observed to be significantly higher in abundance in 'Cresthaven' as compared to 'Sierra Rich'. These included the sesquiterpenoids, anhydroretinol and 2-octa.-3-meth.-6-meth-1,4-benzoquinol and the terpene-glycoside, retinyl beta-glucuronide. The most interesting trends from this interpretation of secondary metabolites analysis throughout the season were the oligosaccharides and terpenes relationship with H_c, and the relationship of flavonoids to abiotic stress. These trends indicate that hardy peach genotypes may express terpenoids and oligosaccharides to help tolerate cold stress.

Principal component analysis of the proteomic data revealed separation between deacclimation and the other dormancy phases, however, maximum hardiness and acclimation overlapped **(Figure 4.4a)**. Genotypic separation was only clear at deacclimation. Repeated measures ANOVA identified 24 significant proteins varying in expression over time, with

peroxidase (8G289400) representing the only significant change between genotypes. Variable clustering was performed to aggregate correlated protein abundance across the samples. Elongation factor tu (EF-Tu) was classified in protein cluster 4.1, and showed peak expression in early acclimation. EF-Tu is involved in translation elongation, which produces proteins. The trend of decreasing abundance in EF-Tu indicates less proteins are needed as dormancy progress, however, in 'Sierra Rich' a there is a second "abundance peak" of this protein after the maximum hardiness frost event. The high expression of EF-Tu on Jan. 9, 2016 may indicate that since 'Sierra Rich' had met its chill requirements and entered ecodormancy prior to the frost there was a stress response necessitating the production of more proteins as a result **(Figure 4.3b and c)**. Protein cluster 4.2 included proteins which were up or down regulated during the time of maximum hardiness. This includes tubulin alpha chain (TAC), which is involved in mitosis, a process which intuitively would be less common during cold temperatures and suspended growth in endodormancy. The slow rise in TAC in 'Sierra Rich' from January 3 to March 3, 2017 may be a result of the onset of ecodormancy following chilling satisfaction. Flavanone-3-hydroxylase (F3H) is critical to the biosynthesis of flavanones, and high expression in 'Sierra Rich' compared to 'Cresthaven' may be because flavonoids tended to be more prevalent in 'Sierra Rich'. Glutathione peroxidase is most highly expressed at the coldest part of the winter, during maximum hardiness, in both genotypes. The glutathione-ascorbate pathway is the principal ROS scavenging pathway, thus the observed expression was expected because of the high levels of ROS produced by cold stress. Protein cluster 4.3 expression tends to follow a relatively linear upward or downward trend across the dormant season. Starch synthase is highly expressed during acclimation, and is not expressed beyond acclimation. High expression in acclimation is expected because sugars are

being synthesized into starch reserves for storage to be used throughout the dormant season and during spring.

4.4.2 Modulations in peach floral bud H_c, metabolome and proteome following acute freezing events at different phases of dormancy.

Following two separate frost events during dormancy the H_c of 'Cresthaven' increased more dramatically than that of 'Sierra Rich'. This is likely because 'Sierra Rich' was not selected for its ability to tolerate cold, whereas cold tolerance was a requisite trait for 'Cresthaven', having been bred in a location with consistently cold dormant seasons. Chilling requirements for peach are not well established in literature, however 650-700 chilling hours (<7.2 ºC) is the reported chilling requirement for 'Sierra Rich' from breeders and nursery sources. Chilling accumulation surpassed this threshold on December 13, 2016 **(Figure 4.1c)**. 'Cresthaven' likely has a chilling requirement of around 850 chilling hours (0-7.2 ºC), which was surpassed in January 23, 2017. These data would suggest that during the maximum hardiness phase, 'Sierra Rich' was in ecodormancy phase, while 'Cresthaven' was still in endodormancy, have not yet fulfilled the chilling requirement. This observation is necessary to consider when comparing post-frost floral bud metabolite and protein responses to cold stress during maximum hardiness between the two cultivars.

Post-frost kinetics of primary metabolites revealed that 'Sierra Rich' had more significantly modulated metabolome than 'Cresthaven', although accompanied by a comparatively minor gain in H_c **(Table 4.1; Figure 4.5)**. Changes in primary metabolites were more common in 'Sierra Rich,' however, many of these changes were negative shifts. The sugar alcohols myo-inositol and glycerol both significantly declined in abundance following the acclimation frost event. These sugar alcohols contribute to the cells' ability to supercool as osmolytes, however literature also

suggests they have a role in scavenging ROS (Ahmad and Wani, 2014; Nishizawa-Yokoi et al., 2008). This suggests that having failed to alleviate sufficient stress as osmolytes in 'Sierra Rich' floral bud tissues (e.g., floral primordia) might have allowed for additional increase of ROS levels following the freezing event. The increased stress and consequently the increased ROS levels might have oxidized more dramatically these sugar alcohols in the non-hardy cultivar, decreasing their abundance following the event. Oxidation of primary metabolites is one way to account for the reduced abundance of primary metabolites in floral buds after a stress event that would result in ROS generation. Raffinose and RFOs are known to be related to cold hardiness and cold stress, preventing cellular damage through several different mechanisms, and there was a significant gain in 'Cresthaven' following the acclimation frost. The increase in raffinose abundances likely played a large role in increasing cold tolerance, and acclimating 'Cresthaven' more quickly than 'Sierra Rich'. However, across the entirety of the season, repeated measures ANOVA did not detect a genotypic difference, and raffinose abundance was remarkably similar between genotypes outside of the acclimation frost response. The similarity between the two genotypes with regards to raffinose suggests that the soluble sugar is a critical primary cryoprotectant for both genotypes, and not a major season-wide difference between the two.

Proline and other AAs, have been associated with cold hardiness in past studies (Hayat et al., 2012). A comparison of the total AA abundance across all significantly changed AAs (glutamic acid, proline, glycine, valine, isoleucine and pyroglutamic acid; **Figure 4.2b and c**) among the analyzed floral bud samples revealed a consistently significant and vast difference in AA abundance between genotypes **(Figure 4.5e)**. A difference of a factor from 2.8-4.0 times was found for the four dormancy dates during acclimation and maximum hardiness between the two cultivars with 'Creshaven' exhibiting higher total abundance of AA levels. This is strong evidence that

genotypes linked to hyper-accumulation of AAs within floral tissues could be more cold-tolerant. Proteins, crucial for enzymatic facilitation of all metabolic pathways in plants, consist of long chains of amino acids. Glutathione, one of the main antioxidant compounds found in plants is the combination of three AA, glycine, glutamate and cysteine (Barba-Espín et al., 2022; Choudhury et al., 2017; Cooke et al., 2012; Di Ferdinando et al., 2012; Gill et al., 2013; Hasanuzzaman et al., 2017; Ruelland et al., 2009). In addition, tetrapyrroles, specialized stress related signaling molecules are also largely made up of AA (Zhang et al., 2015). Significant tetrapyrroles from this study include precorrin 3-B and Uroporphrinogen III, both of which were highly expressed during max hardiness in 'Cresthaven' post-frost **(Figure 4.6c)**.

A high number of changes were expressed in the secondary metabolome of 'Sierra Rich' floral buds **(Figure 4.6d)**. While this included multiple organic acids, organic oxygen compounds, organoheterocyclic compounds and phenylpropanoids and polyketides, the greatest difference was in the change in lipid and lipid-like compounds following freezing events. However, it was observed that the total abundance of all 7 prenol lipids found to be significantly changed across the samples by repeated measures ANOVA. the same statistical analysis approach revealed a much higher abundance of prenol lipids in 'Cresthaven', with 60-170% higher accumulation across all acclimation and maximum hardiness dates **(Figure 4.6e)**. Prenol lipids include terpenes, terpenoids, and xanthophylls, some of which have been found to increase cold tolerance or be express highly as a result of abiotic stress in past studies (Ruelland et al., 2009; Zhang et al., 2017; Zhao et al., 2020; Zhou et al., 2020). The association of prenol lipid accumulation with increases of H_c in a cold hardy peach cultivar is a significant finding for breeders selecting for certain metabolic traits in breeding cold hardy cultivars. Specific subfamilies of compounds within the superclass of prenol lipids which were linked with H_c in 'Cresthaven' in the present data set are

sesquiterpenoids (anhydroretinol), monoterpenoids (pimilprost), terpeneglycosides (retinyl beta-glucuronide) and xanthophylls (1,1',2,2',7,8'-Hexahydro-1'-hydroxy-1-methoxy-psi, psi-caroten-4-one) **(Figure 4.3c and 4.6c)**. One previous study has reported suppression of the gene responsible for expressing a specific sesquiterpene (nerolidol) resulted in reduced the cold tolerance of tea (*Camellia sinensis*) and the ability to reduce ROS levels (Zhao et al., 2020). The same study verified the findings of the molecular analysis by applying sesquiterpene in tea plants that became more tolerant to cold temperatures following treatment. While that study was performed on a non-dormant plant unlike the current study, the findings support the high prevalence of similar compounds in the more cold hardy peach genotype could be related to increased cold tolerance.

Several oligosaccharides, suffriticoside E and Rubrofusarin 6-[glucosyl-(1->3)-glucosyl-(1->6)-glucoside] (RGGG) were strongly linked to 'Cresthaven' throughout dormancy, as well as after acclimation or maximum hardiness frost, while having almost corresponding abundance in the less hardy 'Sierra Rich'. The high levels of abundance of these oligosaccharides supports previous findings in literature with regards to oligosaccharides and cold tolerance. Similar trends were seen in the tetrapyrroles precorrin-3B and uroporphyrinogen III that were detected in the same samples. These tetrapyrroles are large glutamate based molecules similar to heme or chlorophyll a molecules (Bali et al., 2014). Uroporphyrinogen III is a precursor to Mg-protoporphyrin IX, a compound that has been linked to cold tolerance and other abiotic stressors, as well as retrograde signaling leading to upregulation of antioxidant enzymes and compounds during cold stress (Zhang et al., 2016, 2015).

Although comparatively few primary metabolites were found through volcano plot analysis, several significant findings may provide insight into cold stress response of peach floral

buds. Peptidyl-prolyl isomerase (PPase) was increased in abundance following acclimation frost. PPase has a role in catalyzing a rate-limiting folding process involved in proline linkage in proteins, and has been related to cold stress and hormone signaling in plants (Singh et al., 2020; Yoon et al., 2016). This may indicate the up regulation of PPase led to the more efficient use of proline, more efficient use of proline related proteins, and the immediate H_c response of 'Cresthaven' flower buds to the cold stress. 'Sierra Rich' exhibited significant gains in carboxypeptidase and elongation factor 1-alpha (EF1a), both of which have links to translation. Carboxypeptidase aids in the modification of proteins after translation, which could indicate it is allowing damaged proteins to repair following ROS damage, or aiding in modification of proteins to better withstand ROS stress. EF1a is necessary for translation similarly to EF-tu, and is overexpressed at the same time as EF-tu in 'Sierra Rich'. An increase in translation activity after a stressful freezing event may be a symptomatic response of ecodormant floral buds, since this is not seen in 'Cresthaven,' which were still endodormant, or following the acclimation freezing event during endodormancy in 'Sierra Rich'. The consistent up-regulation of 5-(hydroxymethyl) glutathione dehydroxylase following freeze events, although only significant once, suggests the activity of the glutathione-ascorbate cycle is active in the dormant buds of both genotypes for ROS scavenging during abiotic stress.

4.4.3 Combined macro-analysis of peach floral bud metabolome and proteome contextualizes changes across systems during dormancy transitions of a hardy and non-hardy cultivar

Combining variable clustering analysis of all annotated primary, and secondary metabolites and proteins with PCA provided an opportunity to collocate associated variables with their associations along genotypes during dormancy transitions. Combining principal component loadings with cluster analysis of 8.1 it is clear that time is a significant driver of all the proteomic

and metabolic features within that cluster. Clustering suggests positively correlated primary, and secondary metabolites and proteins within cluster 8.1, such as proline, are associated with deacclimation, while negatively correlated ones, such as glucose-6-phosphate isomerase, are associated with acclimation given their placement on the PCA biplot (**Figure 4.8a and b)**. Cluster 8.2 are in the furthest edge of quadrant 3, indicating their influence over the placement of 'Cresthaven' within the biplot, and lack of association with 'Sierra Rich'. Examples of metabolites associated with 'Cresthaven' include: anhydroretinol, retinyl-beta glucuronide, and bistramide C (**Figure 4.8a and b)**. While positively correlated features within cluster 8.5, such as flavanone-3-hydroxylase are highly associated with 'Sierra Rich', and relatively unassociated with 'Cresthaven' (**Figure 4.8a and b)**. This combined analysis provides extra insight into genotype, time and stress associations with different primary and secondary metabolites and proteins which are yet to be found significant across other tests, and confirms findings of other tests. It also provides a way to relativize the effects of different types of metabolic features across different detection platforms.

4.5. Conclusions

This study is the first of its kind to combine a detailed analysis of cold hardiness, and the global metabolic and proteomic framework of dormant peach floral buds in order to identify critical molecules related to H_c and dormancy transitions. Marginal increases in H_c between two peach genotypes in response to two significant frost events, drove differential cold tolerance responses, and distinct metabolic and proteomic changes. Numerous candidate molecules and classifications of molecules have been put forth as being associated with the increasing cold tolerance of 'Cresthaven' peach floral buds. Proline and other AA, the backbones of proteins, glutathione and tetrapyrroles are highly accumulated in the hardy genotype relative to the non-

hardy genotype. Significant prenol lipids including anhydroretinol and retinyl beta-glucuronide in subclasses such as: terpenes, terpenoids and xanthophylls were highly accumulated throughout the dormant season in association with greater H_c. Oligosaccharides such as RGGG, and suffriticoside E as well as raffinose were highly associated with greater H_c. In addition to these associations, this work presents clusters of many other proteomic and metabolic features found to be highly correlated with known contributors to H_c, abiotic stress, and dormancy in peach floral buds.

4.6. References:

Ahmad, P., Wani, M.R., 2014. Physiological mechanisms and adaptation strategies in plants under changing environment: Volume 1, Physiological Mechanisms and Adaptation Strategies in Plants Under Changing Environment: Volume 1. https://doi.org/10.1007/978-1-4614-8591-9

Ashraf, M.A., Iqbal, M., Rasheed, R., Hussain, I., Riaz, M., Arif, M.S., 2018. Environmental stress and secondary metabolites in plants, plant metabolites and Rregulation under environmental stress. Elsevier Inc. https://doi.org/10.1016/B978-0-12-812689-9.00008-X

Ashworth, E.N., 1984. Xylem development in prunus flower buds and the relationship to deep supercooling . Plant Physiol. 74, 862–865. https://doi.org/10.1104/pp.74.4.862

Ashworth, E.N., 1982. Properties of peach flower buds which facilitate supercooling. Low Temp. Stress Physiol. Crop. 153–157. https://doi.org/10.1201/9781351074186

Ashworth, E.N., Abeles, F.B., 1984. Freezing behavior of water in small pores and the possible role in the freezing of plant tissues. Plant Physiol. 76, 201–204. https://doi.org/10.1104/pp.76.1.201

Bai, S., Saito, T., Sakamoto, D., Ito, A., Fujii, H., Moriguchi, T., 2013. Transcriptome Analysis of Japanese Pear (Pyrus pyrifolia Nakai) Flower Buds Transitioning Through Endodormancy. Plant and cell physiology, 54, 1132–1151. https://doi.org/10.1093/pcp/pct067

Baldermann, S., Homann, T., Neugart, S., Chmielewski, F.M., Tz, K.P.G., Deke, K.G., Huschek, G., Morlock, G.E., Rawel, H.M., 2018. Selected plant metabolites involved in oxidation-reduction processes during bud dormancy and ontogenetic development in sweet cherry buds (Prunus avium L.). Molecules 23. https://doi.org/10.3390/molecules23051197

Bali, S., Palmer, D.J., Schroeder, S., Ferguson, S.J., Warren, M.J., 2014. Recent advances in the biosynthesis of modified tetrapyrroles: The discovery of an alternative pathway for the

formation of heme and heme d 1. Cell. Mol. Life Sci. 71, 2837–2863. https://doi.org/10.1007/s00018-014-1563-x

Barba-Espín, G., Hernández, J.A., Díaz-Vivancos, P., 2022. Antioxidant system: The hub of bud dormancy regulation in Prunus sp. Sci. Hortic. (Amsterdam). 305. https://doi.org/10.1016/j.scienta.2022.111396

Beyá-Marshall, V., Herrera, J., Santibáñez, F., Fichet, T., 2019. Microclimate modification under the effect of stationary and portable wind machines. Agric. For. Meteorol. 269–270, 351–363. https://doi.org/10.1016/j.agrformet.2019.01.042

Bonhomme, M., Rageau, R., Lacointe, A., 2010. Optimization of endodormancy release models , ssing series of endodormancy release data collected in France 51–60. incomplete referenceBroeckling, C.D., Afsar, F.A., Neumann, S., Ben-Hur, A., Prenni, J.E., 2014. RAMClust: A novel feature clustering method enables spectral-matching-based annotation for metabolomics data. Anal. Chem. 86, 6812–6817. https://doi.org/10.1021/ac501530d

Broeckling, C.D., Prenni, J.E., 2018. Stacked Injections of Biphasic Extractions for Improved Metabolomic Coverage and Sample Throughput. Anal. Chem. 90, 1147–1153. https://doi.org/10.1021/acs.analchem.7b03654

Burke, M.J., Gusta, L. V, Quamme, H.A., Weiser, C.J., Li, P.H., 1976. Freezing and injury in plants. Annu. Rev. Plant Physiol. 27, 507–528. https://doi.org/10.1146/annurev.pp.27.060176.002451

Choudhury, F.K., Rivero, R.M., Blumwald, E., Mittler, R., 2017. Reactive oxygen species, abiotic stress and stress combination. Plant J. 90, 856–867. https://doi.org/10.1111/tpj.13299

Cooke, J.E.K., Eriksson, M.E., Junttila, O., 2012. The dynamic nature of bud dormancy in trees: Environmental control and molecular mechanisms. Plant, Cell Environ. 35, 1707–1728.

https://doi.org/10.1111/j.1365-3040.2012.02552.

Di Ferdinando, M., Brunetti, C., Fini, Al., Tattini, M., 2012. Flavanoids as antioxidants in plants under abiotic stresses. In P. Ahmad and M.N.V. Prasad (Eds.), *Abiotic stress responses in plants: Metabolism, productivity*. Abiotic Stress New Res. (171–180). Springer Science+Business Media. https://doi.org/10.1007/978-1-4614-0634-1

Djoumbou Feunang, Y., Eisner, R., Knox, C., Chepelev, L., Hastings, J., Owen, G., Fahy, E., Steinbeck, C., Subramanian, S., Bolton, E., Greiner, R., Wishart, D.S., 2016. ClassyFire: automated chemical classification with a comprehensive, computable taxonomy. J. Cheminform. 8, 1–20. https://doi.org/10.1186/s13321-016-0174-y

Fadón, E., Herrera, S., Guerrero, B.I., Guerra, M.E., Rodrigo, J., 2020. Chilling and heat requirements of temperate stone fruit trees (*Prunus* sp.). Agronomy 10, 409. doi10.3390/agronomy10030409

Gill, S.S., Anjum, N.A., Hasanuzzaman, M., Gill, R., Trivedi, D.K., Ahmad, I., Pereira, E., Tuteja, N., 2013. Glutathione and glutathione reductase: A boon in disguise for plant abiotic stress defense operations. Plant Physiol. Biochem. 70, 204–212. https://doi.org/10.1016/j.plaphy.2013.05.032

Götz, K.P., Chmielewski, F.M., Gödeke, K., Wolf, K., Jander, E., Sievers, S., Homann, T., Huschek, G., Rawel, H.M., 2017. Assessment of amino acids during winter rest and ontogenetic development in sweet cherry buds (Prunus avium L.). Sci. Hortic. (Amsterdam). 222, 102–110. https://doi.org/10.1016/j.scienta.2017.05.001

Granot, D., David-Schwartz, R., Kelly, G., 2013. Hexose kinases and their role in sugar-sensing and plant development. Front. Plant Sci. 4, 1–17. https://doi.org/10.3389/fpls.2013.00044

Gusta, L. V., Wisniewski, M., Nesbitt, N.T., Gusta, M.L., 2004. The effect of water, sugars, and

proteins on the pattern of ice nucleation and propagation in acclimated and nonacclimated canola leaves. Plant Physiol. 135, 1642–1653. https://doi.org/10.1104/pp.103.028308

Hasanuzzaman, M., Nahar, K., Anee, T.I., Fujita, M., 2017. Glutathione in plants: biosynthesis and physiological role in environmental stress tolerance. Physiol. Mol. Biol. Plants 23, 249–268. https://doi.org/10.1007/s12298-017-0422-2

Hayat, S., Hayat, Q., Alyemeni, M.N., Wani, A.S., Pichtel, J., Ahmad, A., 2012. Role of proline under changing environments: A review. Plant Signal. Behav. 7, 1456–1466. https://doi.org/10.4161/psb.21949

Hernandez, J.A., Díaz-Vivancos, P., Martínez-Sánchez, G., Alburquerque, N., Martínez, D., Barba-Espín, G., Acosta-Motos, J.R., Carrera, E., García-Bruntón, J., 2021. Physiological and biochemical characterization of bud dormancy: Evolution of carbohydrate and antioxidant metabolisms and hormonal profile in a low chill peach variety. Sci. Hortic. (Amsterdam). 281. https://doi.org/10.1016/j.scienta.2021.109957

Hummel, J., Selbig, J., Walther, D. and Kopka, J., 2007. The Golm Metabolome Database: a database for GC-MS based metabolite profiling. Metabolomics 18, 75-95.

Hummel, J., Strehmel, N., Bölling, C., Schmidt, S., Walther, D. and Kopka, J., 2013. Mass spectral search and analysis using the golm metabolome database. The Handbook of Plant Metabolomics 321-343.

Islam, M.T., Liu, J., Sherif, S.M., 2021. Ethephon-mediated bloom delay in peach is associated with alterations in reactive oxygen species, antioxidants, and carbohydrate metabolism during dormancy. Front. Plant Sci. 12. https://doi.org/10.3389/fpls.2021.765357

Käll, L., Storey, J.D., MacCoss, M.J., Noble, W.S., 2008. Assigning significance to peptides identified by tandem mass spectrometry using decoy databases. J. Proteome Res. 7, 29–34.

https://doi.org/10.1021/pr700600n

Kaur, G., Asthir, B., 2015. Proline: a key player in plant abiotic stress tolerance. Biol. Plant. 59, 609–619. https://doi.org/10.1007/s10535-015-0549-3

Kaur, H., Chowrasia, S., Gaur, V.S., Mondal, T.K., 2016. Allantoin: emerging role inplant abiotic stress tolerance. Plant Mol. Biol. Report. 39, 648–661. https://doi.org/10.1007/s11105-021-01280-z

Kovaleski, A., 2021. Woody species do not differ in dormancy progression: differences in time to budbreak due to forcing and cold hardiness. BioRxiv 1–12. https://doi.org/10.1073/pnas.2112250119/-/DCSupplemental.Published

Lang, G.A., Early, J.D., Martin, G.C., Darnelll, R.L., 1987. Endodormancy, paradormancy, and ecodormancy - physiological terminology and classification for dormancy research. HortScience 22, 371–377.

Li, Y., Wang, L., 2020. Genetic resources, breeding programs in China, and gene mining of peach: a review. Hortic. Plant J. 6, 205–215. https://doi.org/10.1016/j.hpj.2020.06.001

Linsley-Noakes, G.C., Allan, P., 1994. Comparison of two models for the prediction of rest completion in peaches. Sci. Hortic. (Amsterdam). 59, 107–113. https://doi.org/10.1016/0304-4238(94)90077-9

Liu, J., Lindstrom, O.M., Chavez, D.J., 2019. Differential thermal analysis of ‘Elberta’ and ‘Flavorich’ peach flower buds to predict cold hardiness in Georgia. HortScience 54, 676–683. https://doi.org/10.21273/HORTSCI13518-18

Lu, Y., Hu, Y., Zhao, C., Snyder, R.L., 2018. Modification of water application rates and intermittent control for sprinkler frost protection. American Society of Agricultural and Biological Engineers 61, 4.1277–1285.

Luedeling, E., Kunz, A., Blanke, M.M., 2013. Identification of chilling and heat requirements of cherry trees-a statistical approach. Int. J. Biometeorol. 57, 679–689. https://doi.org/10.1007/s00484-012-0594-y

Maurel, K., Leite, G.B., Bonhomme, M., Guilliot, A., Rageau, R., Pétel, G., Sakr, S., 2004a. Trophic control of bud break in peach (Prunus persica) trees: A possible role of hexoses. Tree Physiol. 24, 579–588. https://doi.org/10.1093/treephys/24.5.579

Maurel, K., Sakr, S., Gerbe, F., Guilliot, A., Bonhomme, M., Rageau, R., Pétel, G., 2004b. Sorbitol uptake is regulated by glucose through the hexokinase pathway in vegetative peach-tree buds. J. Exp. Bot. 55, 879–888. https://doi.org/10.1093/jxb/erh087

Michailidis, M., Karagiannis, E., Tanou, G., Sarrou, E., Adamakis, I.D., Karamanoli, K., Martens, S., Molassiotis, A., 2018. Metabolic mechanisms underpinning vegetative bud dormancy release and shoot development in sweet cherry. Environ. Exp. Bot. 155, 1–11. https://doi.org/10.1016/j.envexpbot.2018.06.024

Mills, Lynn J., Ferguson, J.C., Keller, M., 2006. Cold-hardiness evaluation of grapevine buds and cane tissues. Am. J. Enol. Vitic. 57, 194-200.

Minas, I.S., Blanco Cipollone, F., Sterle, D., 2020. Near infrared spectroscopy can non-destructively assess the effect of canopy position and crop load on peach fruit maturity and quality. Acta Hortic. 1281, 407–412. https://doi.org/10.17660/actahortic.2020.1281.54

Minas, I.S., Sterle, D., 2020. Differential thermal analysis sheds light on the effect of environment and cultivar in peach floral bud cold hardiness. Acta Hortic. 1281, 385–391. https://doi.org/10.17660/ActaHortic.2020.1281.51

Nesvizhskii, A.I., Keller, A., Kolker, E., Aebersold, R., 2003. A statistical model for identifying proteins by tandem mass spectrometry. Anal. Chem. 75, 4646–4658.

https://doi.org/10.1021/ac0341261

Nishizawa-Yokoi, A., Yabuta, Y., Shigeoka, S., 2008. The contribution of carbohydrates including raffinose family oligosaccharides and sugar alcohols to protection of plant cells from oxidative damage. Plant Signal. Behav. https://doi.org/10.4161/psb.6738

Okie, W.R., 1998. Handbook of peach and nectarine varieties.

Okie, W.R., Blackburn, B., 2011. Increasing chilling reduces heat requirement for floral budbreak in peach. HortScience 46, 245–252. https://doi.org/10.21273/hortsci.46.2.245

Pelletier, M.K., Winkel-Shirley, B., 1996. Analysis of flavanone 3-hydroxylase in Arabidopsis seedlings. Plant Physiol. 111, 339–345.

Preedy, K., Brennan, R., Jones, H., Gordon, S., 2020. Improved models of the effects of winter chilling on blackcurrant (Ribes nigrum L.) show cultivar specific sensitivity to warm winters. Agric. For. Meteorol. 280, 107777. https://doi.org/10.1016/j.agrformet.2019.107777

Proebsting, E. L. and Mills, H.H., 1978. Low temperature resistance of developing flower buds of 6 deiduous fruit species. Journal Am. Soc. Hortic. Sci. 103, 192–198.

Quamme, H.A., 1991. Application of thermal analysis to breeding fruit crops for increased cold hardiness. HortScience 26, 513–517. https://doi.org/10.21273/hortsci.26.5.513

Quamme, H.A., 1986. A. 1986.Use of thermal analysis to measure freezing resistance of grape buds. Can. J. Plant Sci. 952, 945–952.

Ruelland, E., Vaultier, M.N., Zachowski, A., Hurry, V., 2009. Chapter 2 cold signalling and cold acclimation in plants, 1st ed, Advances in Botanical Research. Elesvier Ltd. https://doi.org/10.1016/S0065-2296(08)00602-2

Salazar-Gutiérrez, M.R., Chaves, B., Anothai, J., Whiting, M., Hoogenboom, G., 2014. Variation in cold hardiness of sweet cherry flower buds through different phenological stages. Sci.

Hortic. (Amsterdam). 172, 161–167. https://doi.org/10.1016/j.scienta.2014.04.002

Sarkar, D., Bhowmik, P.C., Kwon, Y.I., Shetty, K., 2009. Clonal response to cold tolerance in creeping bentgrass and role of proline-associated pentose phosphate pathway. Bioresour. Technol. 100, 5332–5339. https://doi.org/10.1016/j.biortech.2009.03.086

Scandalios, J.G., 2005. Oxidative stress: Molecular perception and transduction of signals triggering antioxidant gene defenses. Brazilian J. Med. Biol. Res. 38, 995–1014. https://doi.org/10.1590/S0100-879X2005000700003

Schauer, K.L., Freund, D.M., Prenni, J.E., Curthoys, N.P., 2013. Proteomic profiling and pathway analysis of the response of rat renal proximal convoluted tubules to metabolic acidosis. Am. J. Physiol. - Ren. Physiol. 305, 628–640. https://doi.org/10.1152/ajprenal.00210.2013

Schulz, E., Tohge, T., Zuther, E., Fernie, A.R., Hincha, D.K., 2016. Flavonoids are determinants of freezing tolerance and cold acclimation in Arabidopsis thaliana. Sci. Rep. 6, 1–10. https://doi.org/10.1038/srep34027

Shen, G., Pang, Y., Wu, W., Deng, Z., Zhao, L., Cao, Y., Sun, X., Tang, K., 2006. Cloning and characterization of a flavanone 3-hydroxylase gene from Ginkgo biloba. Biosci. Rep. 26, 19–29. https://doi.org/10.1007/s10540-006-9007-y

Shin, H., Oh, S., Arora, R., Kim, D., 2016. Proline accumulation in response to high temperature in winter-acclimated shoots of Prunus persica: A response associated with growth resumption or heat stress? Can. J. Plant Sci. 96, 630–638. https://doi.org/10.1139/cjps-2015-0372

Siddique, A., Kandpal, G., Kumar, P., 2018. Proline accumulation and its defensive role under diverse stress condition in plants: An overview. J. Pure Appl. Microbiol. https://doi.org/10.22207/JPAM.12.3.73

Singh, H., Kaur, K., Singh, M., Kaur, G., Singh, P., 2020. Plant cyclophilins: multifaceted proteins

with versatile roles. Front. Plant Sci. 11, 1–30. https://doi.org/10.3389/fpls.2020.585212

Smith, C.A., Want, E.J., O'Maille, G., Abagyan, R., Siuzdak, G., 2006. XCMS: Processing mass spectrometry data for metabolite profiling using nonlinear peak alignment, matching, and identification. Anal. Chem. 78, 779–787. https://doi.org/10.1021/ac051437y

Stushnoff, C., Junttila, O., 1986. Seasonal development of cold stress resistance in several plant species at a coastal and a continental location in North Norway. Polar Biol. 5, 129–133. https://doi.org/10.1007/BF00441691

Szalay, L., Timon, B., Németh, S., Papp, J., Tóth, M., 2010. Hardening and dehardening of peach flower buds. HortScience 45, 761–765. https://doi.org/10.21273/hortsci.45.5.761

Vickers, C.E., Gershenzon, J., Lerdau, M.T., Loreto, F., 2009. A unified mechanism of action for volatile isoprenoids in plant abiotic stress. Nat. Chem. Biol. 5, 283–291. https://doi.org/10.1038/nchembio.158

Vimont, N., Fouché, M., Campoy, J.A., Tong, M., Arkoun, M., Yvin, J.C., Wigge, P.A., Dirlewanger, E., Cortijo, S., Wenden, B., 2019. From bud formation to flowering: Transcriptomic state defines the cherry developmental phases of sweet cherry bud dormancy. BMC Genomics 20, 1–23. https://doi.org/10.1186/s12864-019-6348-z

Waśkiewicz, A., Beszterda, M., Goliński, P., 2014. Nonenzymatic Antioxidants in Plants, Oxidative Damage to Plants: Antioxidant Networks and Signaling. https://doi.org/10.1016/B978-0-12-799963-0.00007-1

Watanabe, S., Kounosu, Y., Shimada, H., Sakamoto, A., 2014. Arabidopsis xanthine dehydrogenase mutants defective in purine degradation show a compromised protective response to drought and oxidative stress. Plant Biotechnol. 31, 173–178. https://doi.org/10.5511/plantbiotechnology.14.0117a

Whiting, M.D., Salazar, M.R., Hoogenboom, G., 2015. Development of bloom phenology models for tree fruits. Acta Hortic. 1068, 107–112. https://doi.org/10.17660/ActaHortic.2015.1068.12

Wisniewski, M., Gusta, L., Neuner, G., 2014. Adaptive mechanisms of freeze avoidance in plants: A brief update. Environ. Exp. Bot. 99, 133–140. https://doi.org/10.1016/j.envexpbot.2013.11.011

Yoon, D.H., Lee, S.S., Park, H.J., Lyu, J. Il, Chong, W.S., Liu, J.R., Kim, B.G., Ahn, J.C., Cho, H.S., 2016. Overexpression of OsCYP19-4 increases tolerance to cold stress and enhances grain yield in rice (Oryza sativa). J. Exp. Bot. 67, 69–82. https://doi.org/10.1093/jxb/erv421

Yu, D.J., Hwang, J.Y., Chung, S.W., Oh, H.D., Yun, S.K., Lee, H.J., 2017. Changes in cold hardiness and carbohydrate content in peach (Prunus persica) trunk bark and wood tissues during cold acclimation and deacclimation. Sci. Hortic. (Amsterdam). 219, 45–52. https://doi.org/10.1016/j.scienta.2017.02.038

Yun, S.K., Bae, H., Chung, K.-H., Yoon, I.K., Nam, E.Y., Kwon, J.H., Jun, J.H., 2014. Sugar, starch, and proline in peach trees exposed to freezing temperatures during dehardening. Agric. Sci. 05, 913–921. https://doi.org/10.4236/as.2014.510099

Zaiger, C.F., Zaiger, G.N., Gardner, L.M., Zaiger, G.G., 2002. United States Plant Patent, Patent No.: US PP12,391 P2, Peach Tree name “Sierra Rich.”

Zhang, X., Da Silva, J.A.T., Niu, M., Li, M., He, C., Zhao, J., Zeng, S., Duan, J., Ma, G., 2017. Physiological and transcriptomic analyses reveal a response mechanism to cold stress in Santalum album L. Leaves. Sci. Rep. 7, 1–18. https://doi.org/10.1038/srep42165

Zhang, Z.W., Wu, Z.L., Feng, L.Y., Dong, L.H., Song, A.J., Yuan, M., Chen, Y.E., Zeng, J., Chen, G.D., Yuan, S., 2016. Mg-protoporphyrin IX signals enhance plant’s tolerance to cold stress.

Front. Plant Sci. 7, 1–12. https://doi.org/10.3389/fpls.2016.01545

Zhang, Z.W., Zhang, G.C., Zhu, F., Zhang, D.W., Yuan, S., 2015. The roles of tetrapyrroles in plastid retrograde signaling and tolerance to environmental stresses. Planta 242, 1263–1276. https://doi.org/10.1007/s00425-015-2384-3

Zhao, J., Davis, L.C., Verpoorte, R., 2005. Elicitor signal transduction leading to production of plant secondary metabolites. Biotechnol. Adv. 23, 283–333. https://doi.org/10.1016/j.biotechadv.2005.01.003

Zhao, M., Zhang, N., Gao, T., Jin, J., Jing, T., Wang, J., Wu, Y., Wan, X., Schwab, W., Song, C., 2020. Sesquiterpene glucosylation mediated by glucosyltransferase UGT91Q2 is involved in the modulation of cold stress tolerance in tea plants. New Phytol. 226, 362–372. https://doi.org/10.1111/nph.16364

Zhou, H.C., Shamala, L.F., Yi, X.K., Yan, Z., Wei, S., 2020. Analysis of Terpene Synthase Family Genes in *Camellia sinensis* with an Emphasis on Abiotic Stress Conditions. Sci. Rep. 10, 1–13. https://doi.org/10.1038/s41598-020-57805-1

4.7. Tables

Table 4.1. Cold hardiness (H_c) of peach floral buds on five dates from November 8, 2016 to March 3, 2017. Acclimation pre- and post- frost measurements were on either side of the first significant frost event (-6.8 °C) of the dormant season on November 18, 2016. Maximum hardiness pre- and post-frost measurements were taken at either side of the most significant frost event of the year (-18.6 °C) on January 6, 2017, after 601 chill units were accumulated. The deacclimation cold hardiness measurement was taken March 3, 2017. Marginal increase in cold hardiness (MICH) represents the increase in H_c between two measurements, while the relative genotypic increase in cold hardiness shows how great the change in hardiness of 'Cresthaven' (CH) was relative to 'Sierra Rich' (SR).

Dates	Dormancy	Chill Accumulation (0-7.2 °C)	Cresthaven			Sierra Rich		
			LT_{10}	LT_{50}	LT_{90}	LT_{10}	LT_{50}	LT_{90}
11/8/2016	**Acclimation Pre-frost**	73	-13.8	-15.9	-18.1	-12.3	-15.5	-18.0
11/21/2016	**Acclimation Post-frost**	189	-17.3	-19.1	-20.9	-13.6	-16.2	-18.8
Marginal Increase in Cold Hardiness (MICH)		-	*-3.5*	*-3.2*	*-2.8*	*-1.3*	*-0.7*	*-0.8*
Relative Genotypic Increase in Cold Hardiness (MICH CH/MICH SR) x100%		-	*269%*	*457%*	*350%*	-	-	-
1/3/2017	**Max Hardiness Pre-Frost**	586	-20.4	-21.9	-22.9	-18.9	-21.2	-22.8
1/9/2017	**Max Hardiness Post-Frost**	619	-22.6	-23.8	-25.0	-19.2	-22.2	-25.2
Marginal Increase in Cold Hardiness (MICH)		-	*-2.2*	*-1.9*	*-2.1*	*-0.3*	*-1.0*	*-2.4*
Relative Genotypic Increase in Cold Hardiness (MICH CH/MICH SR) x100%		-	*733%*	*190%*	*88%*	-	-	-
3/3/2017	**Deacclimation**	-	-12.3	-16.1	-19.6	-7.2	-9.4	-16.6

4.8. Figures

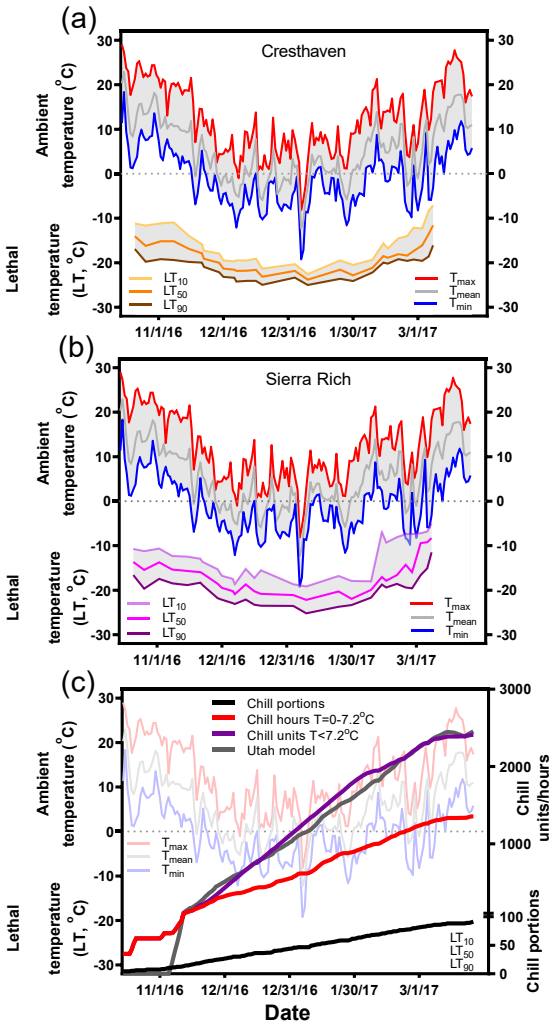

Figure 4.1. Seasonal patterns of temperature, cold hardiness, and chilling accumulation of 'Cresthaven' and 'Sierra Rich' flower buds. (a-b) Daily maximum, minimum and mean temperature data (from October 1, 2016, through April 1, 2017) and cold hardiness data for 'Cresthaven' (a) and 'Sierra Rich' (b) peach floral bud during the dormant season. Cold hardiness as measured by differential thermal analysis (DTA), and expressed as lethal temperature quantiles for 10, 50 and 90% flower bud loss (LT_{10}, LT_{50} and LT_{90}). (c) Chilling accumulation from October 1, 2016, through April 1, 2017, as calculated using four distinct chilling accumulation models: dynamic chill portions model, chill hours 0-7.2 ºC, chill hours <7.2 ºC, and the Utah chilling model. Daily temperature data and observed lethal temperatures were collected at the CSU's experimental orchard at WCRC-OM, Grand Junction, CO.

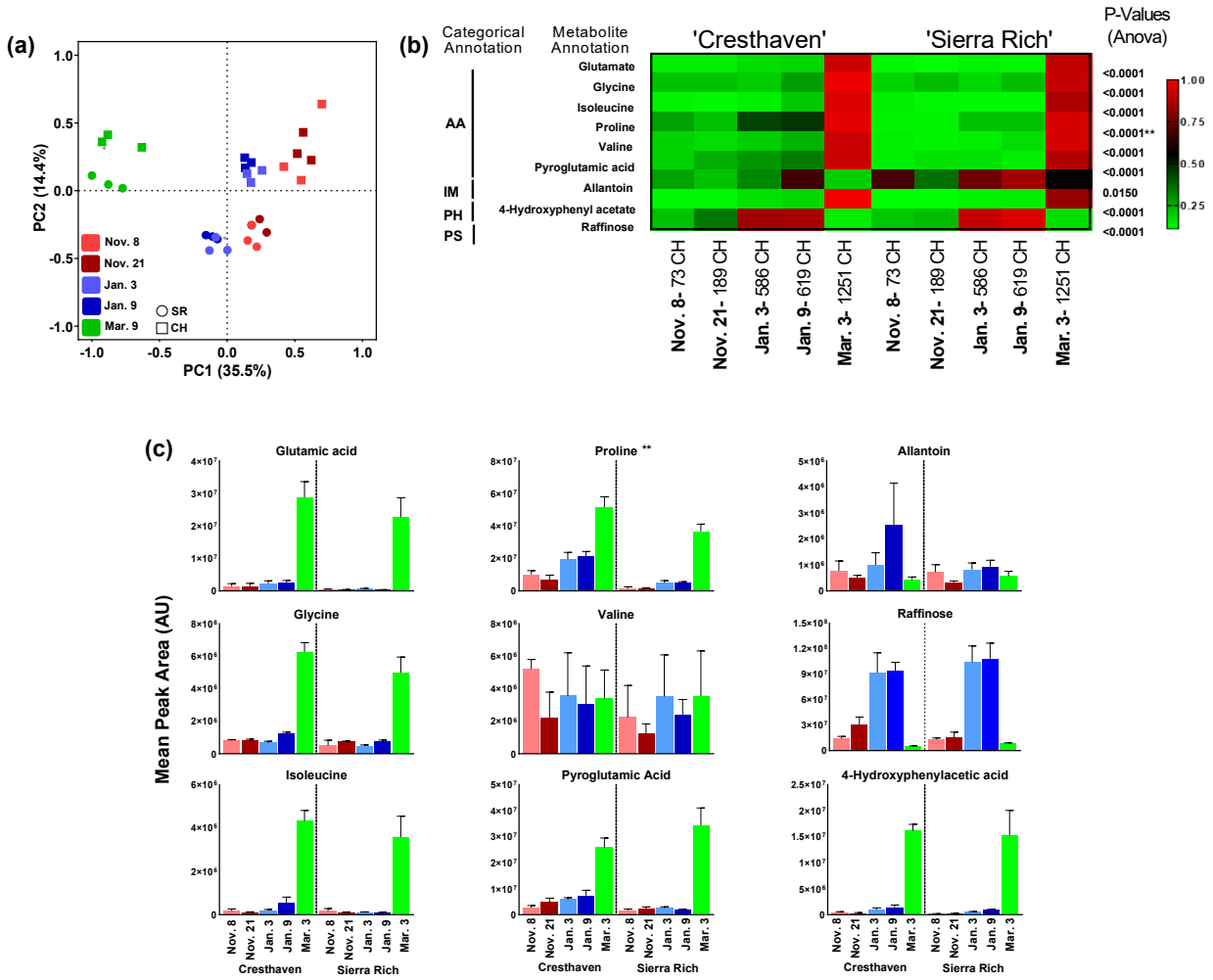

Figure 4.2. Dormant season kinetics of primary metabolites in flower buds of 'Cresthaven' and 'Sierra Rich' peach cultivars. Molecular feature abundance measured by non-targeted gas-chromatography mass spectrometry (GC-MS). (a) Principal component analysis (PCA) bi-plot of relative abundance of primary metabolites, with comparisons between two cultivars among five time points throughout the dormant season. (b) Heat map showing relative abundance, scaled within each cultivar, of primary metabolites determined to significantly change across five time points during the dormant season as determined by repeated measures ANOVA ($p<0.05$). Metabolic abundances differ between cultivars if denoted with "**". Different categorical annotations are indicated by abbreviations: AA-amino acids and derivatives, IM-Imidazole, PH-Phenol, PS-Polysaccharide. (c) Relative abundances of significant primary metabolites, as determine by repeated measures ANOVA to change across five time points. Proline was the only primary metabolite to significantly differ between peach genotypes. Error bars represent one standard deviation.

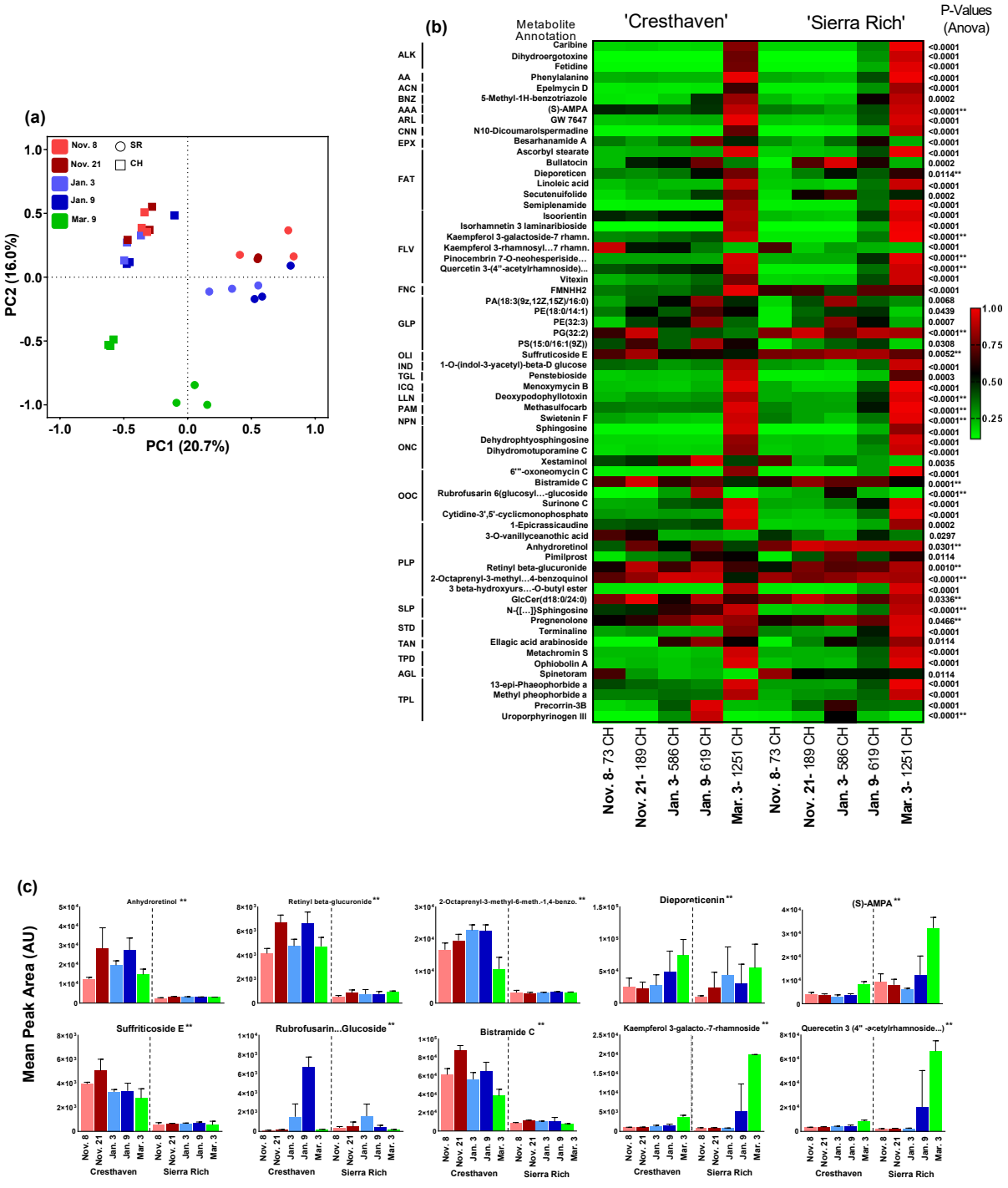

Figure 4.3. Dormant season kinetics of secondary metabolites in flower buds of 'Cresthaven' and 'Sierra Rich' peach cultivars. Molecular feature abundance measured by non-targeted liquid-chromatography mass spectrometry (LC-MS). (a) Principal component analysis (PCA) bi-plot of relative abundance of secondary metabolites, with comparisons between two cultivars

among five time points throughout the dormant season. (b) Heat map showing relative abundance, scaled within each cultivar, of secondary metabolites determined to significantly change across five time points during the dormant season as determined by repeated measures ANOVA ($p<0.05$). Metabolic abundances differ between cultivars if denoted with "**". Different categorical annotations are indicated by abbreviations: ALK-alkaloids, AA-amino acids, ACN-anthracyclines, BNZ-Benzotriazole, ARL-Arylthioethers, AAA-alpha amino acids, CNN-cinnamic acids, EPX-epoxides, FAT-fatty acids, FLV-flavonoids, FNC-flavin nucleotides, GLP-Glycerophospholipids, OLI-oligosaccharides, IND-indolyl carboxylic acids, TGL- Terpene glycosides, ISQ-Isochromanequinones, LLN- lignolactones, PAM-phenylacetamides, NPN-napthopyranones, ONC- organonitrogen compounds, OOC-organooxygen compounds, PLP-prenol lipids, SLP-sphingolipids, STD- steroid, TAN-tannin, TPD-terpenoid,AGL-aminoglycosides, TPL-tetrapyrroles. (c) Individual bar plots of secondary metabolites determined by repeated measures ANOVA to be expressed both differentially across time during dormancy, and between cultivars if denoted with "**". Error bars represent one standard deviation.

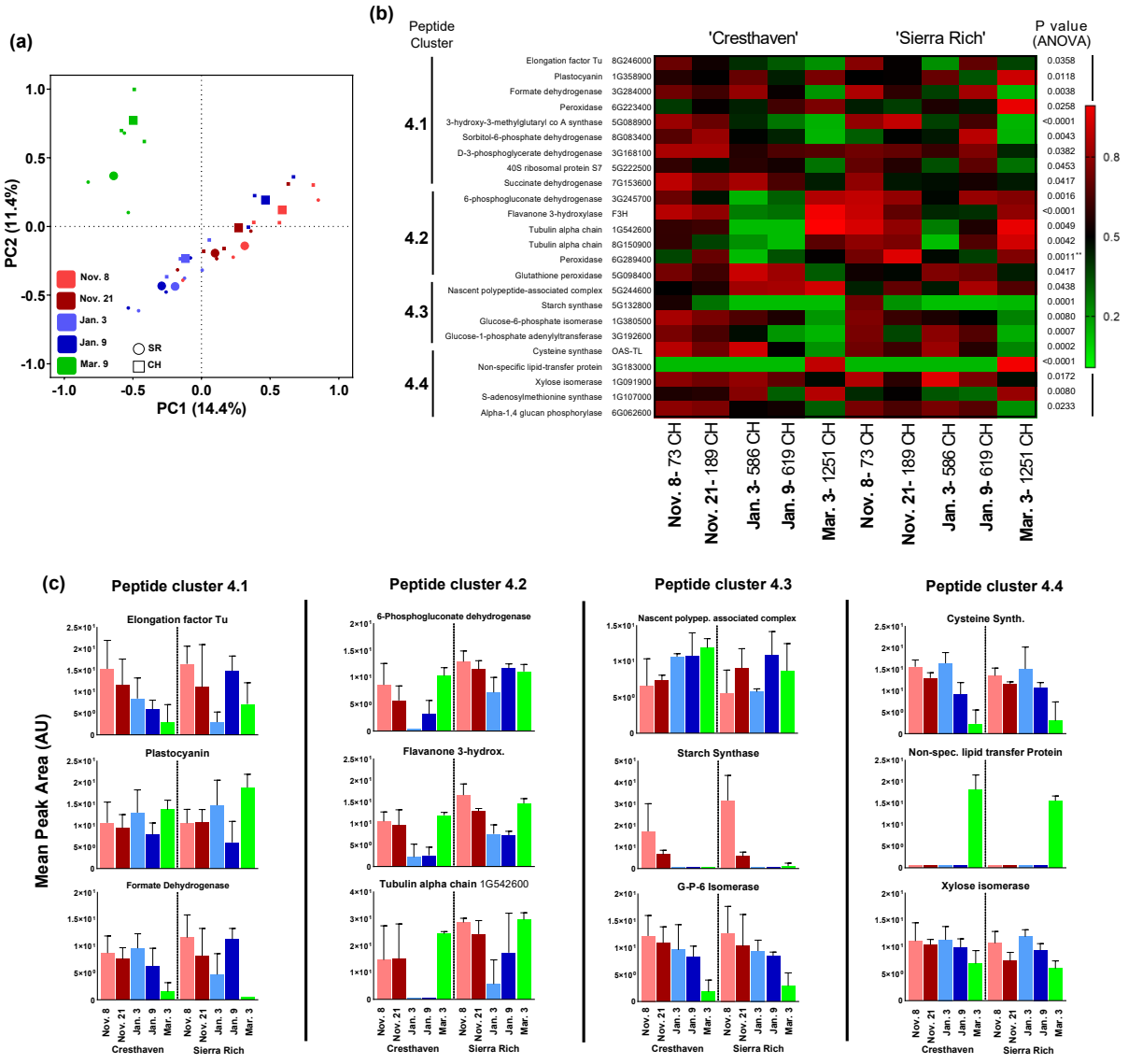

Figure 4.4. Dormant season kinetics of proteins in flower buds of 'Cresthaven' and 'Sierra Rich' peach cultivars. Molecular feature abundance measured by non-targeted liquid-chromatography mass spectrometry (LC-MS). (a) Principal component analysis (PCA) bi-plot of relative abundance of proteins, with comparisons between two cultivars among five time points throughout the dormant season. (b) Heat map showing relative abundance, scaled within each cultivar, of proteins determined to significantly change across five time points during the dormant season as determined by repeated measures ANOVA ($p<0.05$). Protein abundances differ between cultivars if denoted with "**". (c) Individual bar plots for proteins determined to be accumulated significantly different over time by repeated measures ANOVA ($p<0.05$), were aggregated using variable clustering analysis, which combined each protein into a cluster of proteins with which it was most highly correlated. The three proteins from each protein cluster with the highest coefficients of determination (r^2) were ranked from top to bottom within each cluster, and none of the displayed proteins varied significantly by genotype. Error bars represent one standard deviation.

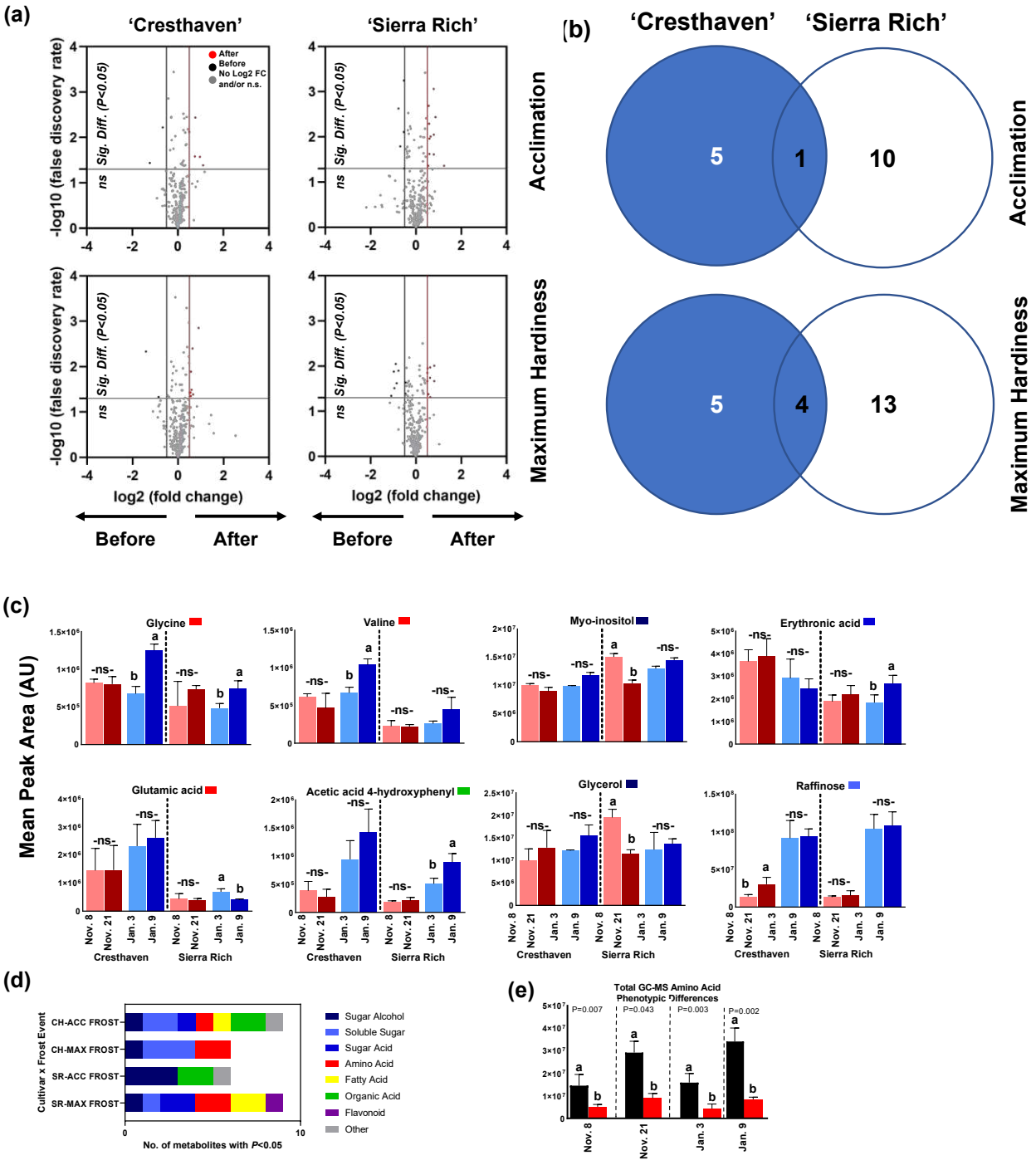

Figure 4.5. Multifaceted comparison of differential primary metabolite abundance for two peach cultivars, 'Cresthaven' and 'Sierra Rich,' following two major frost events. One frost event occurred in November 18, 2016 (-6.8 ºC) during the acclimation phase of endodormancy, and one which happened during maximum hardiness at January 6, 2017 (-18.6 ºC). (a) Volcano plots displaying significant ($p<0.05$, with log2 fold change >0.5) increases and decreases in abundance of primary metabolites before and after two frost events for each of two genotypes. (b)

Venn diagrams showing the numbers of primary metabolites which are differentially and significantly ($p<0.05$, with log2 fold change >0.5) modulated by frost events at different dormancy stages. (c) Bar plots showing abundance of individual metabolites at the different time points pre- and post-frost. Comparisons of pre- and post- frost events determined significant by T-test ($p<0.05$) are indicated by different letters. Error bars represent one standard deviation. (d) Histogram displaying the number of significant ($p<0.05$, with log2 fold change >0.5) metabolic changes in abundance, by class for each frost event and each genotype. (e) Bar plot of T-tests($p<0.05$) showing differences in total accumulation of all GC-MS detected amino acids between genotype for each sampling date from November 2016 and January 2017. Error bars represent one standard deviation.

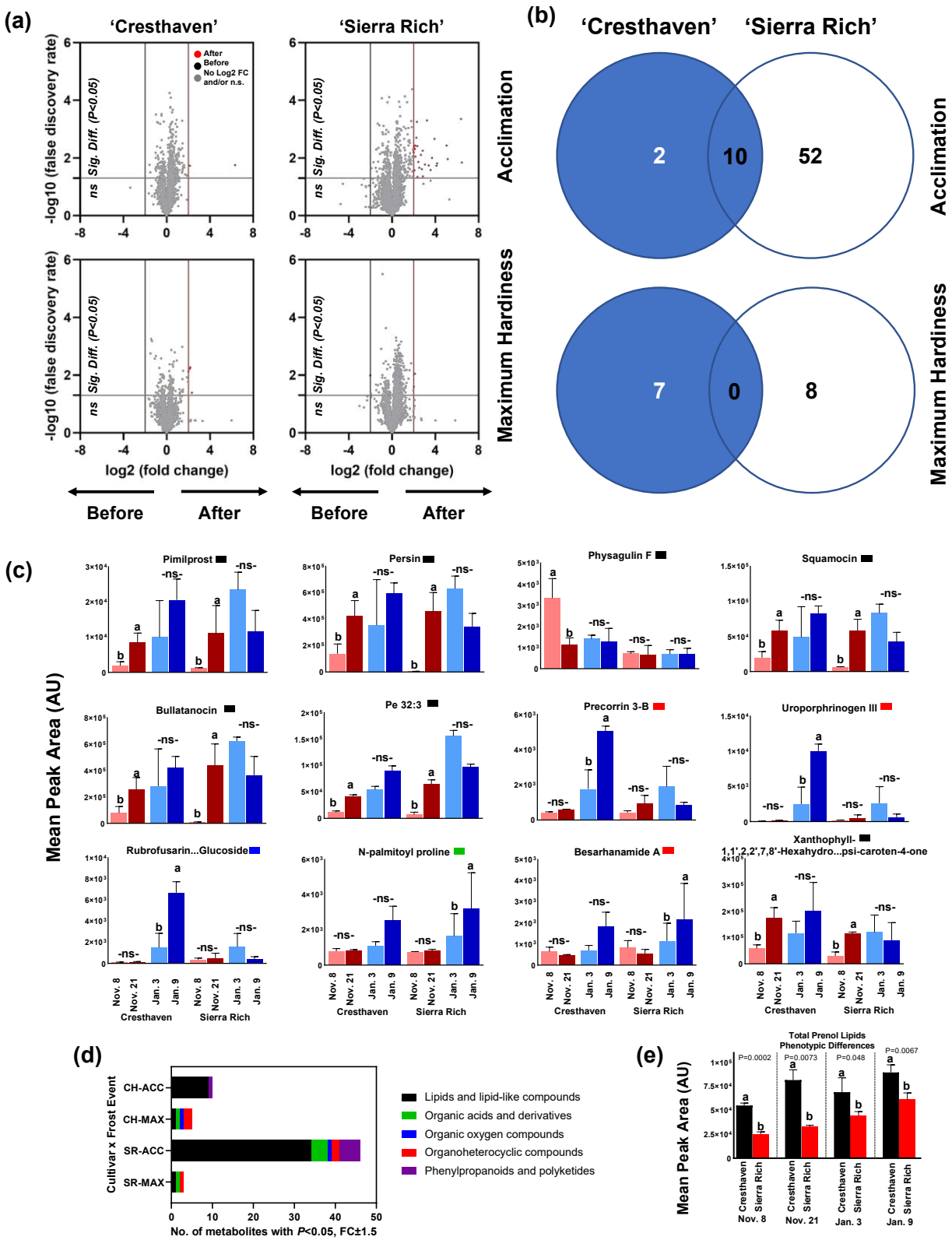
(a)
'Cresthaven'
'Sierra Rich'
After
Before
No Log2 FC and/or n.s.
-log10 (false discovery rate)
ns
Sig. Diff. (P<0.05)
log2 (fold change)
Before
After
Acclimation
Maximum Hardiness
(b)
'Cresthaven'
'Sierra Rich'
2
10
52
7
0
8
(c)
Mean Peak Area (AU)
Pimilprost
Persin
Physagulin F
Squamocin
Bullatanocin
Pe 32:3
Precorrin 3-B
Uroporphrinogen III
Rubrofusarin...Glucoside
N-palmitoyl proline
Besarhanamide A
Xanthophyll-
1,1',2,2',7,8'-Hexahydro...psi-caroten-4-one
-ns-
Nov. 8
Nov. 21
Jan. 3
Jan. 9
Cresthaven
Sierra Rich
(d)
Cultivar x Frost Event
CH-ACC
CH-MAX
SR-ACC
SR-MAX
No. of metabolites with P<0.05, FC±1.5
Lipids and lipid-like compounds
Organic acids and derivatives
Organic oxygen compounds
Organoheterocyclic compounds
Phenylpropanoids and polyketides
(e)
Total Prenol Lipids
Phenotypic Differences
Mean Peak Area (AU)
P=0.0002
P=0.0073
P=0.048
P=0.0067
Cresthaven
Sierra Rich
Nov. 8
Nov. 21
Jan. 3
Jan. 9

Figure 4.6. Multifaceted comparison of differential secondary metabolite abundance for two peach cultivars, 'Cresthaven' and 'Sierra Rich,' following two major frost events. One frost event which happened in November 18, 2016 (-6.8 ºC) during the acclimation phase of endodormancy, and one which happened during maximum hardiness at January 6, 2017 (-18.6 ºC). (a) Volcano plot displaying significant ($p<0.05$, with log2 fold change >1.5) increases and decreases in abundance of secondary metabolites before and after two frost events for each of two genotypes. (b) Venn diagrams showing the numbers of secondary metabolites which are differentially and significantly ($p<0.05$, with log2 fold change >1.5) modulated by frost events at different dormancy stages. (c) Bar plots showing abundance of individual metabolites at the different time points pre- and post-frost. Comparisons of pre- and post- frost events determined significant by T-test ($p<0.05$, with a log2 fold change >1.5) are indicated by different letters. Error bars represent one standard deviation. (d) Histogram displaying the number of significant ($p<0.05$, with log2 fold change >1.5) metabolic changes in abundance, by class for each frost event and each genotype. (e) Bar plot of T-tests($p<0.05$) showing differences in total accumulation of all LC-MS detected prenol lipids between genotype for each sampling date from November 2016 and January 2017. Error bars represent one standard deviation.

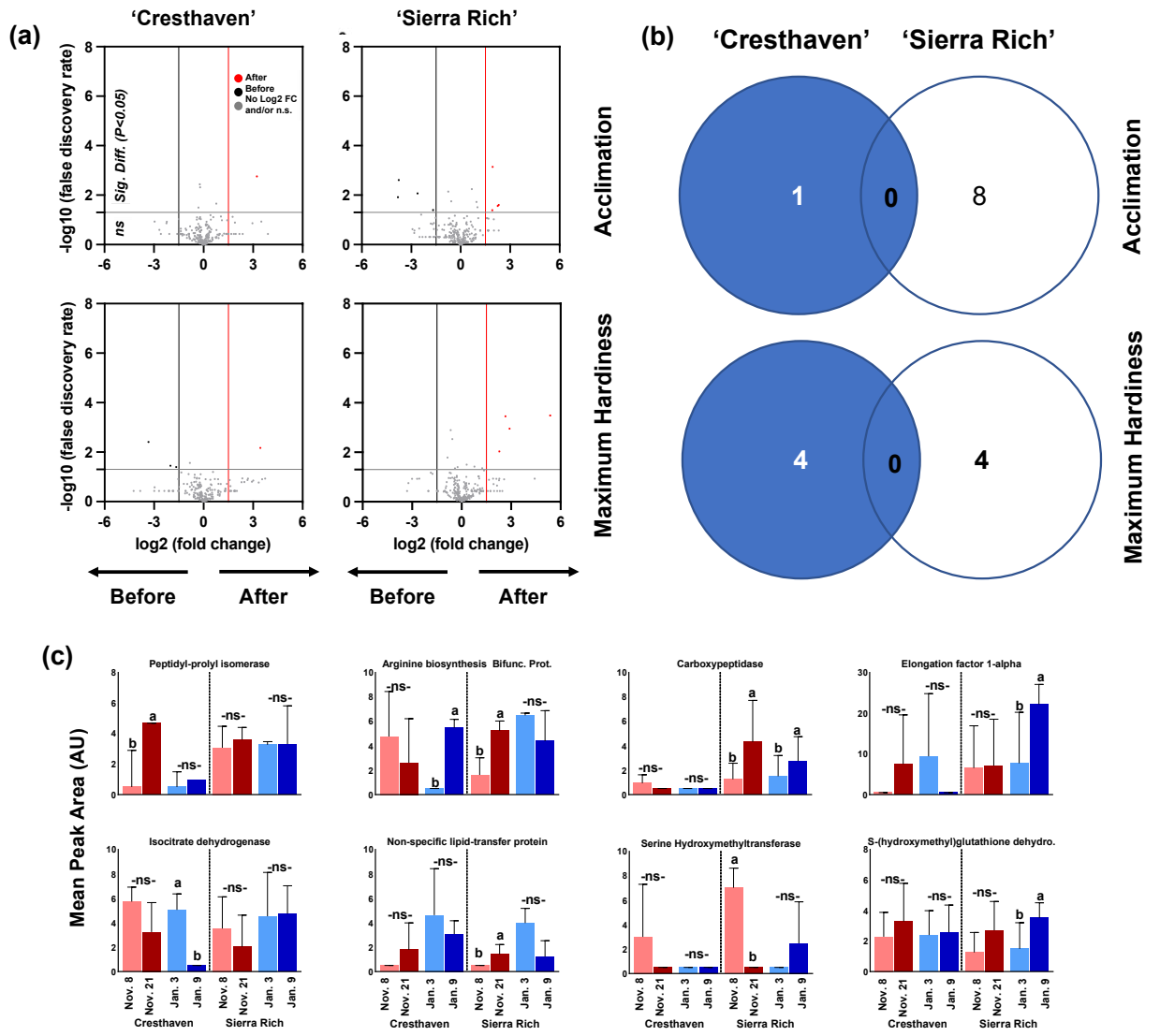

Figure 4.7. Multifaceted comparison of differential protein abundance for two peach genotypes, 'Cresthaven' and 'Sierra Rich,' following two major frost events. One which happened in November 18, 2016 (-6.8 ºC) during the acclimation phase of endodormancy, and one which happened during maximum hardiness on January 6, 2017 (-18.6 ºC). (a) Volcano plot displaying significant ($p<0.05$, with log2 fold change >1.5) increases and decreases in abundance of proteins before and after two frost events for each of two genotypes. (b) Venn diagrams showing the numbers of proteins which are differentially and significantly ($p<0.05$, with log2 fold change >1.5) modulated by frost events at different dormancy stages. (c) Bar plots showing differential abundance of individual proteins at the different time points pre- and post-frost. Comparisons of pre- and post- frost events determined significant by T-test ($p<0.05$) are indicated by different letters. Error bars represent one standard deviation.

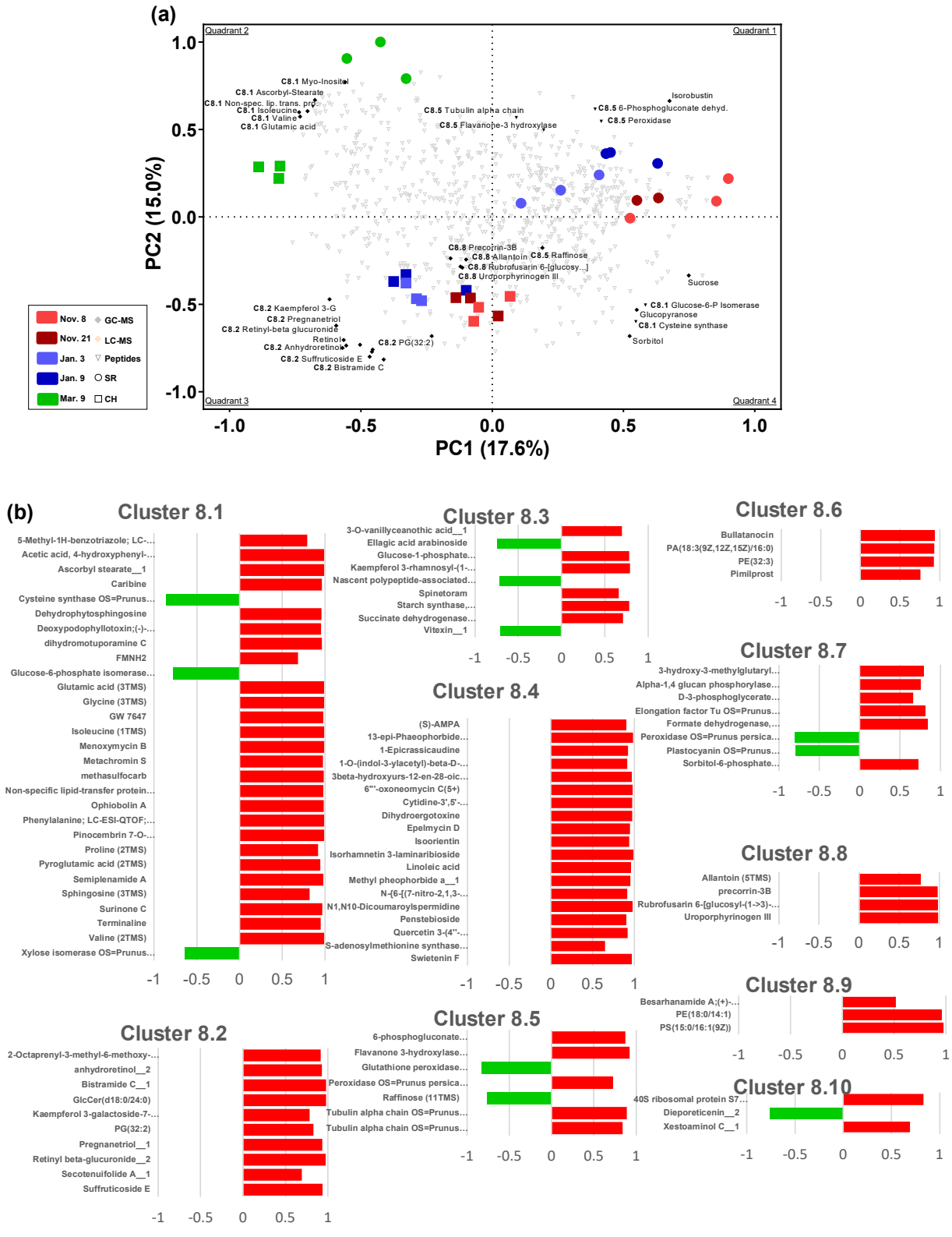
(a)
Quadrant 2
Quadrant 1
Quadrant 3
Quadrant 4
C8.1 Myo-Inositol
C8.1 Ascorbyl-Stearate
C8.1 Non-spec. lip. trans. pr...
C8.1 Isoleucine
C8.1 Valine
C8.1 Glutamic acid
C8.5 Tubulin alpha chain
C8.5 Flavanone-3 hydroxylase
Isorobustin
C8.5 6-Phosphogluconate dehyd.
C8.5 Peroxidase
C8.8 Precorrin-3B
C8.8 Allantoin
C8.5 Raffinose
C8.8 Rubrofusarin 6-[glucosy...]
C8.8 Uroporphyrinogen III
Sucrose
C8.2 Kaempferol 3-G
C8.2 Pregnanetriol
C8.2 Retinyl-beta glucuronide
Retinol
C8.2 Anhydroretinol
C8.2 PG(32:2)
C8.2 Suffruticoside E
C8.2 Bistramide C
C8.1 Glucose-6-P Isomerase
Glucopyranose
C8.1 Cysteine synthase
Sorbitol
Nov. 8 GC-MS
Nov. 21 LC-MS
Jan. 3 Peptides
Jan. 9 SR
Mar. 9 CH
PC2 (15.0%)
PC1 (17.6%)
1.0
0.5
0.0
-0.5
-1.0
(b)
Cluster 8.1
5-Methyl-1H-benzotriazole; LC-...
Acetic acid, 4-hydroxyphenyl-...
Ascorbyl stearate__1
Caribine
Cysteine synthase OS=Prunus...
Dehydrophytosphingosine
Deoxypodophyllotoxin;(-)-...
dihydromotuporamine C
FMNH2
Glucose-6-phosphate isomerase...
Glutamic acid (3TMS)
Glycine (3TMS)
GW 7647
Isoleucine (1TMS)
Menoxymycin B
Metachromin S
methasulfocarb
Non-specific lipid-transfer protein...
Ophiobolin A
Phenylalanine; LC-ESI-QTOF;...
Pinocembrin 7-O-...
Proline (2TMS)
Pyroglutamic acid (2TMS)
Semiplenamide A
Sphingosine (3TMS)
Surinone C
Terminaline
Valine (2TMS)
Xylose isomerase OS=Prunus...
Cluster 8.3
3-O-vanillyceanothic acid__1
Ellagic acid arabinoside
Glucose-1-phosphate...
Kaempferol 3-rhamnosyl-(1-...
Nascent polypeptide-associated...
Spinetoram
Starch synthase,...
Succinate dehydrogenase...
Vitexin__1
Cluster 8.6
Bullatanocin
PA(18:3(9Z,12Z,15Z)/16:0)
PE(32:3)
Pimilprost
Cluster 8.4
(S)-AMPA
13-epi-Phaeophorbide...
1-Epicrassicaudine
1-O-(indol-3-ylacetyl)-beta-D-...
3beta-hydroxyurs-12-en-28-oic...
6'''-oxoneomycin C(5+)
Cytidine-3',5'-...
Dihydroergotoxine
Epelmycin D
Isoorientin
Isorhamnetin 3-laminaribioside
Linoleic acid
Methyl pheophorbide a__1
N-[6-[(7-nitro-2,1,3-...
N1,N10-Dicoumaroylspermidine
Penstebioside
Quercetin 3-(4'''-...
S-adenosylmethionine synthase...
Swietenin F
Cluster 8.7
3-hydroxy-3-methylglutaryl...
Alpha-1,4 glucan phosphorylase...
D-3-phosphoglycerate...
Elongation factor Tu OS=Prunus...
Formate dehydrogenase,...
Peroxidase OS=Prunus persica...
Plastocyanin OS=Prunus...
Sorbitol-6-phosphate...
Cluster 8.8
Allantoin (5TMS)
precorrin-3B
Rubrofusarin 6-[glucosyl-(1->3)-...
Uroporphyrinogen III
Cluster 8.9
Besarhanamide A;(+)-...
PE(18:0/14:1)
PS(15:0/16:1(9Z))
Cluster 8.2
2-Octaprenyl-3-methyl-6-methoxy-...
anhydroretinol__2
Bistramide C__1
GlcCer(d18:0/24:0)
Kaempferol 3-galactoside-7-...
PG(32:2)
Pregnanetriol__1
Retinyl beta-glucuronide__2
Secotenuifolide A__1
Suffruticoside E
Cluster 8.5
6-phosphogluconate...
Flavanone 3-hydroxylase...
Glutathione peroxidase...
Peroxidase OS=Prunus persica...
Raffinose (11TMS)
Tubulin alpha chain OS=Prunus...
Tubulin alpha chain OS=Prunus...
Cluster 8.10
40S ribosomal protein S7...
Dieporeticenin__2
Xestoaminol C__1
-1
-0.5
0
0.5
1

Figure 4.8. Combined analysis of GC-MS and LC-MS detected metabolites and proteins of dormant peach floral buds, across five time points and two cultivars ('Cresthaven' and 'Sierra Rich'). All metabolites and proteins were normalized as z-scores and analyzed across all as a single population. (a) Principal component analysis Bi-plot (PCA) of all detectable metabolites and proteins for observation of which have greatest influence with the shift in abundance across time and genotype. Specific metabolites and proteins are annotated on the PCA Bi-plot. (b) Variable clustering analysis used in conjunction with PCA bi-plot to identify how different metabolites and proteins correlate with one another, and which are associated with different dormancy stages and genotypes.